INFORMATION TO USERS

This manuscript has been reproduced from the microfilm master. UMI films the text directly from the original or copy submitted. Thus, some thesis and dissertation copies are in typewriter face, while others may be from any type of computer printer.

The quality of this reproduction is dependent upon the quality of the copy submitted. Broken or indistinct print, colored or poor quality illustrations and photographs, print bleedthrough, substandard margins, and improper alignment can adversely affect reproduction.

In the unlikely event that the author did not send UMI a complete manuscript and there are missing pages, these will be noted. Also, if unauthorized copyright material had to be removed, a note will indicate the deletion.

Oversize materials (e.g., maps, drawings, charts) are reproduced by sectioning the original, beginning at the upper left-hand corner and continuing from left to right in equal sections with small overlaps. Each original is also photographed in one exposure and is included in reduced form at the back of the book.

Photographs included in the original manuscript have been reproduced xerographically in this copy. Higher quality 6" x 9" black and white photographic prints are available for any photographs or illustrations appearing in this copy for an additional charge. Contact UMI directly to order.

UMI®

Bell & Howell Information and Learning
300 North Zeeb Road, Ann Arbor, MI 48106-1346 USA
800-521-0600

Liquid-Phase Sensing Strategies for the The Thickness Shear Mode Acoustic Wave Sensor

by

Jeffrey John Chance

A thesis submitted to the Faculty of Graduate Studies and Research in partial fulfillment of the requirements for the degree of Doctor of Philosophy

Department of Chemistry
McGill University
Montréal, Québec, Canada

July 1997

Abstract

A thickness-shear mode (TSM) acoustic wave sensor system has been constructed and used to examine binding phenomena that occur in the liquid phase. The work is broadly divided into two sections.

The first section examines the use of cholestyramine as a sensor coating for detection of bile acids. A 10-MHz piezoelectric crystal is coated on one side with cholestyramine resin and mounted in a batch-mode sensor block which exposes the coating to solution. After sample injection, the binding process is observed in real time as a drop in frequency as the bile salt binds to the coating, reaching > 90% completion within 10 minutes with most of the binding occurring within the first minute. Linear calibration curves are generated with sensitivity increasing in the order cholate ≈ glycocholate < taurocholate << taurodeoxycholate. Detection limits in water are in the range 0.2 - 9 nmol and are better than those observed in phosphate buffer. A multi-step regeneration protocol allows the coating to be reused more than 400 times over a period of several months. Precision for replicate injections is about 10% RSD and depends on the reproducibility of the regeneration and injection steps.

In terms of the binding process, hydrophobic interactions are observed to be of importance in the ability of bile salts to displace other counterions. However, anions with greater charge density also appear to compete effectively for binding sites on the resin. In particular, at equimolar concentrations of citrate and bile salt, the trivalent citrate anion reduces the amount of bile salt binding by about 40%. This suggests that the efficiency of cholestyramine-based bile salt sequestering drugs used in the reduction of hypercholesterolemia may be improved by eliminating citric acid as an excipient and avoiding the use of fruit juices during ingestion.

In the second section, a selection of compounds were examined for their potential as stable and reactive liquid-phase coatings with the primary amine group as the functional group of interest. Based on dry TSM sensor frequency changes, all

coating candidates exhibited some degree of stable coating formation after incubation and rinsing. Reactivity of the coatings was then assessed via reaction with succinic anhydride under anhydrous conditions. With pyridine- and thiol-based coatings, the frequency change is negligible or is positive, which may indicate some loss of coating material upon reaction of the amine group. A silane-based coating was stable but exhibited only small frequency decreases for the reaction step. In terms of stability, reproducibility and magnitude of the frequency changes observed, poly(ethyleneimine) (PEI) is seen to be the best choice for providing analytically useful signals where covalent reaction with surface-confined amino groups in the liquid phase is desired.

Reaction of PEI with succinic anhydride also serves as a method for fabrication of sensor coatings with the carboxylic acid group as the reactive functional group of interest. The formation of reactive COOH groups was tested with a carbodiimide-activated covalent immobilization of dopamine. TSM sensor frequency changes, ellipsometry, and x-ray photoelectron spectroscopy provided support for all steps involved. The coating surface structure is uneven and is likely highly branched and three-dimensional. The method is quick and simple, and the films are also sufficiently robust for liquid-phase acoustic wave sensor applications.

Résumé

Un capteur à onde acoustique en mode d'épaisseur par cisaillement ("thickness-shear mode (TSM) acoustic wave sensor") a été construit et utilisé afin d'étudier les phénomènes de liaison qui ont lieu en phase liquide. Ce travail a été divisé en deux parties.

La première partie de ce travail consiste à déposer la cholestyramine sous forme de film afin de pouvoir détecter les acides biliaires. Pour ce faire, un cristal piézoélectrique de 10-MHz est recouvert d'un côté par la résine de cholestyramine et est ensuite assemblé de manière à exposer le film vers la solution; le tout dans une cellule en mode d'analyse discontinu (en lot). Après injection de l'échantillon, le processus de liaison est suivi en temps réel. Une chute de fréquence est observée lorsque le sel biliaire se lie au film, atteignant 90 % de la valeur maximale en 10 minutes. Cependant, le processus de liaison est presqu' entièrement terminé durant la première minute. Des courbes de calibration linéaires ont été réalisées avec une sensibilité croissante pour la série suivante: cholate ~ glycocholate < taurocholate << taurodéoxycholate. Les limites de détection dans l'eau sont de l'ordre de 0,2 à 9 nmol. Celles-ci sont meilleures par rapport à celles mesurées en milieu tampon phosphate. Le protocole de regénération en plusieurs étapes permet de réutiliser le film plus de 400 fois sur une période de temps couvrant quelques mois. La précision des injections successives est d'environ 10% DSR et dépend de la reproductibilité de l'étape de l'injection ainsi que des étapes de regénération.

En ce qui concerne le processus de liaison, les intéractions hydrophobes semblent jouer un rôle important pour ce qui est de la capacité des acides biliaires à déplacer les autres contre-ions. Cependant, les anions ayant une plus grande densité de charge semblent se lier plus efficacement aux sites de liaison de la résine (processus compétitif). Plus spécifiquement, à des concentrations équimolaires de citrate et d'acide bilaire, les anions citrates trivalents réduisent la quantité d'acide biliaire lié à la résine

d'à-peu-près 40%. Ceci suggère que l'efficacité de la complexation entre les acides biliaires et les médicaments à base de cholestyramine utilisés contre l'hypercholestérolémie pourrait être augmentée en éliminant l'acide citrique présent comme excipient et en éliminant les jus de fruits durant l'ingestion.

La seconde partie du travail consiste à étudier plusieurs composés potentiels ayant la particularité d'être stables et de former des films réactifs avec les amines primaires, en milieu liquide. Les mesures de variation de fréquence du capteur TSM à l'air ambient de tous les films étudiés montrent que ceux-ci ont un certain degré de stabilité de formation après les étapes d'incubation et de rinçage. La réactivité de ces films a ensuite été testée par réaction avec l'anhydride succinique sous conditions anhydres. Les films à base de pyridine et de thiol ont montré une variation de fréquence qui est soit négligeable, soit positive. Ceci pourrait indiquer une perte du film après réaction avec le groupement amine. Le film à base de silane était stable mais ne montrait qu'une faible chute de fréquence après réaction avec le groupement amine. En ce qui concerne la stabilité, la reproductibilité et les variations de fréquences observées, le poly(imine d'éthylène) semble être le meilleur candidat. En effet, ce film permet de détecter des signaux analytiques utiles dans les cas où l'on veut observer une réaction covalente avec des surfaces contenant des groupements amines en phase liquide.

La réaction du poly(imine d'éthylène) avec l'anhydride succinique peut aussi être utilisée comme méthode de fabrication de films pour des capteurs ayant un acide carboxylique comme groupement réactif. La formation des groupements COOH réactifs a été testée avec la dopamine immobilisée de manière covalente en utilisant un carbodiimide. Les mesures de variation de fréquence du capteur TSM, les mesures par ellipsométrie ainsi que les spectres de spectrométrie photoélectronique par rayons-X ont confirmé chacune de ces deux étapes. La surface du film est inégale, et probablement réticulée et tridimensionnelle. Cette méthode est rapide et simple. De plus, les films sont suffisament solides pour pouvoir être utilisés pour les applications avec le capteur à onde acoustique en phase liquide.

Acknowledgements

I would like to express many thanks to Professor William C. Purdy for his support and guidance throughout my stay at McGill. The opportunity to pursue my research interests in an environment of independence was greatly appreciated.

I would also like to express my gratitude to some of the people who made my stay at McGill a pleasant one. Brian Spencer and Tanya Tadey for their friendship and for helping me to "learn the ropes"; Dr. Power and Dr. Salin for their periodic assistance and coursework instruction which in both cases complemented my research efforts; and Dr. Lennox for helpful discussions on thin-film systems. I am also grateful to Fred Kluck and Bill Bastians in construction of the housing unit, and Ms. Renée Charron for administrative help with my stay here as a graduate student. The assistance of Ms. Susie Poulin of the École Polytechnique de Montréal with acquisition and interpretation of XPS spectra is also acknowledged.

I would also like to express my gratitude to my family for their encouragement and support while persuing my educational aspirations. Special thanks to Dr. Art Chow of the University of Manitoba for encouraging me to pursue graduate studies.

Finally, I would like to thank the Department of Chemistry at McGill University for demonstrator assistantships, and the Natural Sciences and Engineering Research Council of Canada and the Fonds pour la Formation de Chercheurs et l'Aide à la Recherche for graduate scholarships.

Table of Contents

Abstract i
Résumé iii
Acknowledgements v
Table of Contents vi
List of Figures ix
List of Tables xii
List of Abbreviations and Symbols xiii

1. The Thickness Shear Mode Acoustic Wave Sensor 1
1.1 Introduction 1
1.2 Operation of the TSM Acoustic Wave Sensor 2
1.2.1 The Piezoelectric Effect 2
1.2.2 Measurement Methods 4
1.2.3 The Experimental System 6
1.2.4 Factors Influencing the Frequency Response 9
1.2.5 Signal-to-Noise 11
1.3 Research 12
1.3.1 Evolution of TSM Acoustic Wave Sensor Research 12
1.3.2 Detectors for Chromatography 13
1.3.3 Gas Detection 15
1.3.4 Electrogravimetric Analysis 17
1.3.5 Biosensors 21
1.3.6 Other Research 27
1.4 Commercial Products 29
References 31

2. Construction of Circuit and Housing Apparatus 37
2.1 Introduction 37
2.2 Circuitry 37
2.3 Crystals 42
2.4 Housing Unit for One-Sided Liquid-Phase Experiments 43
2.5 Three-Crystal Design for Accurate Long-Term Frequency Readings 48
References 50

3. Bile Acid Measurements Using a Cholestyramine-Coated TSM Acoustic Wave Sensor 51
3.1 Introduction 51
3.1.1 Atherosclerosis 51
3.1.2 Hypothetical *In Vitro* TSM Sensor Experiment 53
3.2 Bile Acids 54
3.2.1 Structure of Bile Acids 54
3.2.2 Bile Acids and the Enterohepatic Circulation 57
3.2.3 Synthesis of Bile Acids From Cholesterol 59
3.2.4 Bile Acid Sequestrants and Cholesterol Reduction 59
3.3 A TSM Sensor for Bile Acids 61
3.3.1 Materials 61
3.3.2 Apparatus 61
3.3.3 Coating Procedure 62
3.3.4 Determination of Frequency Response 62
3.3.5 Basic Operation 63
3.3.6 Nernst Film Model of System 65
3.3.7 Comparison of Sensor Response with Previous Reports 65
3.3.8 Coating Regeneration 67
3.3.9 Calibration Curves 71
3.3.10 Interferences 78
3.3.11 Implications of Citrate Interference on Action of Cholestyramine 81
3.4 Analytical Methods for Bile Acids 81
3.4.1 Isolation from a Biological Matrix 82
3.4.2 Colorimetric Methods 82
3.4.3 Chromatographic Methods 83
3.4.4 Other Methods 84
3.5 Applications for the Present TSM Acoustic Wave Sensor 85
3.6 Conclusions 87
References 89

4. Functional Group Reactions at Stable Coatings 92
4.1 Introduction 92
4.2 Criteria for TSM Sensor Functional Group Reactions 93
4.3 Attempts to Immobilize Cholesterol on a Gold TSM Electrode 94
4.3.1 Choice of Reaction 95
4.3.2 TSM Sensor Studies 96
4.3.3 Assessment of Results and Direction of Efforts 100
4.4 Experiments Using Peptide Coupling Agents 101
4.4.1 Peptide Synthetic Route Using Coupling Agents 102
4.4.2 Advantages For Use With The TSM Sensor 104
4.4.3 Selection of Alternate Analytical Method for Examining Coatings . . .104
4.4.4 Verification of Coating Stability Using XPS 106
4.4.5 Procedure for Peptide Coupling Agent Experiments 110
4.4.6 Results for Peptide Coupling Agent Experiments 111
4.5 Systematic Evaluation of Amine-Functionalized Coatings 116
4.5.1 Experimental 117
4.5.2 Results and Discussion 119
4.5.3 Conclusions 128
4.6 Fabrication of Carboxylic Acid Terminated Thin Films Using Poly(ethyleneimine) on a Gold Surface 130
4.6.1 Materials and Methods 131
4.6.2 Reactions Steps and TSM Sensor Frequency Data 132
4.6.3 Ellipsometric and XPS Data 134
4.6.4 Conclusions 134
4.7 Chapter Overview 141
References 142

Appendices

A.1 GPIB Software Routine for Data Acquisition 145
A.2 Publications, Presentations and Industry Consulting 147
A.3 Contributions to Original Knowledge 149

List of Figures

Figure 1.1 The piezoelectric effect and converse piezoelectric effect 3
Figure 1.2 Equivalent circuit of an AT-cut quartz crystal (Butterworth-van Dyke model) 5
Figure 1.3 Quartz crystal wafer showing electrode geometry 7
Figure 1.4 TSM sensor experiment instrumentation 8
Figure 1.5 Propagation of the transverse shear wave from the TSM sensor into a liquid 10
Figure 1.6 Comparison of chromatograms using a traditional thermal detector and piezoelectric crystal detector 14
Figure 1.7 Apparatus used for gas-phase detection of organophosphorus compounds and pesticides 16
Figure 1.8 UPD of Pb on Au followed by the EQCM method and cyclic voltammetry 18
Figure 1.9 Response of Prussian Blue-coated TSM sensor crystal to the flow injection of K^+ and H^+ in a stream of nitric acid: current and frequency change 20
Figure 1.10 Experimental setup for liquid-phase TSM biosensor experiment 22
Figure 1.11 Response for the unspecific adsorption of anti-EBV antibody to HIV peptide covered quartz and the specific reaction of anti-HIV antibody 23
Figure 1.12 Schematic representation of the sandwich enzyme-linked immunosorbent assay procedure used with the QCM 25

Figure 2.1 Reference and working oscillators with difference circuitry 39
Figure 2.2 Clock diagram illustrating how the 7474 flip-flop IC outputs the frequency difference between two frequency inputs 40
Figure 2.3 Housing unit (side view) and associated apparatus for liquid sensing applications where only one crystal face (electrode) is exposed to solution 44
Figure 2.4 Top view of the one-sided crystal housing unit 45
Figure 2.5 Photo of plexiglas housing unit where the two blocks are pressed together using a clamp 46
Figure 2.6 Photo of inside faces of the two plexiglas blocks 47
Figure 2.7 3-crystal arrangement for improving accuracy in frequency measurements for coatings applied over long periods of time 49

Figure 3.1 Sketch of foundation for a TSM sensor experimental system for *in vitro* study of processes associated with atherosclerosis 53
Figure 3.2 Chemical structure of cholesterol and bile acids, indicating bile acids studied with the TSM sensor system 55
Figure 3.3 Chemical configurations of cholic acid 56
Figure 3.4 The enterohepatic circulation of bile acids and the digestion of lipids 58
Figure 3.5 Structure of cholestyramine 60
Figure 3.6 Typical response to 1 mM sodium glycocholate in buffer with and without agitation 64
Figure 3.7 Frequency changes during the regeneration protocol 70
Figure 3.8 Scatterplot of frequency response to sodium cholate in buffer and water 73
Figure 3.9 Scatterplot of frequency response to sodium glycocholate in buffer and water 74
Figure 3.10 Scatterplot of frequency response to sodium taurocholate in buffer and water 75
Figure 3.11 Scatterplot of frequency response to sodium taurodeoxycholate in buffer and water 76
Figure 3.12 Frequency response profiles showing interference from citrate in buffer 80

Figure 4.1 Studies examining the use of a thiol as an initial coating for the immobilization of cholesterol via ester formation using thionyl chloride 98
Figure 4.2 Role of coupling agent in amide bond formation 102
Figure 4.3 Flow chart for solid-phase peptide synthesis 103
Figure 4.4 XPS survey scan for a coating of 4-ATP on a gold crystal electrode 108
Figure 4.5 High-resolution N 1s spectrum from a sample coated with 4-ATP . .108
Figure 4.6 Structure of amine-functionalized coating compounds 119
Figure 4.7 Graphical representation of frequency changes for the steps of coating, rinsing and reaction with anhydride 129
Figure 4.8 Reaction of poly(ethyleneimine) thin film with succinic anhydride and subsequent reaction with dopamine 133
Figure 4.9a Carbon high-resolution XPS spectrum for PEI 136
Figure 4.9b Carbon high-resolution XPS spectrum for PEI reacted with succinic anhydride 137
Figure 4.9c Carbon high-resolution XPS spectrum for PEI reacted with succinic anhydride and then dopamine 137
Figure 4.9d Nitrogen high-resolution XPS spectrum for PEI 138

Figure 4.9e Nitrogen high-resolution XPS spectrum for PEI reacted with succinic anhydride 138
Figure 4.9f Nitrogen high-resolution XPS spectrum for PEI reacted with succinic anhydride and then dopamine 139
Figure 4.9g Oxygen high-resolution XPS spectrum for PEI 139
Figure 4.9h Oxygen high-resolution XPS spectrum for PEI reacted with succinic anhydride 140
Figure 4.9i Oxygen high-resolution XPS spectrum for PEI reacted with succinic anhydride and then dopamine 140

List of Tables

Table 3.1 Regeneration and precision data for 1 mM sodium cholate 68
Table 3.2 Sensor response for four bile acids 77

Table 4.1 Ideal criteria for TSM sensor functional group reactions 93
Table 4.2 XPS results for monolayer stability in DMF and DCM 109
Table 4.3 Peptide coupling agent experiments using the TSM sensor 112
Table 4.4 Frequency data for all steps involved in the coating evaluation 121
Table 4.5 XPS data for reaction steps in Figure 4.8 135

List of Abbreviations and Symbols

The abbreviations and symbols for the physical or chemical terms and units used in this thesis are in accordance with those adopted by IUPAC (International Union of Pure and Applied Chemistry), IUPAP (International Union of Pure and Applied Physics) and IUB (International Union of Biochemistry), published in the Handbook of Chemistry and Physics.

2-AET	2-aminoethanethiol hydrochloride
4-AP	4-aminopyridine
4-ATP	4-aminothiophenol
AGC	automatic gain control
AMT	3-amino-5-mercapto-1,2,4-triazole
APM	acoustic plate mode
APS	adenosine 5'-phosphosulfate
APTES	3-aminopropyltriethoxysilane
BCIP	5-bromo-4-chloro-3-indolyl phosphate
BE	binding energy (XPS)
BOP	benzotriazol-1-yloxytris(dimethylamino)phosphonium hexafluorophosphate
CDI	1,1'-carbonyldiimidazole
CMC	critical micelle concentration
CRP	C-reactive protein
CV	cyclic voltammetry
DC	direct current
DCC	1,3-dicyclohexylcarbodiimide
DCM	dichloromethane
DEC	1-(3-dimethylaminopropyl)-3-ethylcarbodiimide methiodide
DL	detection limit
DMF	dimethylformamide
ELISA	enzyme-linked immunosorbent assay
EQCM	electrochemical quartz crystal microbalance
FIA	flow-injection analysis
FPW	flexural plate wave
GC	gas chromatography
GPIB	general purpose interface bus
HDL	high density lipoprotein
HIV	human immunodeficiency virus
HPLC	high performance liquid chromatography
HSV	herpes simplex virus
Hz	hertz

IEEE	Institute of Electrical and Electronic Engineers
IgG	immunogamma globulin G
LDL	low density lipoprotein
LDLR	low density lipoprotein receptor
LPEIA	latex piezoelectric immunoassay
LPIA	latex photometric immunoassay
MHA	mercaptohexadecanoic acid
MHz	megahertz
min	minutes
mL	millilitre
mM	millimolar
MPA	mercaptopropionic acid
MS	mass spectrometry
MUA	11-mercaptoundecanoic acid
MW	molecular weight
n	number of crystal faces used for sensing
NADH	reduced nicotinamide adenine dinucleotide
PB	prussian blue
PBS	phosphate buffered saline
PEI	poly(ethyleneimine)
QCM	quartz crystal microbalance
RIA	radioimmunoassay
RSD	relative standard deviation
SA	succinic anhydride
SAW	surface acoustic wave
SCE	saturated calomel electrode
STM	scanning tunnelling microscopy
STW	surface tranverse wave
TEA	triethylamine
TLC	thin layer chromatography
TSM	thickness shear mode
TTL	transistor-transistor logic
UHV	ultrahigh vacuum
UPD	underpotential deposition
UV	ultraviolet
XPS	x-ray photoelectron spectroscopy
Δf	change in frequency, Hz
Δm/A	change in mass per unit area, g/cm^2
f_o	fundamental frequency of the crystal
µL	microlitre
µM	micromolar
μ_q	shear modulus of quartz, g cm^{-1} s^{-2}
ρ_q	density of quartz, g cm^{-3}
E_f	formal potential

1 The Thickness Shear Mode Acoustic Wave Sensor

1.1 Introduction

Chemical sensors, like all kinds of analytical instrumentation, produce a measurable electrical signal corresponding to an appropriate chemical sensing event. However in common usage, the term *chemical sensors* refers to a subset of instrumentation which is not defined so much by the method involved in probing the sample (e.g., spectroscopic, electrochemical) but by other criteria; chemical sensors are devices which are generally smaller, less expensive and more portable and amenable to *in situ* analyses than conventional instrumentation. The common classes of chemical sensors are mass (piezoelectric), thermal, electrochemical (amperometric, conductimetric and potentiometric) and optical (fibre optic) detection devices. As a recognized field within analytical chemistry, chemical sensors are routinely the subject of book reviews,[1,2] dedicated journals, fundamental research reviews within journals,[3] and specialized conferences.

If one could invent a "universal" sensor, one which could in theory detect any chemical species, then what would be the characteristics of such a sensor? Recognizing the fact that there are a huge number of molecules which cannot readily participate in optical or electrochemical processes, one could then conclude that a truly universal sensor would be one that responds to a property which all chemical species possess: *mass*. Thus, it comes as no surprise that piezoelectric mass sensors have been described in a tremendously diverse array of research journals, including journals specializing in corrosion processes, electroplating, clinical analysis, environmental monitoring, biotechnology, thin-film technology, and surface science, as well as analytical chemistry journals. In addition, mass-sensitive sensors are well suited to

monitoring not only chemical species themselves (both elemental and molecular), but also any imaginable chemical process in which two species join together or dissociate (at a surface). The cornucopia of applications for which mass-sensitive chemical sensors might be used to yield useful information is directly responsible for the significantly increased level of interest in these devices over the past decade. Much of this work is summarized is a number of important review papers.[4-12]

1.2 Operation of the TSM Acoustic Wave Sensor

Mass-sensitive chemical sensors operate via the propagation of acoustic waves through piezoelectric materials. The orientation of the piezoelectric material as well as the geometry of the metal transducers on its surface determine the type of acoustic wave generated. Thus, a variety of acoustic wave devices exist based on the type of wave involved: thickness-shear mode (TSM), surface acoustic wave (SAW), flexural plate wave (FPW) and acoustic plate mode (APM). Acoustic wave sensors also differ in the type of piezoelectric material used. While sensors have been described employing e.g. $LiTaO_3$[13] piezoelectric substrates, quartz is the most useful and widely-used of many piezoelectric materials due to its electrical, mechanical and chemical properties. Commercially-available quartz crystals are usually made from plates that were cut from a single crystal at specific angles to the principal optical axis. Quartz cut at an angle of +35°15' is referred to as AT-cut quartz and has the advantage of a negligible temperature coefficient. The remainder of this chapter will focus on the most common acoustic wave sensor, the TSM sensor based on AT-cut quartz crystal.

1.2.1 The Piezoelectric Effect

The property which enables a quartz crystal to resonate in an oscillator circuit is called the *piezoelectric effect*. This name is derived from the Greek word *piezin*, meaning "to press", and occurs in crystals which do not possess a center of symmetry. When pressure is applied to the crystal, the crystal lattice deforms and causes a separation of the centers of gravity of oppositely charged species. This in turn leads to a partial separation of electrical charge where equal, but opposite, charges build up on opposite crystal surfaces (Figure 1.1). If electrodes are applied to the faces of a

thin wafer of the crystal and an external ammeter is connected, a current will be seen to flow through the external circuit when stress is applied to the crystal. If the stress is released, a transient current flow occurs in the opposite direction.

The converse piezoelectric effect occurs when a potential is applied across a piezoelectric material and produces a stress in the material. If an alternating potential difference is applied, stable oscillations occur within the crystal lattice. Particle displacements at the crystal surface are parallel to the surface (in-plane) and transverse shear waves are generated that travel through the thickness of the crystal in a direction perpendicular to the surface. The thickness d of the crystal wafer determines the wavelengths λ of the fundamental (n = 1) and harmonic (n = 3, 5, 7...) resonances according to $\lambda = 2d/n$. Thus if the crystal is incorporated into the feedback loop of an oscillator circuit, it becomes the frequency determining element of the circuit. Over

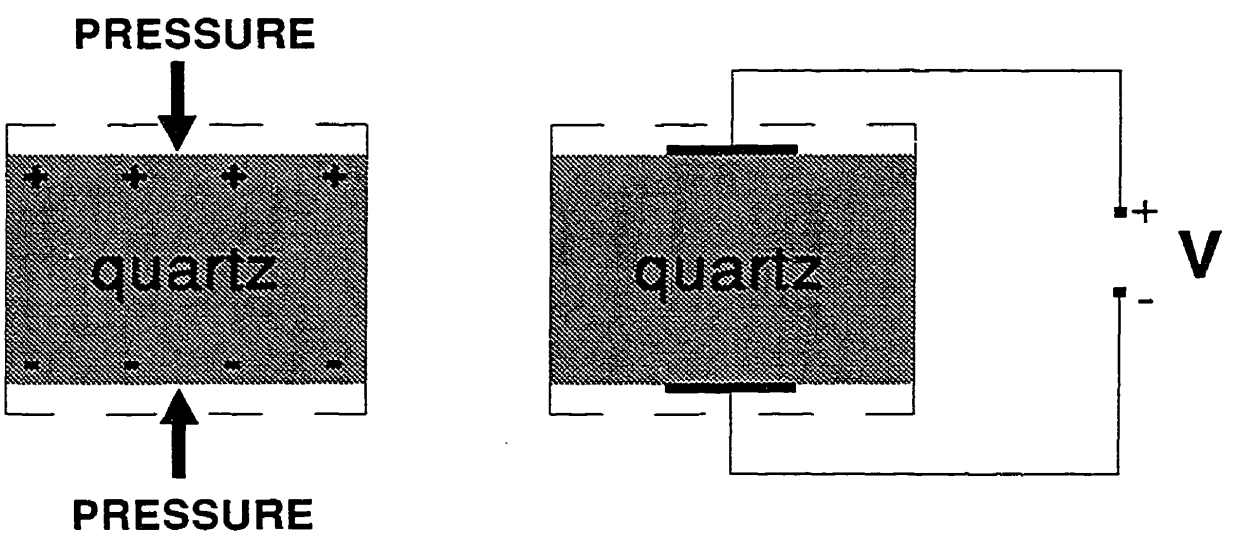

Figure 1.1 The piezoelectric effect (left) is the separation of charge induced by the application of an applied pressure. The converse piezoelectric effect (right) causes a deformation when a potential difference is applied across the substrate.

the past century, piezoelectricity has gone from a scientific curiosity to a widely exploited phenomenon with important applications in consumer goods (e.g. digital wrist-watches) and communications (e.g. radio), as well as chemical sensors.

1.2.2 Measurement Methods

There exist two types of methods to characterize a quartz crystal sensor electrically, which have been called the active and passive methods.[8] The most common method is the active method, also called the oscillator method, in which the crystal serves as the frequency-controlling element in a standard oscillator circuit as mentioned above. The parameter of interest, the resonant frequency of the crystal, is measured by a frequency counter. Although not always described in research reports, the most commonly reported circuit designs are based on the use of transistor-transistor logic (TTL) integrated circuit chips.[14-21] This may involve the use of two TTL inverters connected in series to give a noninverting amplifier (zero phase shift between input and output voltages) with the crystal connected from the output to the input of the amplifier to sustain positive feedback.[17-21] Other circuit designs have also been used, including a Colpitts oscillator,[22] and a Pierce-Miller oscillator.[23,24]

Automatic gain control (AGC) oscillators help to compensate for viscous energy loss when the crystal is exposed to a liquid. This loss results in a decrease in the oscillator loop gain and is compensated by using a feedback system to increase the gain of the driver circuit to maintain a constant oscillation amplitude. In addition to extending the operation of the oscillator to more viscous solutions, use of the AGC circuit allows the direct observation of the viscous loss through measurement of the AGC control circuit. The AGC circuit has been used by a few groups,[25-29] but is not strictly necessary for liquid-phase sensing since the simpler TTL oscillators are also able to function in liquids. An extensive discussion on the use of quartz crystals in oscillator circuits is available.[30]

In the passive method, a network or impedance analyzer is used to apply a sinusoidal voltage at various frequencies across the electrode terminals of the quartz crystal. This method has been used by several workers[31-39] and is mentioned here for the sake of completeness, although it is much less commonly employed than the

oscillator method. Network analyzers obviate the need for oscillator circuitry and allow the mechanical properties of the quartz crystal to be surmised from the electrical characteristics measured with the analyzer, using the Butterworth-van Dyke equivalent circuit model (Figure 1.2). The equivalent circuit has been derived by both Bottom[30] and Cady.[40]

In Fig. 1.2, the m subscripts (for motional) denote elements associated with the large amplitude vibrational motion caused by the piezoelectric effect. The inductance is related to the inertial energy storage in the crystal, the capacitance to the elastic energy storage and the resistance to various energy dissipating processes. The o subscript capacitance is that of the two parallel electrodes plated on the quartz surfaces. The contribution of each element varies with the frequency. When operated far off resonance, the circuit is simply the capacitor C_o, but at the precise resonant frequency the circuit becomes a resistor and capacitor in parallel. Sinusoidal voltages incident on and reflected from the quartz crystal are repeatedly measured for a wide range of frequencies near the resonant frequency. The use of the network analyzer allows not only measurement of the series resonant frequency (as in the oscillator

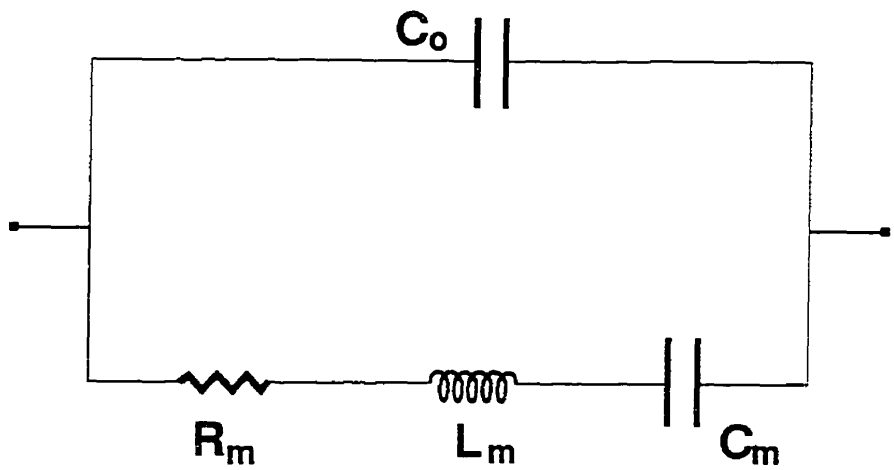

Figure 1.2 Equivalent circuit of an AT-cut quartz crystal (Butterworth-van Dyke model).

method) but also the parallel resonant frequency and the magnitude and phase angle of the impedance as a function of frequency. Plots of R_m or C_o vs. time can be made for analytical sensing processes, in addition to the standard frequency vs. time plots obtained with the oscillator method.[31]

The circuit shown in Fig. 1.2 is the electrical model of the crystal in a gas or vacuum, but it is not a good model of the crystal in liquid media. When the crystal is immersed in a liquid, energy is lost by means of propagation of acoustic waves into the liquid. The extent of this loss is dependant on the properties of the sensor-liquid interface and the bulk properties of the liquid, which are not included in the model. Alternative equivalent circuit models with additional components have been proposed to model the quartz crystal in a liquid.[36,39]

1.2.3 The Experimental System

A number of components are involved in performing a TSM acoustic wave sensor experiment. At a minimum, these include the sensor crystal (with or without a chemically selective coating), the oscillator circuit and a frequency counter (for the oscillator method). Additional equipment may include crystal housing units and structures for reducing noise levels in the system.

The sensor crystals are typically thin, circular wafers of quartz about 1.5 cm in diameter with thin metal films, which serve as electrodes, deposited on both faces (Figure 1.3). Gold is the most common electrode material used, although other metals can be used including aluminum, copper and silver. The choice of electrode material may be influenced by its known adhesion to the coating of interest. Each electrode has the pattern of a small circle in the centre of the wafer, with a flag portion extending to opposite edges which allows for electrical connection to the circuit. The central electrodes usually overlap each other, and the acoustic waves generated through the piezoelectric effect propagate only through this overlapping electroded region. Crystals with fundamental resonant frequencies of 5-10 MHz are most commonly used.

The oscillator circuit has already been discussed in the previous section. In addition, the circuit often has components which provide a difference frequency between the experimental crystal and a second reference crystal, which improves the

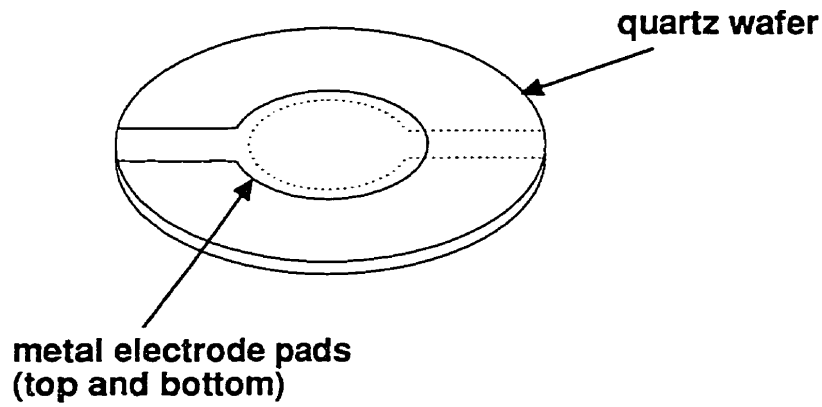

Figure 1.3 Quartz crystal wafer showing electrode geometry.

frequency stability of the overall system. In both gas- and liquid-phase TSM sensor work the reference crystal is usually operated in air. For the liquid phase a dual-QCM design has also been reported with both working and reference crystals having one face exposed to liquid, for improved frequency difference accuracy in studies in which variations in solution viscosity, density or conductivity occur.[41] Crystal oscillator circuits are relatively simple and inexpensive to fabricate, and are suitable for field instruments.

Also necessary in the oscillator method is a DC power supply to power the circuit, which may be provided by simple alkaline batteries, and a frequency counter to provide a digital readout of the resonant frequency signal (Fig. 1.4). The frequency counter, which is the most expensive component in the experimental system, should have a resolution of at least 1 Hz (0.1 Hz is preferred). A computer may also be interfaced to the counter (e.g., via a IEEE-488 or GPIB bus) for facilitated data acquisition. Alternatively, a frequency-to-voltage circuit may be employed for readout of the frequency signal on a strip-chart recorder (this is often an option at the back of commercial frequency counters as well).

The most variable feature in the experimental system is the housing apparatus which surrounds the experimental crystal. The purpose of the crystal housing is generally to reduce the noise or drift in the system and/or to present the crystal to a gaseous or liquid environment in a desired manner. Noise reduction is sometimes attempted through the use of Faraday cages (which reduce electromagnetic interference) or constant-temperature chambers (which reduce drift due to temperature fluctuations). Gas manifolds with dilution/mixing valves and reference paths are employed for gas-phase TSM sensor work. Such systems are often operated under computer control. For liquid-phase experiments, the crystal is usually housed in a material such as Plexiglas which has been machined to allow for the crystal to be sealed in with o-rings. This arrangement allows only one of the two crystal electrodes to be presented to the liquid, which is necessary when real-time frequency monitoring

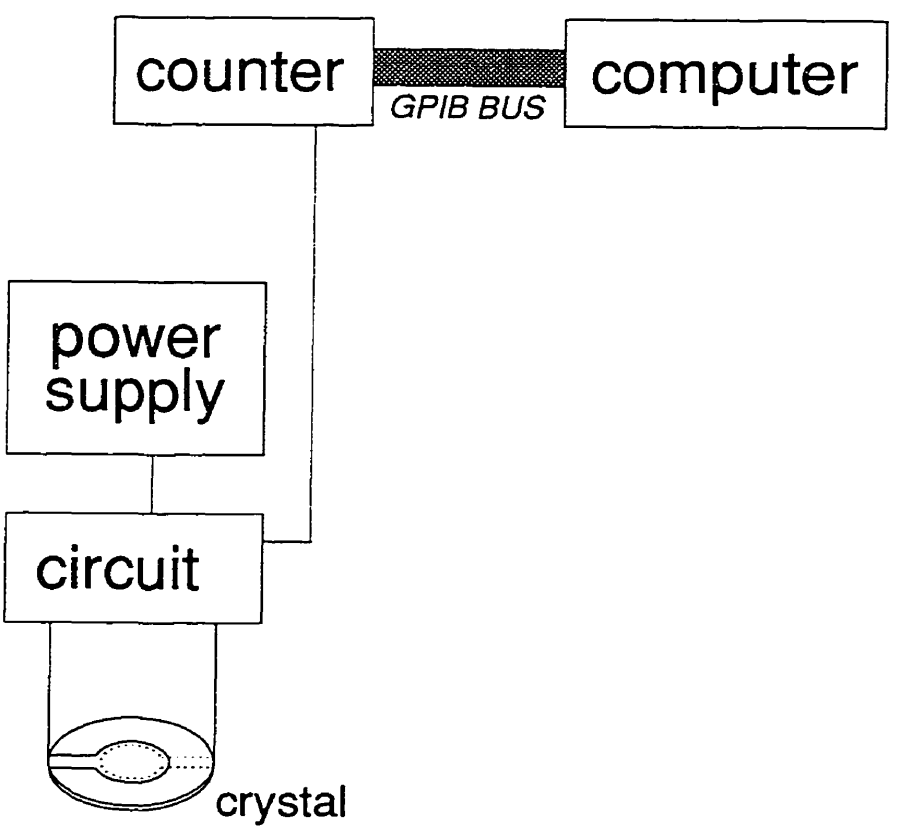

Figure 1.4 TSM sensor experiment instrumentation.

in highly conductive (e.g. buffered) solutions is desired (exposing both electrodes to conductive solution can result in frequency instability or complete loss of crystal oscillation due to short-circuiting). Additional liquid reservoirs and tubing may also be present for flow-through (e.g. flow-injection analysis) experiments.

1.2.4 Factors Influencing the Frequency Response

It is known that by adding mass to the surface of a piezoelectric crystal one obtains a lower oscillation frequency; indeed, this effect has long been used by crystal manufacturers to adjust a crystal to a desired frequency. The first quantitative investigation of this effect was made by Sauerbrey[42] who derived the following expression which relates the change in frequency (Δf, Hz) to the change in mass per unit area (Δm/A, g/cm^2) for a piezoelectric quartz crystal oscillating in air or vacuum:

$$\Delta f = - \frac{2nf_o^2 \Delta m}{A\sqrt{\varrho_q \mu_q}} \qquad (1.1)$$

Here, n is the number of crystal faces used for sensing (1 or 2), f_o is the fundamental frequency of the crystal, μ_q is the shear modulus of quartz (2.947 x 10^{11} g cm^{-1} s^{-2}) and ρ_q is the density of quartz (2.648 g cm^{-3}). Hence Δf is linearly related to Δm and this simple relationship has served as the basis for the mass-sensing capability of the QCM. The term "microbalance" is here seen to be entirely justified; for a 5-MHz crystal, according to eqn. 1-1, a decrease in frequency of 1 Hz is produced by an added mass of 18 ng/cm^2 (n=1). For a 10-MHz crystal, Δm/A = 4.4 ng/cm^2.

It is now well recognized that simple mass loading is not the only mechanism of sensor response, although conceptually it is the simplest response mechanism and the Sauerbrey equation has therefore been a useful benchmark for quantitative or semi-quantitative work. A more accurate description is that the resonant frequency depends on the mechanical impedance of the overall system through which the shear waves propagate and therefore on its viscoelastic properties.[8,21,43,44] The analytical frequency response in a particular sensing application is not always modelled by an

equation; however when it is, the Sauerbrey equation is generally a good model of the frequency response when the frequency is measured with the crystal in air or vacuum and the added mass is thin and rigidly attached. However in liquid-phase applications, where the crystal has one or both faces immersed in an aqueous or non-aqueous liquid, the frequency shift arises from coupling the oscillation of the crystal, involving a standing shear wave, with a damped propagation shear wave in the liquid.[8,45] This shear wave propagates from the crystal electrode into the adjacent liquid with a characteristic decay length (Figure 1.5).

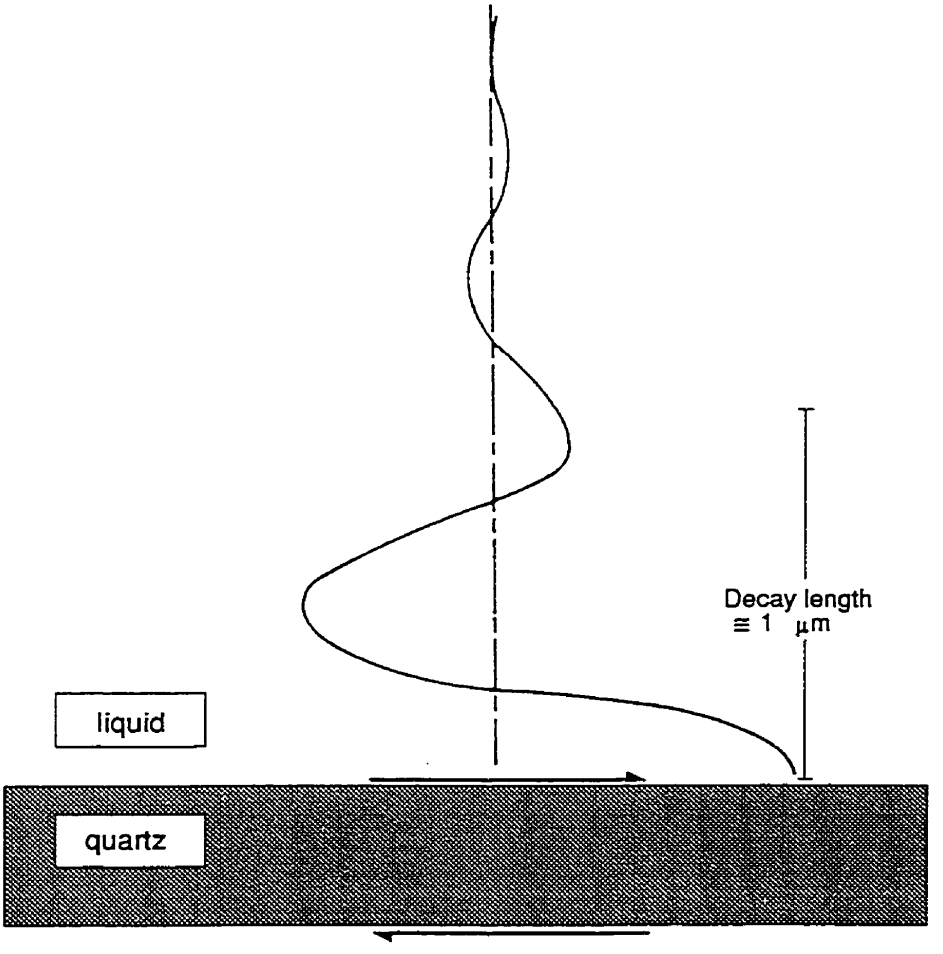

Figure 1.5 Propagation of the transverse shear wave from the TSM sensor into a liquid.

The dependence of the oscillation frequency on the viscosity of the adjacent medium has been conveniently demonstrated by observing the changes in frequency when the crystal is sequentially exposed to various liquids of differing viscosity.[18,19,21,37,39,46,47,50] Several mathematical models have been proposed to describe the liquid phase behaviour of the TSM sensor,[18,19,29,37,45,46,48-52] all of which include constants for the density and/or viscosity of the adjacent liquid.

1.2.5 Signal-to-Noise

In analytical applications, optimization of the signal-to-noise ratio (S/N) is an important goal. Evidently, this involves separate strategies for increasing the signal as well as decreasing the noise, and the successful application of such strategies may often require considerable ingenuity and creative thinking. The extent of application of such strategies in turn depends on the desired detection limits and the expected analyte concentrations in the sample of interest. For the TSM sensor there are a number of known, fundamental factors which directly impact on the S/N and should be considered in attempts to improve the S/N.

According to the Sauerbrey equation, the frequency signal can be increased by using two sides vs. one and especially by using crystals with a higher resonant frequency. In gas-phase work both sides of the crystal are generally used; however in liquid-phase work involving an aqueous system, only one side of the crystal is usually used, since exposing both electrodes can cause the crystal to cease oscillating due to short-circuiting. Since $\Delta f \propto f_o^2$, increasing the crystal resonant frequency can produce a considerable improvement in sensor response. Relatively little comparative work has been done comparing different crystals of different resonant frequency in TSM devices, although high sensitivities have been reported for 30-MHz crystals.[35,53] The frequency response will also be enhanced in applications where the analyte has a favorable geometry for achieving a high mass loading per unit area, or is capable of inducing a large change in the viscoelastic properties of a thin film which is initially coated on the crystal electrode. The most commonly-used means of improving the S/N are by reducing the noise. Two types of noise are generally applicable - random, short-term noise and longer-term frequency drift, both of which can be reduced by the

use of additional apparatus mentioned previously (eg. Faraday cages, constant-temperature chambers).

Since the limit of detection of a method is often defined as the analyte concentration that produces a signal three times larger than the noise, improving the S/N of the method directly improves detection limit. Many devices can be configured as sensors with noise levels of 1 Hz or less, meaning that a signal of only 3 Hz could be resolved, in principle. The real concern however is whether such a small signal has analytical significance. For example, in a typical liquid-phase analysis, one crystal electrode with a particular coating may be exposed to a buffered solution containing analyte and other molecular species, and the mass-attachment mechanism may require up to an hour or more. A number of influences could produce small shifts in frequency, including: uncompensated changes in temperature, humidity, solution viscosity, circuit ground or the electromagnetic environment; loss of coating material; and adsorption of buffer or other matrix species (all in addition to analyte adsorption). Additional factors which are perhaps even more elusive may also be in operation, such as loss of electrode material (e.g., if the electrode had just been cleaned prior to the experiment) or rust formation at electrode flag-clip-connector interfaces in aqueous solutions.

All of these considerations make it clear that device engineering to reduce noise is useful only up to a certain point. Every sensing application has its own unique environment and set of frequency-influencing factors, and for accurate results it is imperative that control experiments are performed which are identical in every way to the actual analyte-sensing experiment except for the presence of analyte. Such control experiments then provide a measure of the true noise in the analytical measurement and not simply a measure of the noise of the device itself.

1.3 Research

1.3.1 Evolution of TSM Acoustic Wave Sensor Research

The piezoelectric effect was first postulated in 1885 by Rayleigh, and quartz was first used in an oscillator circuit in 1920. Soon after Sauerbrey's important work

in the late 1950's, sensing applications based on the mass-frequency relationship of the TSM sensor began to appear. Up until the early 1980's this work was limited strictly to gas-phase analysis, with frequency measurements taken with the crystal oscillating in air. Since about 1985 there has been an explosive growth in the number of research reports on TSM sensing applications, the vast majority of which involve liquid-phase work where the mass-attachment process occurs in liquid (usually aqueous) media. A number of fields of research may be identified, and are briefly presented below. This presentation is by no means exhaustive, and is intended only to give a sampling of the wide range of applications for which the TSM sensor is suited.

1.3.2 Detectors for Chromatography

King,[54] in 1964, in generally credited with the first analytical application using a piezoelectric crystal. He coated 9-MHz AT-cut crystals with gas chromatography (GC) stationary phase materials such as squalene, and used the crystal as a GC "sorption" detector. Separation of components was achieved in the usual fashion, but detection was based on the vapor-phase components adsorbing and desorbing from (partitioning with) the coating (Figure 1.6). King observed that the detectors were rugged, fast, and exhibited increasing sensitivity with increasing solute molecular weight. In addition, linear responses were obtained and the nature of the signal (i.e., a frequency, read with a digital counter) facilitated readout and peak integration. Gas chromatography detectors based on the partitioning of a component between the carrier gas and a stationary-phase coating applied to a piezoelectric quartz crystal have also been investigated by other researchers. Karasek contributed several papers,[55-57] which included the development of a portable room-temperature GC, and reported that the instrument response was rapid and proportional to the sample size, with a sensitivity in the ppm concentration range. Karasek pointed out that while an adequate component vapor pressure is a requisite for GC, the QCM sensitivity increases as component vapor pressure decreases; thus this trade-off requirement defines the useful range of component volatility over which the QCM detector can be used with adequate sensitivity. Edmonds and West[58] also developed a GC detector for n-alkanes

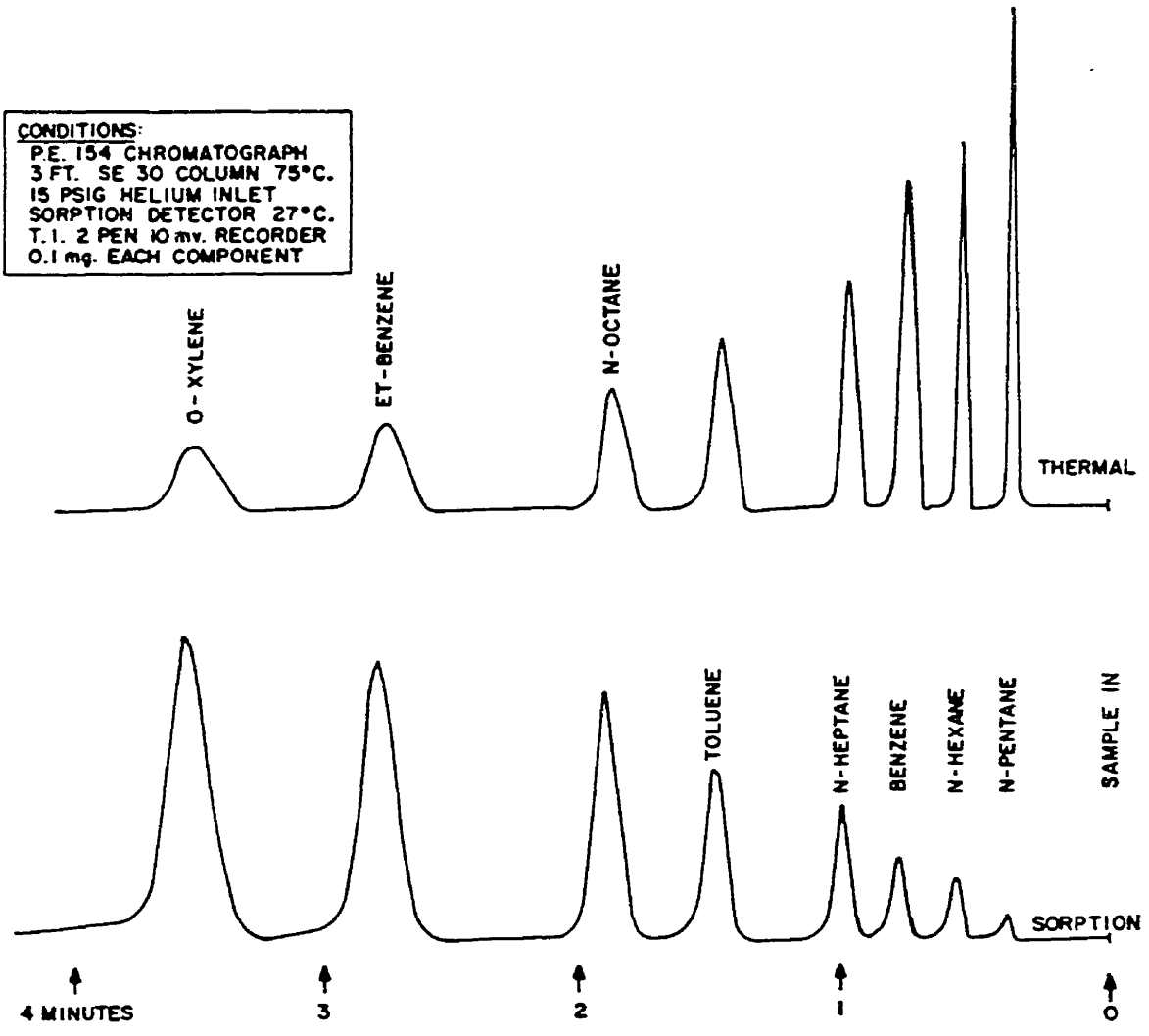

Figure 1.6 Comparison of chromatograms using a traditional thermal detector (top) and piezoelectric crystal detector (bottom) by King.[54]

and chloroform. Rajakovic *et al.*[59] described a gas detector using coatings of valproic acid antiserum and parathion antibody, with nitrogen carrier gas for the detection of toluene, valproic acid, o-nitrotoluene and parathion, as well as a number of other pesticides. They reported good detection limits (10 ng/L), but that the antibody-coated crystal was not selective to the corresponding antigen. They concluded that the responses were associated with conventional chemisorption on the surface of protein particles, and confirmed this by denaturing the antibody at an elevated temperature.

Crystal detectors for liquid chromatography have also been employed. The idea was first suggested by Shulz and King in 1973,[60] although their design was not a true *in situ* one since the effluent was simply sprayed onto the crystal surface. The solvent

evaporated and the mass of any residual solute was determined from the change in oscillation frequency; a complete cycle took 60 s. The results obtained compared favorably with those from a refractive index detector, and better base-line return was claimed for the crystal. The first genuine flow-through design was reported by Konash and Bastiaans,[61] in which the liquid eluent came in contact with only one face of the crystal. Although stable and mass sensitive detection was achieved, the system suffered from poor reproducibility. Since then there have only been a few reports on the use of TSM sensor crystals as liquid chromatographic detectors.[62,63]

1.3.3 Gas Detection

Detection of compounds in the gaseous state dominated TSM sensor research efforts in the 1970's and early 1980's. Since about 1985 the field became overwhelmingly focused on liquid-phase sensing, a trend which has continued to the present day. While this shift is partly explained by the fact that liquid-phase sensing was not even demonstrated as feasible until the early 1980's, and hence a whole new range of potential applications was opened up for exploration, the shift in focus is also explained by the fact that a great number of gas-phase sensing reports had already been published by this time and the field of gas-phase sensing was already mature. After his GC detector work, King[64-66] continued to be one of the early proponents of the use of piezoelectric crystals as sorption detectors in which the crystal is coated with a substrate that will react with or adsorb the material of interest. A typical gas-phase sensing apparatus is depicted in Figure 1.7.

Guilbault and co-workers[67] were able to detect nitrogen dioxide and ammonia in the ppb range using coatings of modified Ucon 75-H-90000 or Ucon LB-300X. Guilbault and Hlavay[68] later developed an even more sensitive (parts per trillion) ammonia detector using coatings of L-glutamic acid hydrochloride and pyridoxine hydrochloride. A sensor for ammonia and alkylamines based on a zinc phosphonate coating has also been reported.[69] Guilbault and coworkers also developed selective detectors for toluene[70] and other aromatic hydrocarbons[71] such as xylenes, benzaldehyde, anisole and butylbenzene. Other detectors have been developed for: anaesthetic gases (nitrous oxide, halothane and enflurane),[72] carbon dioxide,[16,73] carbon

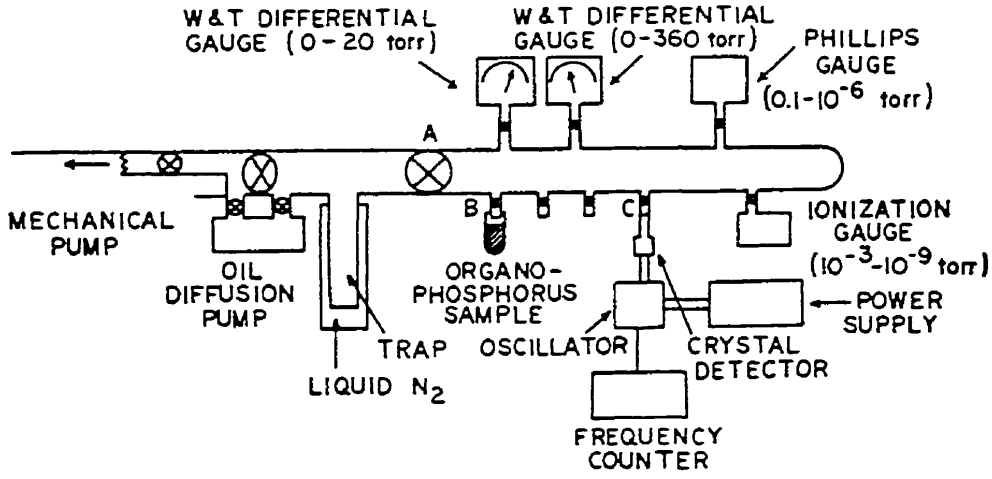

Figure 1.7 Apparatus used for gas-phase detection of organophosphorus compounds and pesticides.[90]

monoxide,[74] hydrogen,[75] hydrogen chloride,[76] hydrogen cyanide,[77] hydrogen sulphide,[78,79] mercury,[80-85] methane and other hydrocarbons,[86] methanol vapor,[87] nitrogen dioxide[16] organophosphorus compounds,[88-94] sulphur dioxide,[95-104] toluene diisocyanate,[105-106] formaldehyde,[107] and water vapor.[108-110]

In some cases the analyte is in solution but a vapor is produced by sweeping a carrier gas through the solution. This approach was used to detect parathion with TSM sensor crystals coated with antibodies against parathion.[111] If necessary, additional reagents can be added to the solution to increase volatilization, such as the addition of tin(II) chloride to reduce mercury species in a water sample and allow production of mercury vapor which is then detected by an uncoated TSM sensor crystal with gold electrodes.[112] In both of these examples, the gaseous sample is passed through a drying tube to minimize frequency changes due to moisture adsorption.

Application of coatings to the crystal can be accomplished by several methods. One method involves simply dipping the crystal in an appropriate solution for a

specified period of time followed by rinsing. Alternatively, a syringe can be used to directly deposit a coating on the crystal electrodes. More elaborate approaches involve the use of plasma-deposition techniques in which coating precursor vapors such as ethylenediamine and 4-vinylpyridine[113] are allowed to react with reactive species produced by a plasma glow discharge to initiate polymerization and coating deposition on the sensor surface. Copper phthalocyanine has also been plasma-polymerized onto TSM crystals to form highly stable coatings which had a lifetime as long as 60 days.[114] Regardless of the method of application, the properties of an ideal sensor coating include ease of application, stability (long life-time), selectivity towards the analyte, the ability to regenerate the coating for repeated usage, and quick response time. Sensor applications where the coating material exhibits all of these properties are rare; in particular, poor selectivity and limited ease of coating regeneration are often reported. These limitations have been discussed in two reviews on gas-phase sensing using piezoelectric crystals.[115,116]

1.3.4 Electrogravimetric Analysis

Electrochemistry deals with charge-transfer reactions that occur at an electrode in solution. Such reactions are often greatly affected by the character of the electrode-solution interface. In order to advance the understanding of heterogeneous electron transfer, electrochemists attempt to couple surface-sensitive probes to conventional electrochemical experiments. Probes that can be used in solution, as charge transfer proceeds, are especially useful. The TSM sensor is one such probe which has been successfully used in electrochemical research to investigate many electrochemical processes.

The earliest use of AT-cut crystals in electrochemical measurements were in 1969 by Mieure and Jones,[117,118] who used the crystal as the cathode in an electrochemical cell to examine cadmium solutions over the range 5×10^{-4} to 5×10^{-8} M. A current was allowed to pass for a known period of time and the crystal was removed from the cell, washed and dried. The mass increase was then determined from the frequency change. These *ex situ* studies are in contrast to those that were predominant starting in the 1980's, with one side of the crystal exposed to liquid and

functioning simultaneously as a working electrode and a mass sensor in a configuration commonly referred to as the electrochemical quartz crystal microbalance (EQCM).

The EQCM has been used in a number of studies to investigate electrochemical processes occurring at an uncoated electrode. One such example is the measurement of the deposition of metal atom monolayers onto electrode surfaces. When a metal is reduced onto a different metal surface, it is often found that the first monolayer deposits at potentials more positive than the predicted Nernstian potential for bulk deposition. Referred to as underpotential deposition (UPD), this process is a simple way to create a single atomic layer of a metal. Figure 1.8 shows one example of UPD, that of Pb on the gold electrode of a TSM sensor crystal with one face only exposed

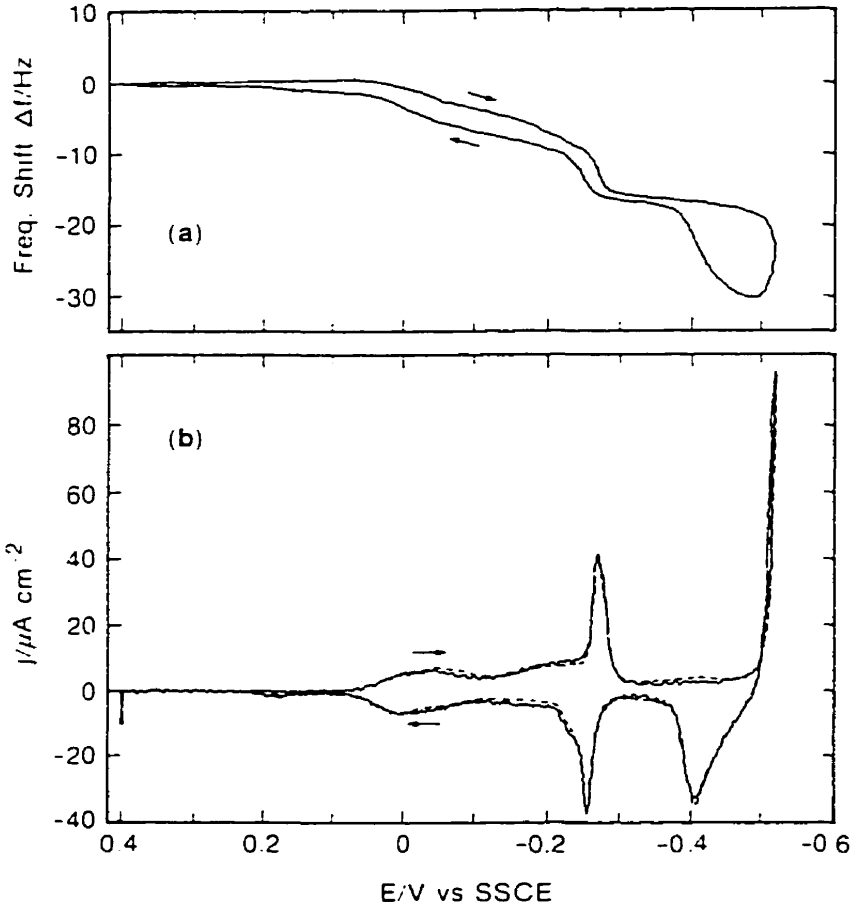

Figure 1.8 UPD of Pb (1.0 mM in 0.1 M $HClO_4$) on Au at 10 mV/s, average of 20 scans, followed by the EQCM method (a) and cyclic voltammetry (b).[119]

to the solution.[119] In (b), the peaks in the negative going scan which occur before the bulk deposition at -0.5 V vs. SCE are due to deposition of submonolayer amounts of Pb. The different peaks are attributed to either changes in the packing of lead atoms on the surface, or varying crystal structure on the gold surface. On the return scan, bulk Pb is oxidized off the surface followed by the oxidative removal of the UPD layer. Each current peak in the CV is mirrored by a frequency shift in the frequency-potential plot (a), and the mass returns to the initial value at the end of the potential cycle. In this example the frequency change during UPD was 18.0 Hz or 0.32 $\mu g/cm^2$ (using the Sauerbrey equation) or 1.5 $nmol/cm^2$, and is the coverage expected for a hexagonal close-packed layer of Pb on Au. When the mass coverage data are plotted against the integrated current, the electrosorption valency for Pb is found to be 2.0 and is approximately independent of potential. The authors thus concluded that the EQCM responded to changes in interfacial mass as predicted by the Sauerbrey equation. Underpotential deposition processes followed by the EQCM have also been the subject of other papers.[120-123] Other EQCM applications with uncoated electrodes have examined growth or dissolution of thin metal films on electrode surfaces,[22,23,124-126] observation of morphological redox relaxation of Cu and Ag electrodes,[127] investigation of the mechanism of gold oxidation,[128] electrosorption of monolayers of Br^- and I^- on an electrode surface,[129] and determination of iodide in solution.[19,130]

Figure 1.9 demonstrates the use of a coating with the EQCM for the detection of cations in a flow-injection analysis (FIA) mode.[131] One face of a crystal was coated with a film of Prussian Blue (PB), an electroactive ion exchanger, and exposed to solution. 0.005 M K^+ was injected into a stream of 0.01 M HNO_3 flowing across the crystal, and the current (a) and frequency (b) were measured vs. time with the potential held at 0.1 V (solid line) or 0.5 V (dashed line) vs. SCE. The current-time plot reflects the change in the formal potential, E_f, which occurs when K^+ replaces H^+ in the film; since the film is held at a potential (0.1 V) near its E_f, the slight change in E_f caused by the replacement of H^+ by K^+ results in a cathodic current, and when the K^+ leaves the film an anodic current is observed. The lower plot shows that the frequency changes mirror the current response and demonstrates the utility of the QCM to follow such events. No redox event occurs at 0.5 V vs. SCE since this is too

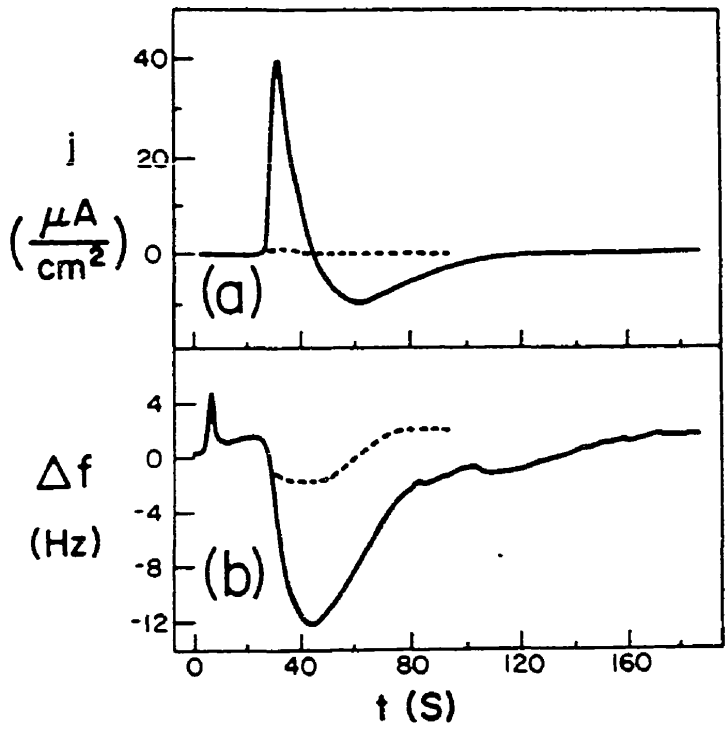

Figure 1.9 Response of Prussian Blue-coated TSM sensor crystal to the flow injection of 0.005 M K^+ and 0.005 M H^+ in a stream of 0.01 M HNO_3: (a) current, (b) frequency change. The applied potential was (solid) 0.1 V and (dashed) 0.5 V vs. SCE.[131]

far removed from the film's E_f. Regarding the use of coatings in the design of a QCM-based detector, the authors note that an electroinactive polymer can change mass only through ion exchange between the polymer and solution, and that no change in redox state is possible with an electroinactive film. As such, for films with approximately the same density of ion-exchange sites, electroactive films held near their E_f will prove to be much more sensitive. The authors also demonstrated the utility of the PB-QCM to detect several other cations by FIA: NH_4^+, Na^+, Ca^{2+} and Ba^{2+}. Other coated EQCM applications have examined ion, solvent, or redox couple transport accompanying redox processes occurring in thin films of inorganic polymers,[25,132-134] organic redox polymers,[135-136] and conducting polymers,[137] and other films.[138-140] Potentiodynamic investigations of the growth or dissolution of thin polymer films such as polypyrrole,[141] diheptylviologen bromide[142] polyvinylferrocene,[135] and

polyaniline,[137,143] as well as long chain alkyl thiol monolayers[144] on TSM sensor electrode surfaces have also been conducted.

Evidently the electrochemical quartz crystal microbalance technique, which utilizes an AT-cut TSM sensor crystal, is well suited not only to purely analytical applications but also to a wide variety of fundamental electrochemical investigations. A review of this area has been published by Deakin and Buttry.[11]

1.3.5 Biosensors

Biosensors are detection devices which combine biologically active sensing materials with transducers. In these devices, the biological system provides the requisite selectivity and sensitivity for the target substrate while the transducer generates a detectable signal for data collection and processing. The biological components of biosensors can include antibodies, antigens, enzymes, nucleic acid, whole cells, plant slices, and receptors. Among chemical sensors, biosensors have been paid an especially high level of attention due to the large potential markets which exist in both clinical and non-clinical settings and the surge of interest in chemical processing using biomaterials and the consequent needs for real-time sensing of biomolecules for use in production control systems. The direct detection of such analytical pairs is also an attractive prospect for alternatives to existing, indirect procedures. Not surprisingly, the appropriate possibilities for TSM acoustic wave sensors in this area have been explored.

Several techniques have been employed for immobilization of biosensor coatings on the crystal electrode surface. These may be grouped into the following categories. (i) The coating is adsorbed directly onto the metal electrode surface. (ii) The crystal is precoated with a thin layer capable of direct hydrophobic and/or covalent bond formation with the biomaterial. These materials may include nyebar C, 3-aminopropyltriethoxysilane, protein A, polyethyleneimine, poly(butylmethacrylate), poly(2-hydroxy-3-dimethylamine-1,4-butane), polyacrylamide, avidin, streptavidin and biotin. (iii) The crystal is precoated as in (ii) and a coupling agent such as glutaraldehyde is used to couple the biomolecule to the surface. (iv) The selective coating material is immobilized via entrapment within a lightly crosslinked

poly(acrylamide) gel. (v) The coating is immobilized by irradiation.

Figure 1.10 shows a typical experimental setup for a liquid-phase TSM biosensing application.[145] Both the oscillator circuit and the crystal were placed in a chamber to protect the frequency measurements against thermal, mechanical and electrical influences. The crystal was secured in a housing apparatus such that only one face was exposed to solution. The following steps were then employed for the detection of anti-human immunodeficiency virus (HIV) antibodies: the gold electrode was cleaned with chloroform; 50 µL of phosphate-buffered synthetic HIV peptide was deposited onto the electrode and allowed to incubate for 18 h at 37 °C; the crystal was cleaned with PBS-Tween; remaining unspecific binding sites were saturated with gelatine followed by rinsing with PBS-Tween; the reaction vessel was filled with 5 mL PBS; the frequency was allowed to stabilize; and then 5 µL of anti-HIV antibody

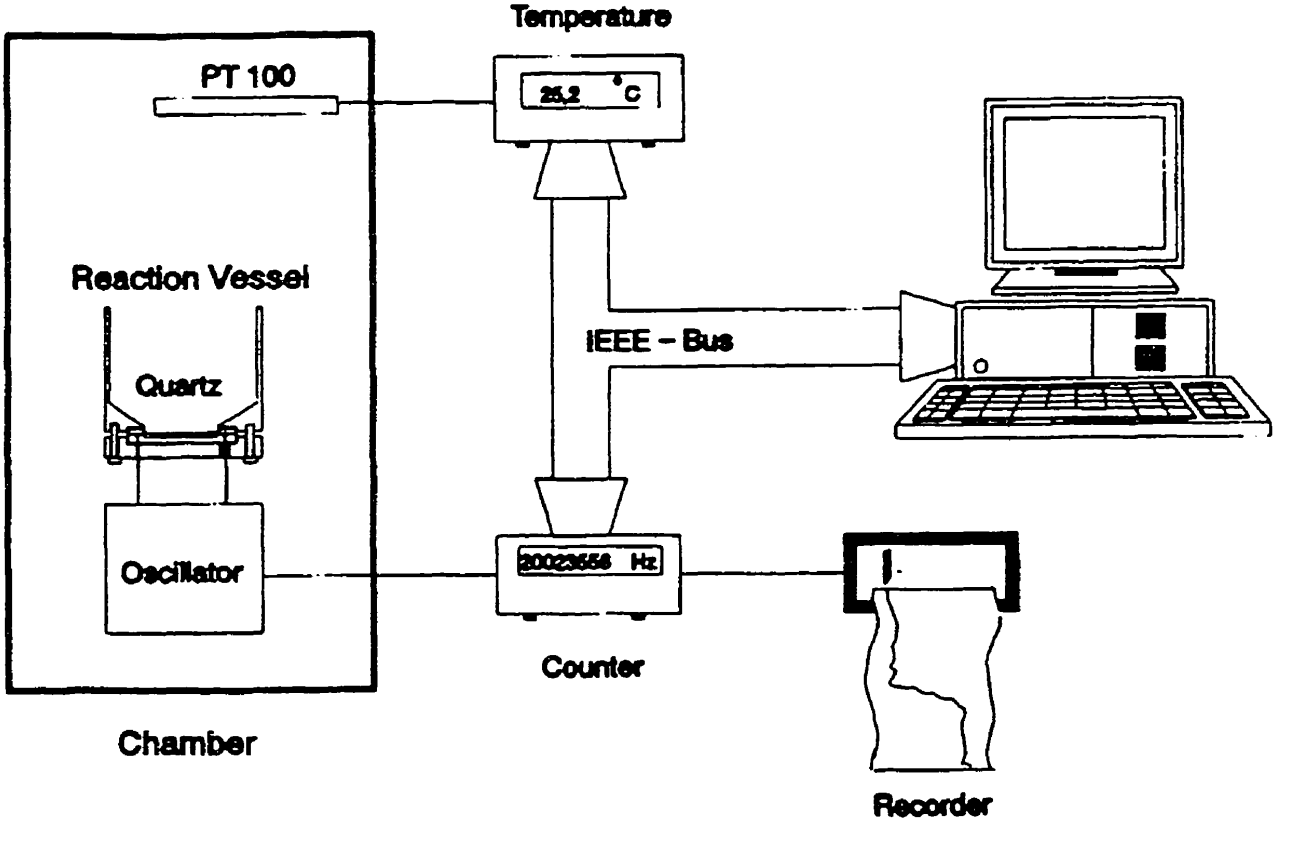

Figure 1.10 Experimental setup for liquid-phase TSM biosensor experiment.[145]

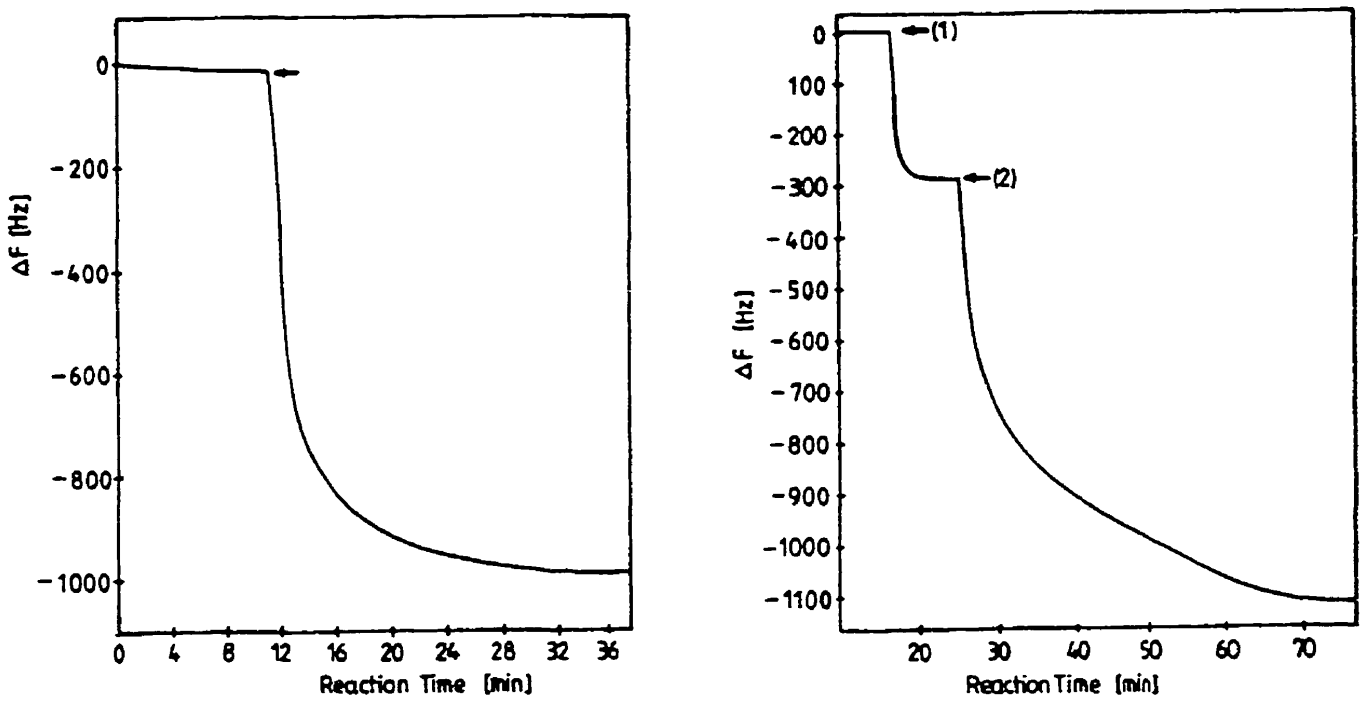

Figure 1.11 Response for the reaction of anti-HIV antibody with the adsorbed HIV peptide (left). Response for the unspecific adsorption of anti-EBV antibody to HIV peptide covered quartz (1) and the specific reaction of anti-HIV antibody (2) (right).[145]

in PBS was added. This sequence of steps is illustrative of those commonly required in a liquid-phase TSM sensor experiment involving a coating. Frequency changes associated with addition of the antibody are shown in Figure 1.11, where it is seen that the analytical signal involves an initial rapid change followed by a slower approach to an equilibrium response. This is a common response curve in liquid-phase TSM sensor experiments. Another common feature is shown in (b) in Fig. 1.11 - that of non-specific adsorption, in this case of a different antibody to the HIV peptide coating. This demonstrates the importance of investigating the influence of non-specific adsorption on the frequency response, even when supposedly "specific" antigen-antibody couples are involved, for proper evaluation of the analytical signal. As described in section 1.2.5, proper controls are essential in TSM sensor experiments.

Many other TSM immunosensors have also been developed. Detection of human transferrin,[146] human albumin,[147,148] *Salmonella typhimurium*,[149] *Candida albicans*,[150] immuno gamma globulins (IgG),[151] atrazine herbicides,[152] Herpes viruses[153] and several viruses and bacteria related to acute diarrhea[154] has been accomplished by first immobilizing the respective corresponding antibody on the sensor crystal. Plomer et al.[155] reported the use of an anti-enterobacterial antibody coating enabling the detection of the class of bacteria which possess the enterobacterial common antigen - including *Salmonella*, *Citrobacter* and *E. Coli*. Alternatively, the antigen can serve as the coating, such as in the detection of monoclonal antibodies Mab anti-2,4-D with immobilized pesticide 2,4-D.[156] This scheme could then be used for a competitive immunoassay for 2,4-D in tap water. IgG immunoglobulins have been immobilized via protein A on gold and used to monitor the kinetics of immunoreaction with sheep antihuman IgG antibody.[157] Sensor reversibility was also achieved, not by antibody-antigen dissociation but by the complete dissociation of the entire immunocomplex from the protein A coating using sodium acetate buffer pH 3.

A novel approach was reported by Ebersole and Ward[158] for the detection of adenosine 5'-phosphosulfate (APS) reductase. APS reductase detection was accomplished by binding APS reductase to an anti-APS reductase antibody immobilized on the crystal surface, followed by addition of anti-APS-alkaline phosphatase reductase conjugate and subsequent exposure of this bound sandwich complex to 5-bromo-4-chloro-3-indolyl phosphate (BCIP) which resulted in enzymatically amplified deposition of the oxidized dimer of BCIP on the sensor crystal (Figure 1.12). The enzymatic amplification resulted in a significant enhancement of the detection limit, down to levels of ca. 5 ng/mL (10^{-14} M), whereas direct binding of APS reductase at even more elevated concentrations could not be detected. Ebersole *et al.*[159] also used the BCIP enzymatic amplification method in another report. An avidin coating was used to bind biotin-alkaline phosphatase conjugate, which in turn was used for the enzymatic hydrolysis of BCIP and deposition of the insoluble dimer product. In the same paper, they further extended the ingenuity of the system by exposing a streptavidin-coated crystal to a solution of biotin and alkaline-phosphatase, both of which had previously been linked to

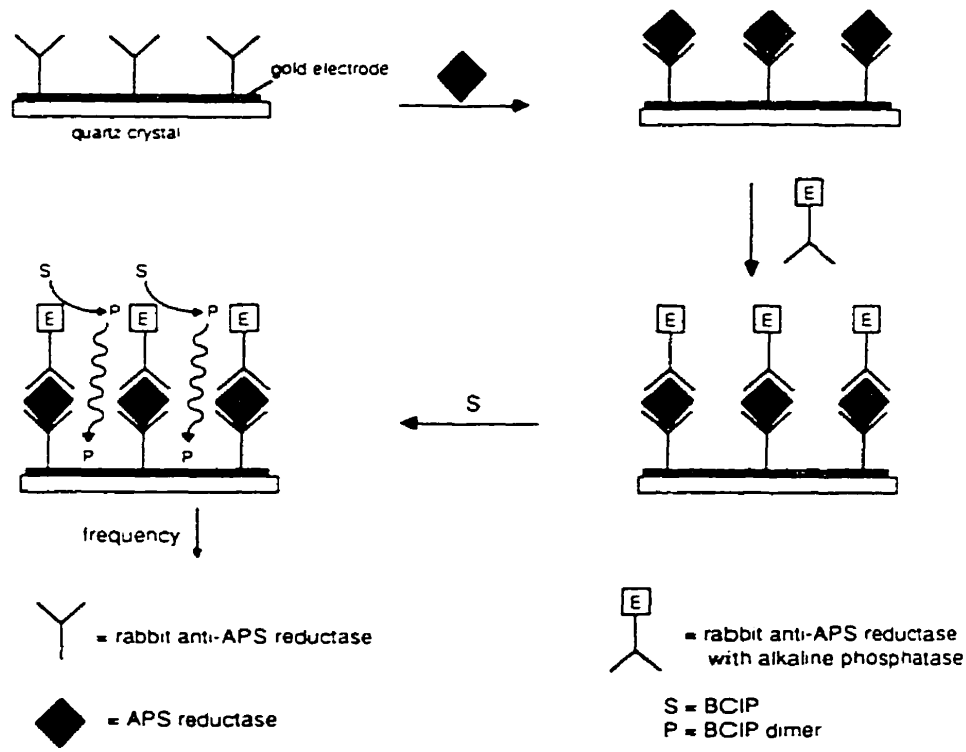

Figure 1.12 Schematic representation of the sandwich enzyme-linked immunosorbent assay procedure used with the QCM. The final step involving conversion of the BCIP substrate to the insoluble blue BCIP dimer, which deposits on the QCM, results in a decrease in the resonant frequency of the quartz crystal.[158]

oligonucleotide sequences specific for different regions of herpes simplex virus HSV-1. Thus only in the presence of HSV-1 nucleic acid target strands, which bound to both the enzyme and biotin, could the enzyme become surface-immobilized. After washing, BCIP was then added to provide enzymatically amplified deposition of dimer. Biotin can also be used as a coating material for the detection of streptavidin in solution.[160]

An entirely different approach to liquid-phase immunoassay has been demonstrated by Kurosawa and coworkers.[161,162] Their method, dubbed a *latex piezoelectric immunoassay* (LPEIA), did not require immobilization of either antigen

or antibody on the crystal surface. Rather, an antibody-bearing latex was employed in the bulk solution to which one crystal face was exposed. Addition of antigen then induces an agglutination reaction of the antibody-bearing latex, which results in a change in the solution bulk viscosity and a resultant change in the oscillation frequency of the crystal. Essentially this approach was a variation of the traditional latex photometric immunoassay (LPIA) used in clinical analyses in which the agglutination reaction is followed in terms of light scattering/turbidimetric or absorbance changes. The LPEIA method was used to determine C-reactive protein (CRP)[161] and antistreptolysin O antibodies[162] in serum, with comparable results to the corresponding LPIA method. The effect of bulk viscosity on crystal frequency has also been exploited for the determination of fibrinogen concentration via the gelation reaction that occurs between fibrinogen, an important factor in blood coagulation processes, and thrombin.[15] Approaches that modify bulk solution properties rather than deposit mass on the crystal surface are attractive since they obviate the need for reproducible application of coating and regenerating the coating for multiple analyses. The antigen-antibody interaction in particular is generally very strong and irreversible and piezoelectric immunosensor applications have often suffered from limited reusability, although adequately creative strategies can be devised to circumvent this problem as illustrated in ref.157 (described earlier). Gas-phase immunoassays are less common but have also been attempted[59,111] (see description in section 1.3.2 re. ref.59). Reviews on piezoelectric immunosensors are available.[5,163]

Other TSM biosensors that have been investigated include the determination of IgG immunoglobulins via the affinity reaction with a protein A coating,[164] development of a real-time glucose sensor by immobilization of hexokinase entrapped within a crosslinked poly(acrylamide) gel matrix,[165] detection of glucose[166,167] and erythrocytes[167] with fully-immersed crystals coated with lectins, detection of galactosyltransferase using a glucosamine coating,[168] and nucleic acid hybridization studies for both RNA[169,170] and DNA[159,171,172] as well as investigation of platinum anticancer drug binding to immobilized DNA.[173] Most of these biosensor reports have involved liquid-phase binding, although gas-phase sensing has been reported, e.g. for determination of formaldehyde using crystals coated with formaldehyde

dehydrogenase.[107] TSM biosensors involving liquid-phase binding either involve measurement of the oscillation frequency *in situ* or after the crystal is rinsed and dried. Experimental design can also involve a static reaction chamber or the use of a flow cell. A general review on piezoelectric biosensors has recently been published.[4]

1.3.6 Other Research

Presented in this section is a sampling of the wide range of other applications for which the TSM acoustic wave sensor has been used. Several microbial growth sensors have been developed which employ uncoated AT-cut crystals. Fengjiao *et al.* reported the detection of *Escherichia Coli*[174] and *Staphylococcus Aureus*.[175] Their approach was unconventional and highly innovative, since detection was accomplished without contacting the crystal with the culture medium. The crystal was kept dry with one terminal of the crystal connected to the input terminal of the oscillator circuit and the other crystal terminal to two platinum electrodes, one exposed to a sample cell and the other to a reference cell. Two different platinum electrodes, again one connected to the sample cell and one to the reference cell, were connected to the output terminal of the oscillator circuit. Both sample and reference cells contain growth medium; microbial growth occurring after inoculation of the sample cell causes changes in the conductivity of the growth medium which in turn causes a shift in the frequency of oscillation. Microbe concentrations were determined by a frequency detection time (FDT) limit method where the time required for the metabolizing bacteria to reach a threshold concentration and cause a sharp change in slope of the frequency signal was measured. The FDT was inversely proportional to the initial microbe concentration (C) and a linear regression equation between FDT and log C was established.

Nivens *et al.*[176] reported a long-term, on-line monitoring system for microbial film growth. The system involved a flow cell and the frequency shift was produced by simple attachment and surface growth of the microbe. The detection limit of the technique was determined to be 3×10^5 cells/cm^2, and it was suggested that the methodology could be used as a sensitive remote sensing device for microbial contamination in ultrapure water systems. A reusable cell growth sensor was also developed by Ebersole *et al.*[177] The sensing strategy involved the use of a pH-sensitive

amphoteric polymer. Metabolic end products produced by the microbes alter the pH of the growth medium, and as the pH approaches the isoelectric point of the polymer, the polymer solubility decreases and the polymer precipitates and adheres to the uncoated crystal electrode surface.

Other applications include investigation of Langmuir-Blodgett (LB) films;[178-182] interaction of liposomes[183] and proteins[184] with phospholipid monolayers; association of cyclodextrins with lipid of cholesterol multibilayers;[185] binding of concanavalin A to glycolipid monolayers;[186] detection of phase transitions in lipid multibilayers[187] and self-assembled thiol monolayers with carboxylic acid functionality;[188] adsorption processes of poly(ethylene glycol) at monolayers of poly(methacrylic acid)-based amphiphiles;[189] monitoring of osteoblast attachment to the electrode surface;[190] adsorption of bovine serum albumin on a polysulfone coating[191] and on gold;[192] studies of Au exposed to sulfide, thiocyanate and n-octadecanethiol;[193] kinetics of polystyrene adsorption onto gold;[194] kinetics of alkanethiolate adsorption onto gold;[195] kinetics of fluorination of polyethylene films;[196] adsorption of 3-aminopropyltriethoxysilane on aluminum and subsequent reactivity with chlorodimethylsilane;[197] simultaneous microgravimetric and FTIR measurements of tetrahydrofuran adsorption on gold;[198] determination of bromide,[199] cyanide[200,201] and mercury[202] in solution with uncoated electrodes; determination of copper in solution using coatings of poly(2-vinylpyridine) and poly(4-vinylpyridine);[203] determination of lead in solution with a copper oleate coating;[204] determination of metal ions in solution using polymer-coated crystals;[205] and determination of sulpha drugs.[206]

In addition to the tremendous variety of applications that have been reported, there has been a great deal of work done to investigate the fundamental aspects of TSM sensor operation. Many of these reports have already been described or cited in section 1.2. Other reports of this nature include the investigation of mass sensitivity by using a separate scanning electrode in close proximity to the crystal electrode[207,208] or by copper electrodeposition in holes etched in a photoresist polymer on the crystal;[209] investigation of the effect of surface roughness,[210] liquid conductivity[211] and longitudinal waves[34] on the sensor response; investigation of the effect of changes in depletion layer viscosity and density on the frequency change of an EQCM;[212] and

determination of an optimal operating frequency for solution-phase sensing, based on phase-frequency relationships.[213] The sensitivity of the TSM sensor to changes in mass and viscosity can enable entirely new ways of examining physicochemical interactions, such as in the determination of contact angles and surface tensions of liquid-air and liquid-liquid interfaces.[214] This novel approach represents an alternative to traditional goniometry and is based on the frequency changes accompanying the introduction of a small liquid droplet to the center of a vibrating TSM quartz resonator.

It is clear from the examples in this section, as well as throughout the chapter, that the only significant limit to the possible applications and uses of a TSM sensor device is that imposed by the researcher's creative faculty.

1.4 Commercial Products

Unlike most research in analytical chemistry, the main apparatus in TSM sensor experiments (i.e. the quartz crystal housing unit) is usually constructed in-house, with the frequency counter being purchased separately. This is because the construction of the housing unit is usually relatively inexpensive and not a great technological challenge (e.g. compared with the construction of a spectrometer). In-house construction also allows the researchers to tailor the design to their particular application. Nevertheless, there still exist a few companies which sell these devices.

Probably the most well-known and publicized piezoelectric TSM sensor is the one sold by Universal Sensors Inc., Metairie, LA, USA. Universal Sensors sells a basic piezoelectric detector as well as a more expensive unit designed specifically for biosensor applications. Both are complete units which include the crystal housing assembly (made from Plexiglas and allows for both gas- and liquid-phase operation), temperature sensor, a pump for flow-through experiments, a frequency counter which can be interfaced to a computer or recorder, and software. Universal Sensors also offers several accessories, including a range of uncoated and precoated crystals with various electrode and coating materials for specific sensing applications.

An electrochemical quartz microbalance system is available from Elchema, Potsdam, NY, USA. The system includes the frequency counter, Faraday cage and a remote probe unit. The potentiostat, data acquisition software, Rotacell crystal housing

unit, crystals, reference and counter electrodes are sold separately. EG&G Instruments, Princeton, NJ, USA also sells an EQCM analyzer unit for use with their industry standard 273A and 263A potentiostats. Electrochemistry software must be purchased separately. Key features include the ability to track potential, current and frequency or admittance intensity simultaneously; monolayer mass sensitivity; quantification of elastic and viscous changes; real-time graphics display; front panel display of frequency and admittance, and analog outputs for frequency and admittance. Both of these commercial EQCM units can also be used for non-EQCM sensing applications.

Maxtek Inc., Torrance, CA, USA also sells a device somewhat similar to a traditional EQCM, but designed specifically for monitoring metal plating and etching processes. Changes in thickness (as small as 1 Å) and rate (down to 0.1 Å/s) during the process can be determined from the frequency changes using metal constants which are stored inside the instrument's microprocessor.

References

1. D.S. Ballantine Jr., R.M. White, S.J. Martin, A.J. Ricco, G.C. Frye, E.T. Zellers and H. Wohltijen, *Acoustic Wave Sensors*, Academic Press, Orlando FL, 1996.
2. S. Yamaguchi, Ed. *Chemical Sensor Technology, Vol.4*, Kodansha Ltd., Tokyo, Japan, 1991.
3. J. Janata, M. Josowicz and D.M. DeVaney, *Anal. Chem.* **1994**, *66(12)*, 207R-228R.
4. M. Minunni, M. Mascini, G.G. Guilbault and B. Hock, *Anal. Lett.* **1995**, *28(5)*, 749-764.
5. A.A. Suleiman and G.G. Guilbault, *Analyst* **1994**, *119*, 2279-2282.
6. J.W. Grate, S.J. Martin and R.M. White, *Anal. Chem.* **1993**, *65(21)*, 940A-948A.
7. J.W. Grate, S.J. Martin and R.M. White, *Anal. Chem.* **1993**, *65(22)*, 987A-996A.
8. M. Thompson, A.L. Kipling, W.C. Duncan-Hewitt, L.V. Rajakovic, B.A. Cavic-Vlasak, *Analyst* **1991**, *116*, 881-890.
9. G.G. Guilbault and J.H.T. Luong, *Diag. Clin. Testing* **1990**, *28*, 22-30.
10. D.S. Ballantine Jr. and H. Wohltjen, *Anal. Chem.* **1989**, *61(11)*, 704A-715A.
11. M.R. Deakin and D.A. Buttry, *Anal. Chem.* **1989**, *61(20)*, 1147A-1154A.
12. R. Schumacher, *Angew. Chem. Int. Ed. Engl.* **1990**, *29(4)*, 329-343.
13. W. Welsch, C. Klein, M. von Schickfus and S. Hunklinger, *Anal. Chem.* **1996**, *68(13)*, 2000-2004.
14. Y. Shou-Zhuo and M. Zhi-Hong, *Anal. Chim. Acta* **1987**, *193*, 97-105.
15. H. Muramatsu, E. Tamiya, M. Suzuki and I. Karube, *Anal. Chim. Acta* **1989**, *217*, 321-326.
16. R. Lucklum, B. Henning, P. Hauptmann, K.D. Schierbaum, S. Vaihinger and W. Göpel, *Sens. Actuators A* **1991**, *25-27*, 705-710.
17. S. Bruckenstein and M. Shay, *Electrochim. Acta* **1985**, *30(10)*, 1295-1300.
18. T. Nomura and T. Nagamune, *Anal. Chim. Acta* **1985**, *155*, 231-234.
19. T. Nomura, M. Watanabe and T.S. West, *Anal. Chim. Acta* **1985**, *175*, 107-116.
20. J.J. Chance and W.C. Purdy, *Anal. Chem.* **1996**, *68(18)*, 3104-3111.
21. L.V. Rajakovic, B.A. Cavik-Vlasak, V. Ghaemmaghami, K.M.R. Kallury, A.L. Kipling and M. Thompson, *Anal. Chem.* **1991**, *63(6)*, 615-621.
22. G.C. Dunham, N.H. Benson, D. Petelenz and J. Janata, *Anal. Chem.* **1995**, *67(2)*, 267-272.
23. M. Benje, M. Eiermann, U. Pittermann and K.G. Weil, *Ber. Bunsenges. Phys. Chem.* **1986**, *90(5)*, 435-439.
24. R. Beck, U. Pittermann and K.G. Weil, *J. Electrochem. Soc.* **1992**, *139(2)*, 453-461.
25. G.C. Komplin, F. Schleifer and W.J. Pietro, *Rev. Sci. Instrum.* **1993**, *64(6)*, 1530-1535.
26. G. Hayward, *Anal. Chim. Acta* **1992**, *264*, 23-30.
27. M. Thompson, C.L. Arthur and G.K. Dhaliwal, *Anal. Chem.* **1986**, *58(6)*, 1206-1209.
28. M. Thompson, G.K. Dhaliwal, C.L. Arthur and G.S. Calabrese, *IEEE Trans. Ultrasonics Ferroelectrics and Frequency Control* **1987**, *UFFC-34*, 127.
29. H.E. Hager, *Chem. Eng. Commun.* **1986**, *43(1-3)*, 25-38.
30. V.E. Bottom, *Introduction to Quartz Crystal Unit Design*; Van Nostrand Reinhold Co.: New York, 1982.
31. M. Yang, F.L. Chung and M. Thompson, *Anal. Chem.* **1993**, *65(24)*, 3713-3716.
32. A.L. Kipling and M. Thompson, *Anal. Chem.* **1990**, *62(14)*, 1514-1519.
33. M. Yang and M. Thompson, *Anal. Chem.* **1993**, *65(24)*, 3591-3597.
34. Z. Lin and M.D. Ward, *Anal. Chem.* **1995**, *67(4)*, 685-693.
35. Z. Lin, C.M. Yip, I.S. Joseph and M.D. Ward, *Anal. Chem.* **1993**, *65(11)*, 1546-1551.
36. S.J. Martin, V.E. Granstaff and G.C. Frye, *Anal. Chem.* **1991**, *63(20)*, 2272-2281.
37. H. Muramatsu, E. Tamiya and I. Karube, *Anal. Chem.* **1988**, *60(19)*, 2142-2146.
38. H. Muramatsu, E. Tamiya, M. Suzuki and I. Karube, *Anal. Chim. Acta* **1988** *215(1-2)*, 91-98.

39. Z. Tiean, N. Liehua and Y. Shouzhuo, *J. Electroanal. Chem.* **1990**, *293*, 1-18.
40. W.G. Cady, *Piezoelectricity*; Dover: New York, 1964.
41. S. Bruckenstein, M. Michalski, A. Fensore, Z. Li and A.R. Hillman, *Anal. Chem.* **1994**, *66(11)*, 1847-1852.
42. G. Sauerbrey, *Z. Phys.* **1959**, *155*, 206-212.
43. J.P. Jones and T.J. Lewis, *J. Chem. Soc. Faraday Trans.* **1995**, *91(18)*, 3147-3155.
44. C. Barnes, C. D'Silva, J.P. Jones and T.J. Lewis, *Sens. Actuators A* **1992**, *31*, 159-163.
45. K.K. Kanazawa and J.G. Gordon II, *Anal. Chim. Acta* **1985**, *175*, 99-105.
46. K.K. Kanazawa and J.G. Gordon II, *Anal. Chem.* **1985**, *57*, 1770-1771.
47. S. Kurosawa, E. Tawara, N. Kamo and Y. Kobatake, *Anal. Chim. Acta* **1990**, *230*, 41-49.
48. Z.A. Shana, D.E. Radtke, U.R. Kelkar, F. Josse and D.T. Haworth, *Anal. Chim. Acta* **1990**, *231*, 317-320.
49. K.E. Heusler, A. Grzegorzewski, L. Jäckel and J. Pietrucha, *Ber. Bunsenges. Phys. Chem.* **1988**, *92(11)*, 1218-25.
50. S. Yao and T. Zhou, *Anal Chim. Acta* **1988**, *212*, 61-72.
51. R. Schumacher, G. Borges and K.K. Kanazawa, *Surf. Sci.* **1985**, *163*, L621-L626.
52. T. Nomura and M. Okuhara, *Anal. Chim. Acta.* **1982**, *142*, 281-284.
53. K. Bodenhöfer, A. Hierlemann, G. Noetzel, U. Weimar and W. Göpel, *Anal. Chem.* **1996**, *68(13)*, 2210-2218.
54. W.H. King Jr, *Anal. Chem.* **1964**, *36(9)*, 1735-1739.
55. F.W. Karasek and K.R. Gibbons, *J. Chromatogr. Sci.* **1971**, *9(9)*, 535-40.
56. F.W. Karasek and J.M. Tierney, *J. Chromatogr.* **1974**, *89(1)*, 31-38.
57. F.W. Karasek, P. Guy, H.H. Hill Jr. and J.M. Tierney, *J. Chromatogr.* **1976**, *124(2)*, 179-186.
58. T.E. Edmonds and T.S. West, *Anal. Chim. Acta* **1980**, *117*, 147-157.
59. L. Rajakovic, V. Ghaemmaghami and M. Thompson, *Anal. Chim. Acta* **1989**, *217*, 111-121.
60. W.W. Shulz and W.H. King, *J. Chromatog. Sci.* **1973**, *11(7)*, 343-348.
61. P.L. Konash and G.J. Bastiaans. *Anal. Chem.* **1980**, *52(12)*, 1929-1931.
62. S. Oda and T. Sawada, *Anal. Chem.* **1981**, *53(3)*, 471-474.
63. J.M. Charlesworth, *Anal. Chem.* **1990**, *62(1)*, 76-81.
64. W.H. King Jr., U.S. Pat. 3164004, 1965.
65. W.H. King Jr., *Res./Develop.* **1969**, *20(4)*, 28-34.
66. W.H. King Jr., *Res./Develop.* **1969**, *20(5)*, 28-33.
67. K.H. Karmarker and G.G. Guilbault, *Anal. Chim. Acta* **1975**, *75*, 111.
68. J. Hlavay and G.G. Guilbault, *Anal. Chem.* **1978**, *50(8)* 1044-1046.
69. K. Aoki, L.C. Brousseau and T.E. Mallouk, *Sens. Actuators B* **1993**, *13-14* 703-704.
70. M.H. Mo, G.G. Guilbault and B. Reitz, *Anal. Chem.* **1980**, *52*, 1489-1492.
71. K.H. Karmarker and G.G. Guilbault, *Environ. Lett.* **1975**, *10(3)*, 237-246.
72. R. Boufenar, T. Boudjerda, F. Benmakroha, F. Djerboua and J.J. McCallum, *Anal. Chim. Acta* **1992**, *264*, 31-42.
73. W.W. Fogelman and M.S. Shuman, *Anal. Lett.* **1976**, *9(8)*, 751-765.
74. M.H. Ho, G.G. Guilbault and E.P. Scheide, *Anal. Chem.* **1982**, *54(12)*, 1998-2002.
75. R.V. Bucur, *Rev. Roum. Phys.* **1974**, *19(8)*, 779-786.
76. J. Hlavay and G.G. Guilbault, *Anal. Chem.* **1978**, *50(7)*, 965-967.
77. J.F. Alder, A.E. Bentley and P.K.P. Drew, *Anal. Chim. Acta* **1986**, *182*, 123-131.
78. L.M. Webber, K.H. Karmarker and G.G. Guilbault, *Anal. Chim. Acta* **1978**, *97*, 29-35.
79. L.M. Webber and G.G. Guilbault, *Anal. Chim. Acta* **1977**, *93*, 145-151.
80. Q. Bristow, *J. Geochim. Explor.* **1972**, *1(1)*, 55-76.
81. E.P. Scheide and J.K. Taylor, *Am. Chem. Soc. Div. Environ. Chem. Prepr.* **1974**, *14(1)*, 329-335.
82. E.P. Scheide and J.K. Taylor, *Am. Ind. Hyg. Assoc. J.* **1975**, *36(12)*, 897-901.

83. E.P. Scheide and J.K. Taylor, *Environ. Sci. Technol.* **1974**, *8(13)*, 1097-9.
84. E.P. Scheide and R.B.J. Warner, *Am. Ind. Hyg. Assoc. J.* **1978**, *39(9)*, 745-9.
85. E.P. Scheide and J.K. Taylor, *Prepr. Pap. Natl. Meet., Div. Environ. Chem., Am. Chem. Soc.* **1975**, *15(2)*, 36-39.
86. W.H. King Jr., *Environ. Sci. Technol.* **1970**, *4(12)*, 1136-41.
87. J.M. Slater, E.J. Watt, N.J. Freeman, I.P. May and D.J. Weir, *Analyst* **1992**, *117*, 1265-1270.
88. O.S. Milanko, S.A. Milinkovic and L.V. Rajakovic, *Anal. Chim. Acta* **1992**, *269*, 289-300.
89. G.G. Guilbault, *Anal. Chim. Acta* **1967**, *39(2)*, 260-264.
90. E.P. Scheide and G.G. Guilbault, *Anal. Chem.* **1972**, *44(11)*, 1764-1768.
91. W.M. Shackelford and G.G. Guilbault, *Anal. Chim. Acta* **1974**, *73(2)*, 383-389.
92. Guilbault, G.G.; Affolter, J.; Tomita, Y.; Kolesar Jr., E.S. *Anal. Chem.* **1981**, *53(13)*, 2057-2060.
93. G.G. Guilbault, Y. Tomita, and E.S. Kolesar Jr. *Sensors Actuators* **1981**, *2(1)*, 43-57.
94. J. Kristoff and G.G. Guilbault, *Anal. Chim. Acta* **1983**, *149*, 337-341.
95. G.G. Guilbault and A. Lopez-Roman, *Environ. Lett.* **1971**, *2(1)*, 35-45.
96. A. Lopez-Roman and G.G. Guilbault, *Anal. Lett.* **1972**, *5(4)*, 225-235.
97. M.W. Frechette, J.L. Fasching and D.M. Rosie, *Anal. Chem.* **1973**, *45(9)*, 1765-1766.
98. M.W. Frechette and J.L. Fasching, *Environ. Sci. Technol.* **1973**, *7(13)*, 1135-7.
99. K.H. Karmarker and G.G. Guilbault, *Anal. Chim. Acta* **1974**, *71*, 419-424.
100. K.H. Karmarker, L.M. Webber and G.G. Guilbault, *Environ. Lett.* **1975**, *8(4)*, 345-352.
101. K.H. Karmarker, L.M. Webber and G.G. Guilbault, *Anal. Chim. Acta* **1976**, *81(2)*, 265-271.
102. J.L. Cheney and J.B. Homolya, *Anal. Lett.* **1975**, *8(3)*, 175-193.
103. J.L. Cheney and J.B. Homolya, *Sci. Total Environ.* **1976**, *5(1)*, 69-77.
104. J.L. Cheney, T. Norwood and J.B. Homolya, *Anal. Lett.* **1976**, *9(4)*, 361-377.
105. J.F. Alder and C.A. Isaac, *Anal. Chim. Acta* **1981**, *129*, 163-174.
106. J.F. Alder and C.A. Isaac, *Anal. Chim. Acta* **1981**, *129*, 175-188.
107. G.G. Guilbault, *Anal. Chem.* **1983**, *55(11)* 1682-1684.
108. D.T. Gjessing, C. Holm and T. Lanes, *Electron. Lett.* **1967**, *3*, 156.
109. W.H. King Jr., *U.S. Pat.* **1969**, *3 427 864*.
110. C.W. Lee, Y.S. Fung and K.W. Fung, *Anal. Chim. Acta* **1982**, *135(2)*, 277-283.
111. J. Ngeh-Ngwainbi, P.H. Foley, S.S. Kuan and G.G. Guilbault, *J. Am. Chem. Soc.* **1986**, *108(18)*, 5444-5447.
112. M.H. Ho, G.G. Guilbault and E.P. Scheide, *Anal. Chim. Acta* **1981**, *130*, 141-147.
113. M.E. Dominguez, J. Li, R.L. Curiale, E.J. Poziomek and A. Queré, *Anal. Lett.* **1995**, *28(6)*, 945-958.
114. S. Kurosawa, N. Kamo, D. Matsui and Y. Kobatake, *Anal. Chem.* **1990**, *62(4)*, 353-359.
115. J. Hlavay and G.G. Guilbault, *Anal. Chem.* **1977**, *49(13)*, 1890-1898.
116. J.F. Alder and J.J. McCallum, *Analyst* **1983**, *108(1291)*, 1169-1189.
117. J.P. Mieure and J.L. Jones, *Talanta* **1969**, *16(1)*, 149-150.
118. J.L. Jones and J.P. Mieure *Anal. Chem.* **1969**, *41(3)*, 484-490.
119. M.R. Deakin and O. Melroy, *J. Electroanal. Chem.* 239, 321-331, 1988.
120. S. Swathirajan and S. Bruckenstein, *Electrochim. Acta* **1983**, *28(7)*, 865-867.
121. S. Bruckenstein and S. Swathirajan, *Electrochim. Acta* **1985**, *30(7)*, 851-855.
122. O.R. Melroy, K.K. Kanazawa, J. Gordon II and D. Buttry, *Langmuir* **1986**, *2(6)*, 697-700.
123. M. Hepel, K. Kanige and S. Bruckenstein, *J. Electroanal. Chem.* **1989**, *266*, 409-421.
124. R. Schumacher, A. Muller and W. Stockel, *J. Electroanal. Chem.*, **1987**, *219(1-2)*, 311-317.
125. W. Hinsberg, C. Wilson and K.K. Kanazawa, *J. Electrochem. Soc.*, **1986**, *133(7)*, 1448-1451.
126. H. Hager, R. Ruedisueli and M. Beuhler *Corrosion*, **1986**, *42(6)*, 345-351.
127. R. Schumacher, J.G. Gordon and O. Melroy, *J. Electroanal. Chem.* **1987**, *216*, 127-135.
128. S. Bruckenstein and M.J. Shay, *J. Electroanal. Chem.* **1985**, *188*, 131-136.

129. M.R. Deakin, T. Li and O.R. Melroy, *J. Electroanal. Chem.* **1988**, *243(2)*, 343-351.
130. T. Nomura and T. Mimatsu, *Anal. Chim. Acta* **1982**, *143*, 237-241.
131. M.R. Deakin and H. Byrd, *Anal. Chem.* **1989**, *61(4)*, 290-295.
132. S. Lasky and D. Buttry *J. Am. Chem. Soc.*, **1988**, *110(18)*, 6258-6260.
133. B.J. Feldman and O.R. Melroy *J. Electroanal. Chem.*, **1987**, *234*, 213-227.
134. S. Ikeda and N. Oyama, *Anal. Chem.* **1993**, *65(14)*, 1910-1915.
135. P. Varineau and D. Buttry, *J. Phys. Chem.* **1987**, *91(6)*, 1292-1295.
136. M. Ward, *J. Phys. Chem.* **1988**, *92(7)*, 2049-2054.
137. D. Orato and D.A. Buttry, *J. Am. Chem. Soc.* **1987**, *109(12)*, 3574-3581.
138. S. Bruckenstein, C.P. Wilde, M. Shay and A.R. Hillman, *J. Phys. Chem.* **1990**, *94*, 787-793.
139. W. Kutner and K. Doblhofer, *J. Electroanal. Chem.* **1992**, *326*, 139-160.
140. H.O. Finklea and R.S. Vithanage, *J. Electroanal. Chem.* **1984**, *161*, 283-294.
141. C.K. Baker and J.R. Reynolds, *Polym. Prep. Am. Chem. Soc. Div. Polym. Chem.* **1987**, *28(2)*, 284-285.
142. G.S. Ostrom and D.A. Buttry, *J. Electroanal. Chem. Interfacial Electrochem.* **1988**, *256(2)*, 411-431.
143. A. Hochfeld, R. Kessel, J.W. Schultze and A. Thyssen, *Ber. Bunsenges. Phys. Chem.* **1988**, *92(11)*, 1406-1412.
144. T.W. Schneider and D.A. Buttry, *J. Am. Chem. Soc.* **1993**, *115(26)*, 12391-12397.
145. C. Köblinger, S. Drost, F. Aberl, H. Wolf, S. Koch and P. Woias, *Biosens. Bioelectron.* **1992**, *7*, 397-404.
146. E. Prusak-Sochaczewski and J.H.T. Luong, *Anal. Lett.* **1990**, *23(2)*, 183-194.
147. E. Prusak-Sochaczewski and J.H.T. Luong, *Anal. Lett.* **1990**, *23(2)*, 401-409.
148. M. Muratsugu, F. Ohta, Y. Miya, T. Hosokawa, S. Kurosawa, N. Kamo and H. Ikeda, *Anal. Chem.* **1993**, *65(20)*, 2933-2937.
149. J.H.T. Luong, E. Prusak-Sochaczewski and G.G. Guilbault, *Ann. N.Y. Acad. Sci.* **1990**, *613*, 439-443.
150. H. Muramatsu, E. Tamiya and I. Karube, *J. Membr. Sci.* **1989**, *41*, 281-290.
151. N.J. Geddes, E.M. Paschinger, D.N. Furlong, Y. Ebara, Y. Okahata, K.A. Than and J.A. Edgar, *Sens. Actuators B* **1994**, *17*, 125-131.
152. G.G. Guilbault, B. Hock and R. Schmid, *Biosens. Bioelectron.* **1992**, *7*, 411-419.
153. B. König and M. Grätzel, *Anal. Chem.* **1994**, *66(3)*, 341-344.
154. B. König and M. Grätzel, *Anal. Lett.* **1993**, *26(8)*, 1567-1585.
155. M. Plomer, G.G. Guilbault and B. Hock, *Enzyme Microb. Technol.* **1992**, *14*, 230-235.
156. M. Minunni, P. Skladal and M. Mascini, *Anal. Lett.* **1994**, *27(8)*, 1475-1487.
157. K.A. Davis and T.R. Leary, *Anal. Chem.* **1989**, *61(11)*, 1227-1230.
158. R.C. Ebersole and M.D. Ward, *J. Am. Chem. Soc.* **1988**, *110(26)*, 8623-8628.
159. R.C. Ebersole, J.A. Miller, J.R. Moran and M.D. Ward, *J. Am. Chem. Soc.* **1990**, *112(8)*, 3239-3241.
160. A. Näbauer, P. Berg, I. Ruge, E. Muller, P. Woias, C. Kösslinger and H. Drobe, *Sens. Actuators B* **1990**, *1*, 508-509.
161. S. Kurosawa, E. Tawara, N. Kamo, F. Ohta and T. Hosokawa, *Chem. Pharm. Bull.* **1990**, *38(5)*, 1117-1120.
162. M. Muratsugu, S. Kurosawa and N. Kamo, *Anal. Chem.* **1992**, *64(21)*, 2483-2487.
163. A.A. Suleiman and G.G. Guilbault, *Anal. Lett.* **1991**, *24(8)*, 1283-1292.
164. H. Muramatsu, J.M. Dicks, E. Tamiya and I. Karube, *Anal. Chem.* **1987**, *59(23)*, 2760-2763.
165. S.J. Lasky and D.A. Buttry, *Am. Biotech. Lab.* **1990**, *8(3)*, 8-16.
166. C. Barnes, C. D'Silva, J.P. Jones and T.J. Lewis, *Sens. Actuators B* **1991**, *3*, 295-304.
167. C. Barnes, C. D'Silva, J.P. Jones and T.J. Lewis, *Sens. Actuators B* **1992**, *7*, 347-350.
168. L.H. Grande, C.R. Geren and D.W. Paul, *Sens. Actuators* **1988**, *14*, 387-403.

169. N.C. Fawcett, J.A. Evans, L. Chien and N. Flowers, *Anal. Lett.* **1988**, *21(7)*, 1099-1114.
170. H. Su, M. Yang, K.M.R. Kallury and M. Thompson, *Analyst* **1993**, *118(3)*, 309-312.
171. H. Su, K.M.R. Kallury, M. Thompson and A. Roach, *Anal. Chem.* **1994**, *66(6)*, 769-777.
172. H. Su and M. Thompson, *Biosens. Bioelectron.* **1995**, *10*, 329-340.
173. H. Su, P. Williams and M. Thompson, *Anal. Chem.* **1995**, *67(5)*, 1010-1013.
174. H. Fengjiao, Z. Wenhong, G. Qing, N. Lihua and Y. Shouzhuo, *Anal. Lett.* **1994**, *27(4)*, 655-669.
175. H. Fengjiao, D. Le, X. Qingji, N. Lihua and Y. Shouzhuo, *Anal. Lett.* **1995**, *28(2)*, 213-224.
176. D.E. Nivens, J.Q. Chambers, T.R. Anderson and D.C. White, *Anal. Chem.* **1993**, *65(1)*, 65-69.
177. R.C. Ebersole, R.F. Foss and M.D. Ward, *Biotechnol.* **1991**, *9*, 450-454.
178. R.R. McCaffrey, S. Bruckenstein and P.N. Prasad, *Langmuir* **1986**, *2(2)*, 228-229.
179. Y. Okahata and K. Ariga, *J. Chem. Soc., Chem. Commun.* **1987**, 1535-1537.
180. Y. Okahata and K. Ariga, *Langmuir* **1989**, *5(5)*, 1261-1262.
181. K. Ariga and Y. Okahata, *Langmuir* **1994**, *10(9)*, 3255-3259.
182. H. Muramatsu and K. Kimura, *Anal. Chem.* **1992**, *64(21)*, 2502-2507.
183. S. Tanaka, Y. Iwasaki, K. Ishihara and N. Nakabayashi, *Macromol. Rapid Commun.* **1994**, *15*, 319-326.
184. Y. Ebara and Y. Okahata, *Langmuir*, **1993**, *9(2)*, 574-576.
185. Y. Okahata and X. Ye, *J. Chem. Soc., Chem. Commun.* **1989**, 1147-1149.
186. Y. Ebara and Y. Okahata, *J. Am. Chem. Soc.* **1994**, *116(25)*, 11209-11212.
187. Y. Okahata and H. Ebato, *Anal. Chem.* **1989**, *61(19)*, 2185-2188.
188. J. Wang, L.M. Frostman and M.D. Ward, *J. Phys. Chem.* **1992**, *96(13)*, 5224-5228.
189. M. Niwa, K. Yokoyama, A. Fuchino and N. Higashi, *J. Chem. Soc., Chem. Commun.* **1995**, 637-638.
190. J. Redepenning, T.K. Schlesinger, E.J. Mechalke, D.A. Puleo and R. Bizios, *Anal. Chem.* **1993**, *65(23)*, 3378-3381.
191. M. Laatikainen and M. Lindström, *J. Colloid Interface Sci.* **1988**, *125(2)*, 610-614.
192. F. Lacour, R. Torresi, C. Gabrielli and A. Caprani, *J. Electrochem. Soc.* **1992**, *139(6)*, 1619-1622.
193. R.L. McCarley, Y. Kim and A.J. Bard, *J. Phys. Chem.* **1993**, *97(1)*, 211-215.
194. T.Z. Fu, U. Stimming and C.J. During, *Macromolecules* **1993**, *26(13)*, 3271-3281.
195. D.S. Karpovich and G.J. Blanchard, *Langmuir* **1994**, *10(9)*, 3315-3322.
196. N. Hara, H. Fukumoto and M. Watanabe, *Bull. Chem. Soc. Jpn.* **1995**, *68(4)*, 1232-1238.
197. D.G. Kurth and T. Bein, Angew. Chem. Int. Ed. Engl. 31(3), 336-338, 1992.
198. G. Zhuang, G. Chottiner, I.T. Bae, E. Hwang and D.A. Scherson, *Rev. Sci. Instrum.* **1994**, *65(8)*, 2494-2499.
199. S. Yao, L. Nie and Z. Mo, *Anal. Chim. Acta* **1989**, *217*, 327-334.
200. T. Nomura and O. Hattori, *Anal. Chim. Acta*, **1980**, *115*, 323-326.
201. T. Nomura, *Anal. Chim. Acta*, **1981**, *124(1)*, 81-84.
202. T. Nomura and M. Fujisawa, *Anal. Chim. Acta* **1986**, *182*, 267-270.
203. T. Nomura and M. Sakai, *Anal. Chim. Acta* **1986**, *183*, 301-305.
204. T. Nomura, T. Okuhara and T. Hasegawa, *Anal. Chim. Acta* **1986**, *182*, 261-265.
205. T.C. Hunter and G.J. Price, *Analyst* **1995**, *120(1)*, 161-165.
206. L. Nie, T. Wang and S.Z. Yao, *Talanta* **1992**, *39(2)*, 155-158.
207. A.C. Hillier and M.D. Ward, *Anal. Chem.* **1992**, *64(21)*, 2539-2554.
208. N. Oyama, T. Tatsuma, S. Yamaguchi and M. Tsukahara, *Anal. Chem.* **1997**, *69(6)*, 1023-1029.
209. M.D. Ward and E.J. Delawski, *Anal. Chem.* **1991**, *63(9)*, 886-890.
210. M. Yang and M. Thompson, *Langmuir* **1993**, *9(8)*, 1990-1994.

211. M. Rodahl, F. Hook and B. Kasemo, *Anal. Chem.* **1996**, *68(13)*, 2219-2227.
212. W. Lee, H.S. White and M.D. Ward, *Anal. Chem.* **1993**, *65(22)*, 3232-3237.
213. G.C. Komplin and W.J. Pietro, *Rev. Sci. Instrum.* **1995**, *66(2, Pt. 1)*, 1131-1135.
214. Z. Lin and M.D. Ward, *Anal. Chem.* **1996**, *68(8)*, 1285-1291.

2 Construction of Circuit and Housing Apparatus

2.1 Introduction

As mentioned in Chapter 1, the minimum requirements for a TSM sensor experiment include an AT-cut quartz crystal with plated electrodes, an oscillator circuit, a power supply and a readout device (e.g., a frequency counter or strip-chart recorder). Additionally, the crystal will generally require a housing unit tailored to the particular sensing application. While complete systems incorporating all of these features can be purchased commercially, most researchers in the field construct their own circuit and housing unit and then purchase a frequency counter for readout. In this chapter the circuit used for all experiments is described, as well as the housing apparatus that was used for liquid-phase work and a simple multiple crystal drift-correction system that was used for accurate estimation of frequency changes during long-term coating.

2.2 Circuitry

The first oscillator circuit that was examined was one that was purchased commercially from the same supplier as the crystals - International Crystal Manufacturing (ICM; Oklahoma City, OK). This was a simple, inexpensive plug-in Colpitts oscillator, model OT-13, designed to work with crystal frequencies between 3 - 11 MHz. Stable and successful oscillation was achieved using this circuit with 5- and 9-MHz crystals exposed to air. However, when one side of the crystal was exposed to liquid, oscillation ceased. Since it was decided early on that the research project would focus on liquid-phase sensing, this circuit was deemed unsuitable and

another one was sought. Another early attempt involved using a pre-fabricated oscillator located on a CGA video card. This arrangement also provided successful oscillation, both with the crystal in air and with one crystal face exposed to an aqueous environment. The drawbacks with this arrangement however included an undesirable degree of frequency drift and a general lack of understanding of circuit operation since it was not straightforward to decipher whether certain circuit board components were or were not involved in the oscillator.

At this point it was decided to construct a number of circuits from scratch, based on designs indicated in general electronics textbooks. In general these attempts did not produce satisfactory results, with the circuits exhibiting high levels of noise, overtone oscillation, and/or inability to oscillate in liquid. A literature search was thus made to locate published circuits which had been used with liquid-phase QCM devices. A modification of the TTL based circuit published in 1985 by Bruckenstein and Shay,[1] variations of which have since been used by a number of workers, was constructed and found to provide excellent performance in terms of frequency stability and continuous operation with the crystal in solution.

The TTL circuit constructed and used in all experiments is shown in Figure 2.1. On the left side of the figure is shown two oscillators, one for the working crystal (nominal resonant frequency 10 MHz) and one for the reference crystal (nominal resonant frequency 9-MHz, sealed in a HC-6/U holder). Each oscillator consists of two inverters with the crystal placed in the feedback loop. On any one inverter, the low-input (i.e., 0 V) condition drives the output high (i.e., 5 V).[2] The high-input condition drives the output low. The oscillator is tuned to operate in the 9-10 MHz frequency range with an LC-network between the two inverters. The output of each oscillator passes through a third inverter which simply serves as an output buffer. All six inverters were contained in one 7404 TTL logic chip (IC1). The outputs of the two oscillators were directed into a single 7474 TTL logic chip (IC2). Both logic chips had pin 14 connected high (5 V) and pin 7 tied to ground. Power was supplied by a Micronta variable DC power supply using a 7805 voltage regulator to provide 5 V and a bypass capacitor for added voltage stability (none of these shown in Figure 2.1).

The 7474 is a dual D edge-triggered flip-flop whose function was to provide

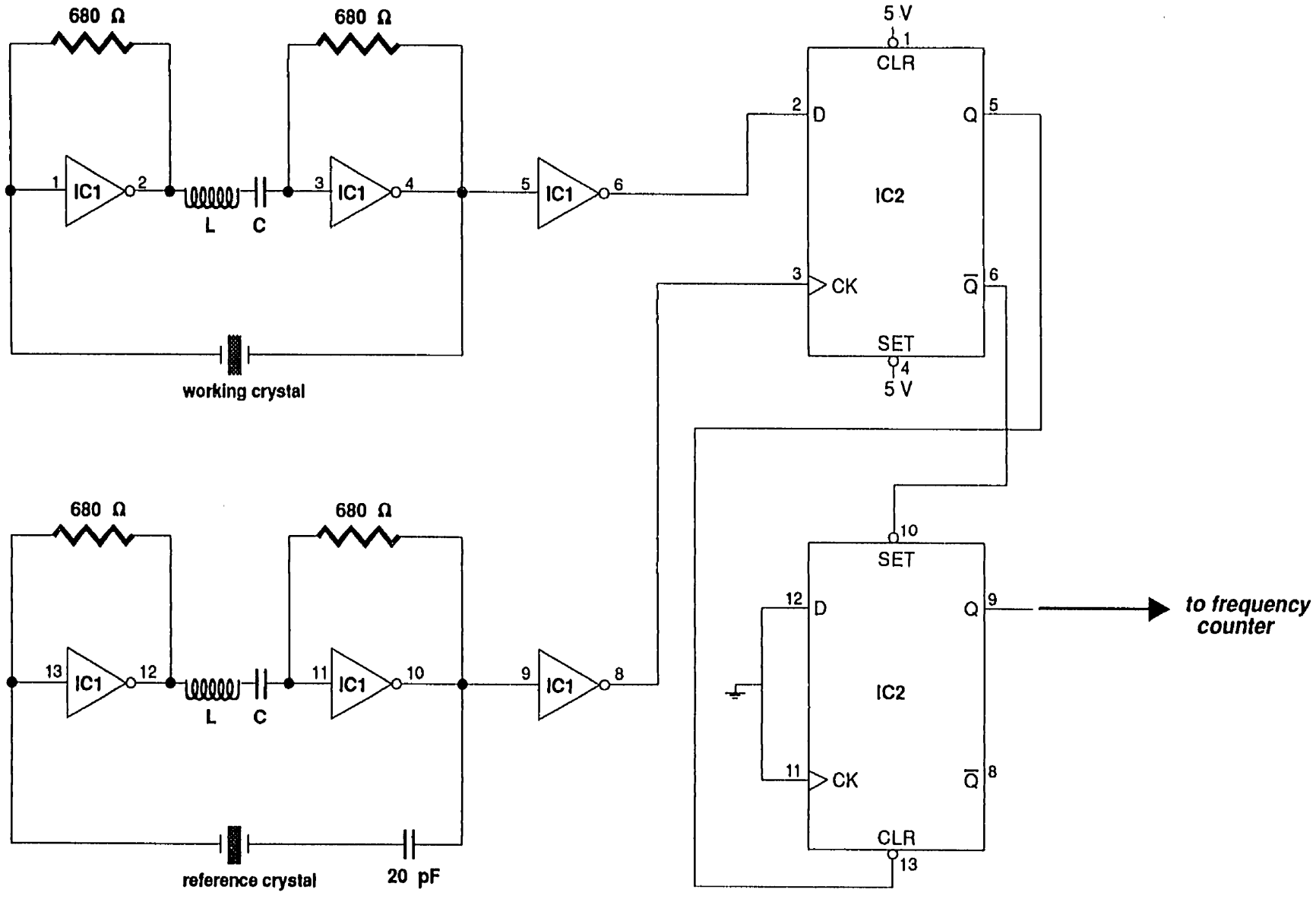

Figure 2.1 Separate reference and working oscillators with difference circuitry. IC1 = SN74LS04N HEX INVERT; IC2 = SN74LS74A Dual D Flip-Flop; L = 10μH; C = 25 pF.

the frequency difference between the two oscillators.[2] The reference crystal output was used as the clock pulse (CK) of the first flip-flop while the working crystal output was sent into the data channel (D). Each flip-flop is a clocked logic block with two outputs, Q and its complement $\overline{Q}$. The information presented to the D input goes on to the Q output whenever the clock input changes from a low to a high level. The only time the output can change is when the clock goes positive. If D is high, on clocking, Q goes high and $\overline{Q}$ goes low. If D is low, on clocking, Q goes low and $\overline{Q}$ goes high. Information on the D input can be changed at any time. It is only its value at the instant of the positive clock edge that matters; this is what is entered into the

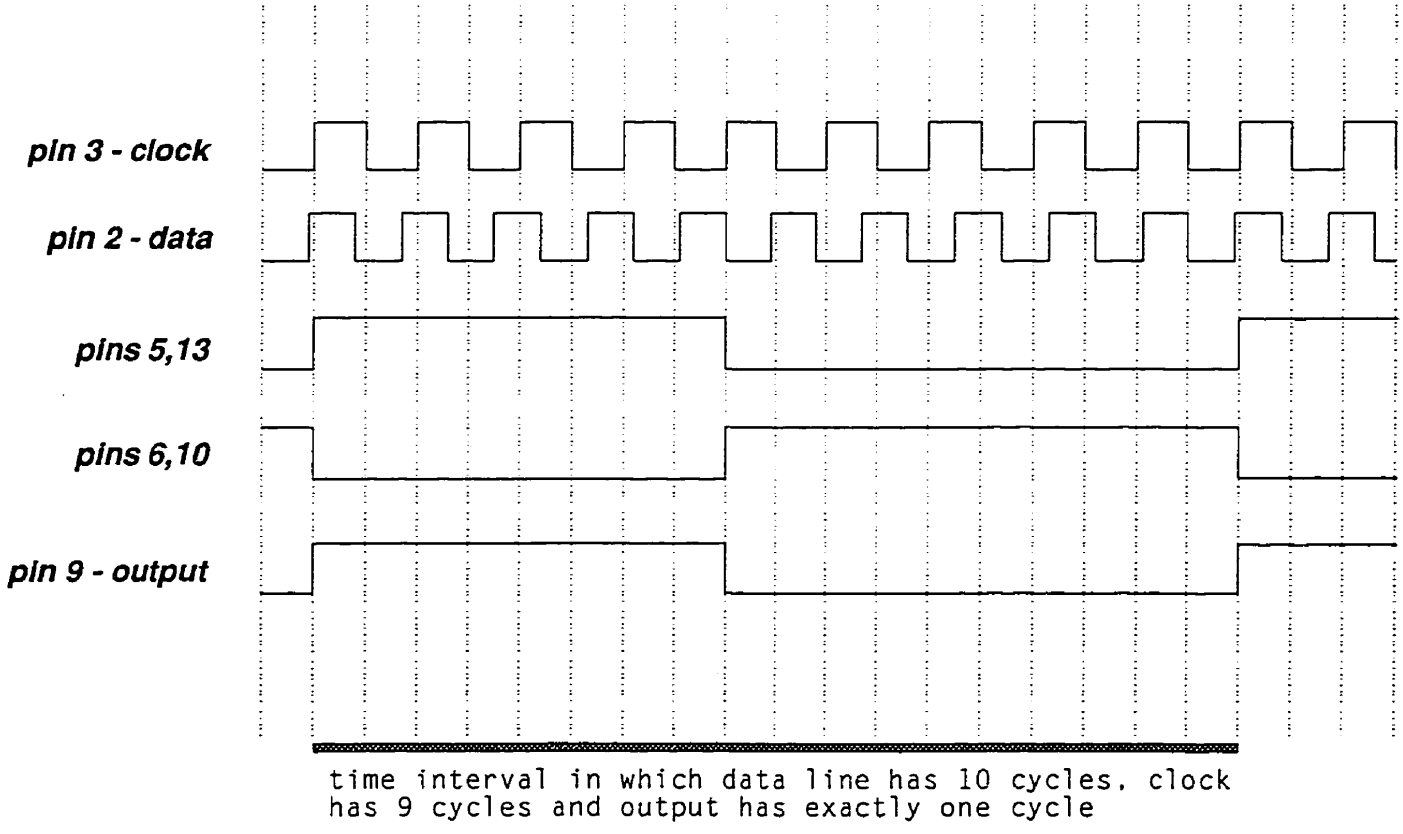

Figure 2.2 Clock diagram illustrating how the 7474 flip-flop IC outputs the frequency difference between two frequency inputs.

flip-flop. This configuration yields the absolute value of the difference in frequency between the reference and working crystals, provided there is at least a few hundred hertz difference in the frequencies. As shown in Figure 2.2, a 9-MHz clock and a 10-MHz data line will result in a 1-MHz output at pins 5 and 6. The use of the second flip-flop (pins 8-13) is thus not strictly necessary but was employed as an output buffer. Of importance here is the operation of the clear (CLR) and set (SET) pins on each flip-flop. When tied positive, these inputs allow for normal operation as described above. If the CLR input is grounded, the flip-flop immediately goes into the state with Q low and $\overline{Q}$ high. If the SET input is grounded, the flip-flop immediately goes into the state with Q high and $\overline{Q}$ low (SET and CLR should never be simultaneously grounded or a disallowed state will occur). As seen in Figure 2.2, when Q and $\overline{Q}$ of the first flip-flop serve as CLR and SET, respectively, of the second flip-flop, the outputs of the second flip-flop mirror those of the first.

The Q output of the second flip-flop was connected to the frequency counter via a standard BNC cable connection. The frequency counter was a Philips Model PM6680 universal counter equipped with a GPIB (IEEE-488) bus interface for computer data acquisition. The PM6680 has a resolution better than 0.01 Hz, and a wide range of features including time averaging of the signal, calculation of duty cycle, etc. The GPIB interface board was model PC<>488, purchased from Capital Equipment Corp. (Burlington, MA). Asystant-GPIB, a software program from Asyst Software Technologies Inc. (Rochester, NY), was used for data acquisition unless frequency readings were taken manually. The software routine used for GPIB data acquisition is documented in Appendix A. A number of different grounding schemes were investigated, involving grounding of the circuit, power supply and counter in various arrangements, in order to improve long-term frequency drift. No particular arrangement, even when a Faraday cage was used and a connection to the grounding network in the building was used, provided markedly improved stability over any other. It was however observed that frequency stability was consistently better during the evenings than during the daytime. For all experiments reported in this work, the circuit was not grounded to the building ground and no Faraday cage was used; all equipment was used under "ambient" conditions and the daytime drift was generally

no worse than ± 3-4 Hz/hour, after allowing approx. 20 minutes for stabilization after power-on.

2.3 Crystals

All crystals used in the experiments were obtained commercially from International Crystal Manufacturing Co. (Oklahoma City, OK). Although other suppliers exist, according to the literature this company is probably the most frequently cited supplier of crystals for TSM sensor research. The crystals are AT-cut with electrodes already deposited. A range of nominal crystal frequencies and electrode materials are available. The electrode may be purchased rough or polished, with specified surface finishes of 3-5 μm and ≤ 1 μm, respectively. In addition it may be specified whether the crystals are to have bonded or unbonded electrodes. This refers to whether or not the electrode flags are cemented or not to the metal clip holder which holds the crystal and which fits inside a standard HC-6/U lid.

10-MHz working crystals were chosen for all experiments for several reasons. The limiting reason was that the circuit itself was designed to work in this frequency range. 10-MHz is also a good choice for nominal frequency since it is higher than the 5- and 6-MHz crystals that have been used in some TSM sensor reports, and hence provides greater sensitivity according to the Sauerbrey equation, yet is not of such a high frequency that the crystal becomes too thin and fragile for being clamped into the housing unit. Gold (1000 Å) was chosen as the electrode material for all experiments since it is an excellent electrical conductor and lends itself to examination of coatings based on alkylthiol compounds, which were of interest in some experiments and are widely known to form self-assembled monolayers on gold substrates. Gold is also the most common electrode material used in the literature. In addition, a 50-Å chromium underlayer was used to improve adhesion. The crystal electrodes have a diameter of 0.201" (0.51 cm) and the crystals themselves a diameter of 0.538" (1.37 cm).

2.4 Housing Unit for One-Sided Liquid-Phase Experiments

One of our early ideas for a TSM sensing application involved real-time sensing in an aqueous environment. Since crystal oscillation is known to be unstable when both crystal electrodes are exposed to conductive media (e.g., buffered solutions), it was decided that a housing unit should be constructed that would secure the crystal in a position in which only one face was exposed to the liquid. This housing unit is shown in Figures 2.3 - 2.6.

In the housing unit the crystal (unbonded) is secured vertically between 2 blocks of plexiglas. Although there have been literature reports of housing units with the crystal in both horizontal and vertical positions, we decided that a vertical position was preferable in our experiments in order to better distinguish frequency changes resulting from actual binding from those arising from sedimentation phenomena. The design in Figure 2.3 exposes one electrode (onto which a coating can be placed) to a 400-μL chamber accessible by syringe through a vertical channel (block 1), while the other electrode remains exposed to a closed air chamber. As mentioned, the exposure of only one electrode to solution is employed in order to avoid the frequency instability (ie. short-circuiting) that would occur with two electrodes being exposed to a common, conductive medium. The use of a closed chamber (constant environment) for the uncoated electrode helps minimize noise/drift due to mass or temperature changes at this electrode. This design is simpler and less expensive than other designs which employ a constant flow of nitrogen across the unused electrode.[3,4]

The two blocks are clamped together with a steel clamp support. Two o-rings, one on each side of the crystal, are used to minimize direct pressure on the crystal and to provide a watertight seal. Electrical contact between the circuit and the crystal electrodes is achieved by the use of two strips of gold (cut from a piece of 99.99 % gold foil, 0.1 mm thick, Aldrich catalog number 26,581-0) which contact the extreme 1 mm of each electrode flag and extend horizontally to the outside of the clamped blocks. 1-cm long springs located in drilled holes within block 2 press the strips against the electrode flags, ensuring electrical contact. The small section of each gold strip extending out of each side of the clamped blocks is connected to the circuit using an alligator clip.

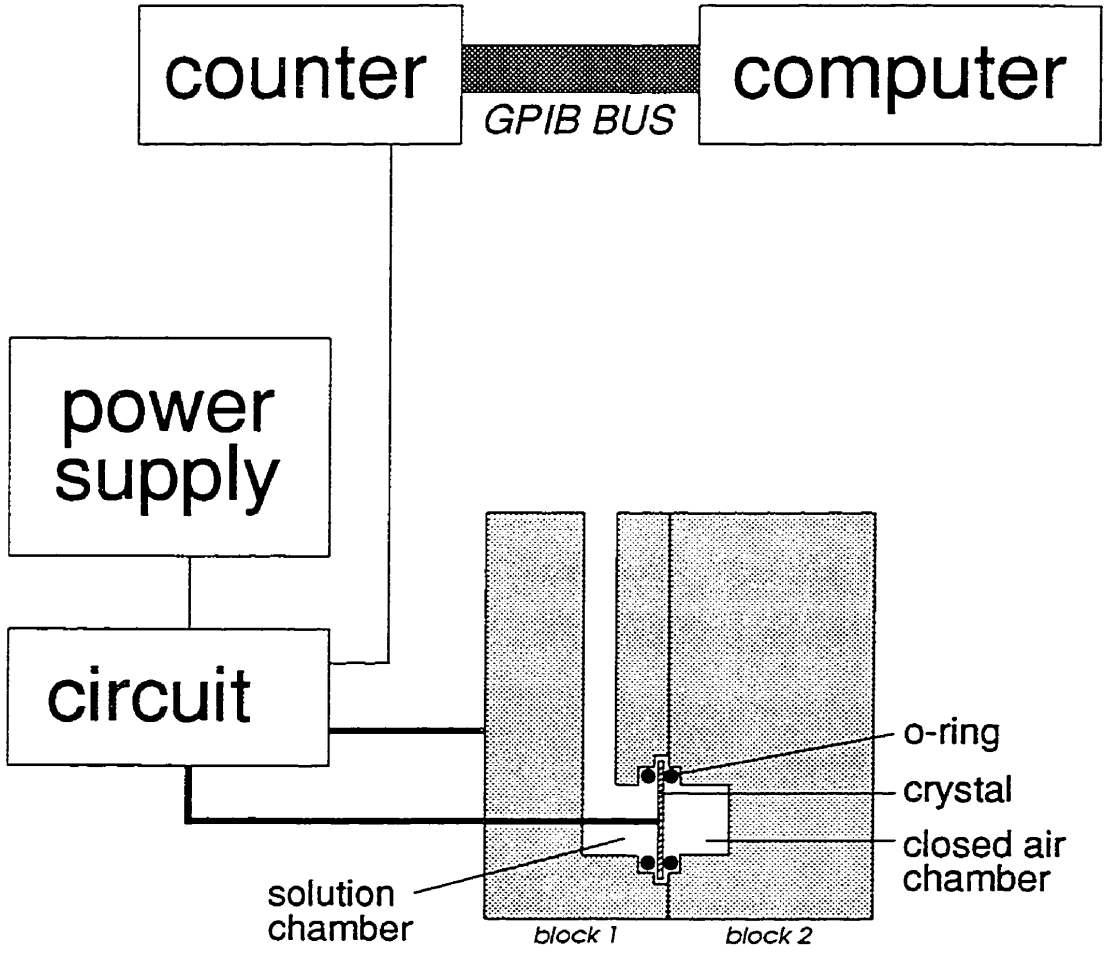

Figure 2.3 Housing unit (side view) and associated apparatus for liquid sensing applications where only one crystal face (electrode) is exposed to solution.

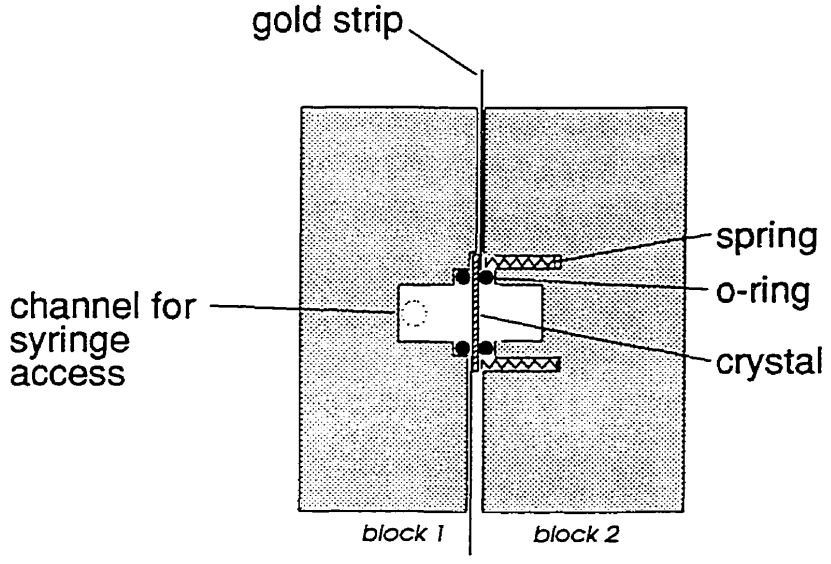

Figure 2.4 Top view of the one-sided crystal housing unit. The springs push the gold strips and crystal together to ensure electrical contact. Note that one gold strip contacts the electrode flag on one side of the crystal, while the other gold strip contacts the electrode flag on the other crystal face.

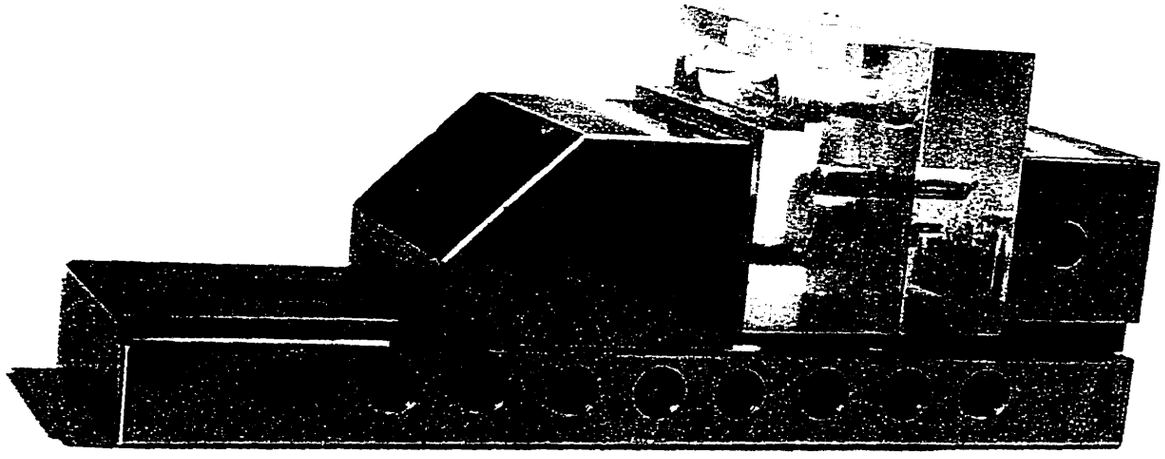

Figure 2.5 Photo of plexiglas housing unit where the two blocks are pressed together using a clamp.

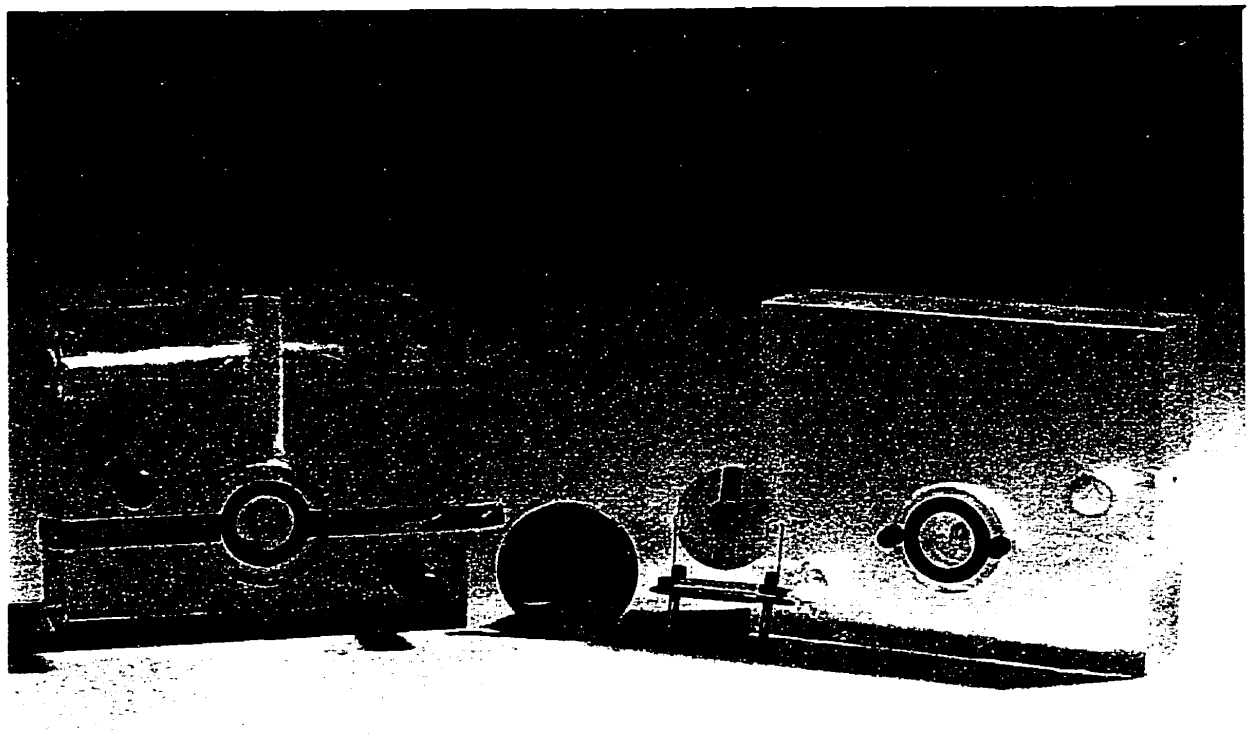

Figure 2.6 Photo of inside faces of the two plexiglas blocks. The piece holding the crystal is not used with the blocks, but *is* used with the full-immersion experiments described in chapter 4.

2.5 Three-Crystal Design for Accurate Long-Term Frequency Readings

Certain experiments involved fully-immersing the working crystal in organic solvent without the use of the housing apparatus described in the previous section. In these experiments, there were several occasions where the crystal was incubated in a coating solution for long periods of time (e.g., overnight). It was found that there was often a significant degree of drift during such long incubations, which was random in direction and not attributable to power-off/power-on switching (the power was switched off during overnight incubations). In order to overcome this problem and allow for accurate measurement of frequency changes due to coatings which were applied during long incubations, a special three-crystal modification was made to the circuit.

The three-crystal design is illustrated in Figure 2.7. Here, two of the crystals are the same as previously described, but an additional crystal is added. The third crystal (C3)(10-MHz, sealed in a HC-6/U holder) is located adjacent to the working/experimental crystal (C2) and connected to the same oscillator circuit in a similar manner. A toggle switch determines whether the frequency counter reads the difference between the circuit's reference 9-MHz crystal (C1)(sealed in a HC-6/U holder) and C2, or the difference between C1 and C3. Since C3 is sealed, any drift in its frequency is likely due to fluctuation in circuit ground or electromagnetic effects, which will have a similar effect on the frequency of C2. Thus, the frequency of C3 can be monitored periodically including before and after overnight incubations (during which the system is shut off), and frequency drift (typically < 10 Hz) observed at C3 is applied as a correction to the frequency changes occurring at the working crystal. The validity of this arrangement was confirmed with control experiments and proved invaluable in the accurate determination of the usually small frequency shifts obtained from both coating application and reaction of the coating with analyte. To the best of our knowledge, such a three-crystal compensation design has not been utilized previously.

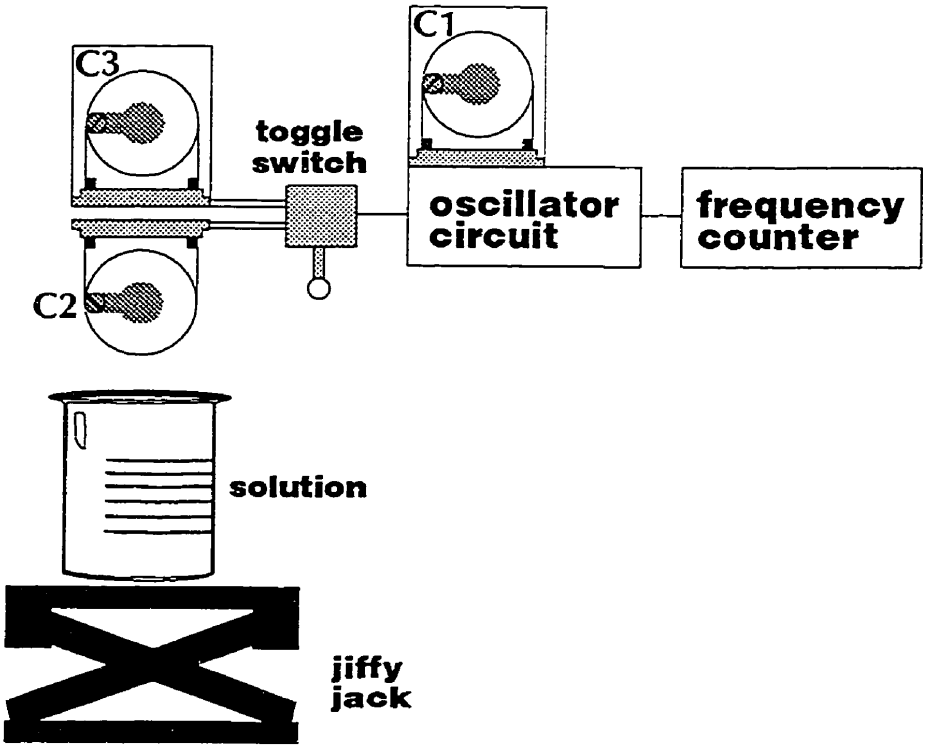

Figure 2.7 3-crystal arrangement for improving accuracy in frequency measurements for coatings applied over long periods of time.

References

1. S. Bruckenstein and M. Shay, *Electrochim. Acta* **1985**, *30(10)*, 1295-1300.
2. D. Lancaster, *TTL Cookbook*, Howard W. Sams & Co., Inc., Indianapolis IN, 1974, Chapter 2.
3. H. Su, K.M.R. Kallury, M.Thompson and A.Roach, *Anal. Chem.* **1994**, *66(6)*, 769-777.
4. H. Su and M. Thompson, *Biosens. Bioelectron.* **1995**, *10(3/4)*, 329-340.

3 Bile Acid Measurements Using A Cholestyramine-Coated TSM Acoustic Wave Sensor

3.1 Introduction

The earliest idea that was put forward for a novel application of the TSM sensor was a clinical one, which was in keeping with the tradition of research in Professor Purdy's lab. However owing to the contrast of the exacting technological demands of the project and our relative inexperience with acoustic wave sensing devices, we quickly beat a hasty retreat and opted for a simpler application, but still with clinical significance. The original idea however remains of considerable interest and we briefly make note of it here, both as a marker of how the bile acid project came into being and as a suggestion for further research. The research project that was envisioned involved constructing an artificial arterial system and using a suitably coated piezoelectric crystal as a mass-sensitive insert within this system to monitor deposition processes associated with atherosclerosis. A short summary of atherosclerosis follows (modified from reference 1).

3.1.1 Atherosclerosis

Atherosclerosis is often referred to as "hardening of the arteries". This is actually a complex disease which involves tumor-like growths in the walls of arteries. These tumors accumulate high-cholesterol fat and grow to obstruct blood flow through the artery. As the fatty tumors age and grow, they become scarred and often calcified. Restricted blood flow to any organ reduces its ability to function and obstruction leads to death of tissue. Sudden obstruction of a narrowed blood vessel is often caused by a clot forming in a narrowed region of the vessel (thrombosis). If the tissue is vital,

such as heart or brain, arterial obstruction may be lethal or, at best, disabling.

Serum cholesterol is a predictor of coronary heart disease (but not strokes), and current recommendations set target goals of less than 200 mg % for blood levels. Cholesterol is incorporated with protein into transport packages, travelling in the blood. These are lipoproteins. Low density lipoprotein (LDL) is "bad cholesterol" since it seems to accumulate in blood vessel walls, plugging them. This fatty tumor growth in arterial walls is known as atherosclerosis. Atherosclerosis causes half of all deaths in the U.S. Half of all North Americans have high fat diets associated with elevated blood LDL. High density lipoprotein (HDL), another form of cholesterol travelling in the blood, is "good cholesterol". The ratio of HDL to LDL should be as high as possible.

Circulating LDL is a spherical packet containing 1500 molecules of cholesterol attached to fatty acids and surrounded by an envelope of phospholipid. A single protein, attached to the LDL sphere like a handle, allows it to bind to receptors (LDLR) on the surfaces of cells. The protein handle, apolipoprotein, is essential for LDL clearing, and deficiencies in it lead to another type of "fat transport disorder". Circulating LDL is removed when the apolipoprotein binds to LDLR on cell surfaces. The receptor moves the LDL packet into the cell which then metabolically processes its contents. Liver cells remove half the circulating LDL. A typical LDL sphere lasts 2-3 days in the blood stream. If LDL clearing is impaired, fat accumulates in the blood.

Some of the LDL in the blood makes its way into the arterial wall where it tends to lodge as an extracellular deposit. Oxidation of LDL by oxygen free radicals seems to damage arterial wall by activating macrophages, immune cells which then organize a damaging inflammatory response. Gradually, a fat-containing inflammatory tumor develops in the arterial wall, growing outward to obstruct the flow of blood. Fat tends to accumulate in the arterial surface where blood flow is turbulent. Arteries branch like trees, and the first turbulent areas to develop fatty plaque are the points of bifurcation of the blood vessels. Once a fatty plaque pushes into the lumen of the artery, more turbulence develops, which promotes more fatty deposition. Obviously, any deficiency or defects of LDLR will reduce the ability of clearing blood LDL. A

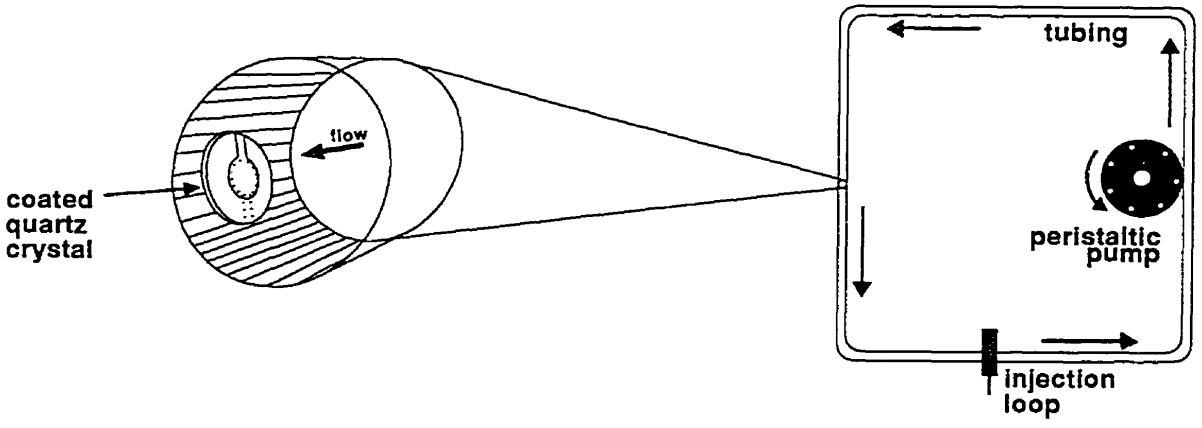

Figure 3.1 Sketch of foundation for a TSM sensor experimental system for *in vitro* study of processes associated with atherosclerosis.

genetic disorder, familial hypercholesterolemia, arises when the LDLR is defective and blood LDL cannot be cleared.

3.1.2 Hypothetical *In Vitro* TSM Sensor Experiment

Figure 3.1 provides an illustration of what the experimental system might look like. Atherosclerosis, as indicated in the preceding section, is a complicated process in which many factors come into play. No experimental system, however well-designed, would be able to thoroughly mimic the *in-vivo* situation. Aside from the complexity and interdependent nature of arterial processes, the experimental design would ideally also entail temperature and internal pressure control to simulate physiological conditions. Nevertheless, it is clear that a suitably designed system could still allow for a large number of relevant *in-vitro* investigations relating to processes involved in atherosclerosis. For example, phospholipid bilayer coatings with incorporated receptors for LDL could be used to monitor interactions with circulating LDL, or fat- and cholesterol-rich coatings could be used to examine deposition rates

of several species under various conditions. Certainly many other studies could be envisioned, and the project remains an intriguing prospect for an interdisciplinary collaboration.

It was in the course of doing background research on atherosclerosis that the idea for investigating bile salt/bile salt sequestrant interactions with the TSM sensor presented itself. The idea had appeal not only because it involved a simpler and more focused system but was also a highly relevant system as well, since bile acid sequestrants are used by millions of people for lowering cholesterol. Bile acids and their relationship to serum cholesterol levels are described in the following section.

3.2 Bile Acids

3.2.1 Structure of Bile Acids

The structure for several of the most common bile acids is given in Figure 3.2. The structure of cholesterol is also provided for comparison. Most of the naturally occurring bile acids are C-24 saturated carboxylic acids that belong to the steroid family. The cyclopentanophenanthrene nucleus of bile acids contains 19 carbon atoms and consists of three six-membered rings and one five-membered ring. The skeleton with a C-5 chain is termed the cholane nucleus, and so the bile acid without hydroxylic substituents is termed cholanoic acid. In the bile acids of vertebrates, the rings A and B are usually of *cis* (5ß) configuration, but in some animal species the AB *trans* (5α or allo) configuration can occur. The BC and CD ring junctures are *trans* and the methyl group at position C13 is *cis* to that of position C10.

Cholic, glycocholic and taurocholic acids are all trihydroxy bile acids, having three hydroxyl groups attached to the otherwise hydrophobic steroid backbone. The side chains of the conjugated bile acids are longer and more polar than in the unconjugated cholic acid, as the carboxyl group is covalently bonded in a polar peptide linkage to an amino acid (glycine or taurine). Dihydroxy bile acids include deoxycholic, chenodeoxycholic, glycodeoxycholic, glycochenodeoxycholic, taurodeoxycholic and taurochenodeoxycholic acid. The greater variety of dihydroxy species occurs since the two hydroxyl groups can be attached to carbons 3/7 or to

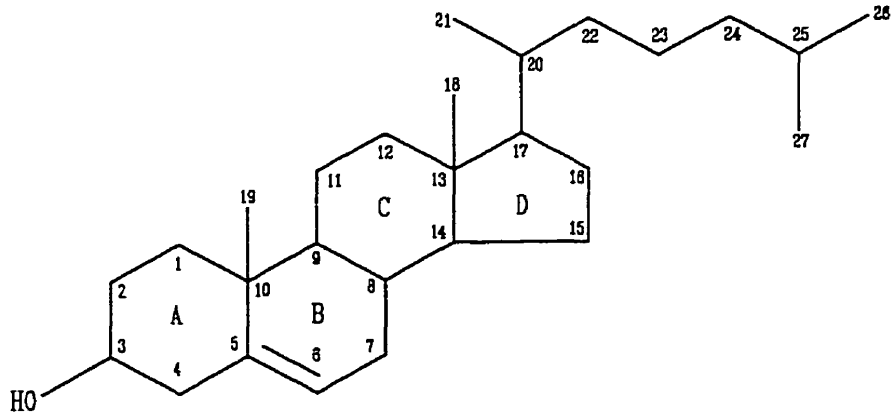

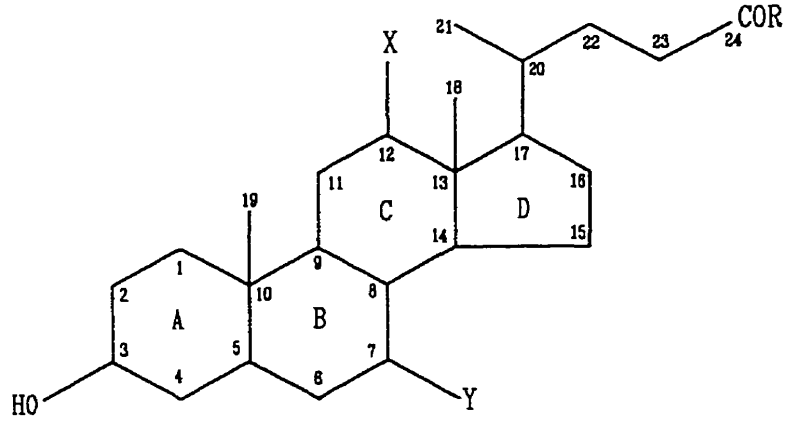

R	X	Y	bile acid
OH	OH	OH	cholic
	OH	H	deoxycholic
	H	OH	chenodeoxycholic
	H	H	lithocholic
NH-CH2-COOH	OH	OH	glycocholic
	OH	H	glycodeoxycholic
	H	OH	glycochenodeoxycholic
NH-CH2-SO3H	OH	OH	taurocholic
	OH	H	taurodeoxycholic
	H	OH	taurochenodeoxycholic

Figure 3.2 Chemical structure of cholesterol (top) and bile acids (below). The numbering of the steroid skeleton system is also given. Bile acids studied with the TSM sensor are underlined.

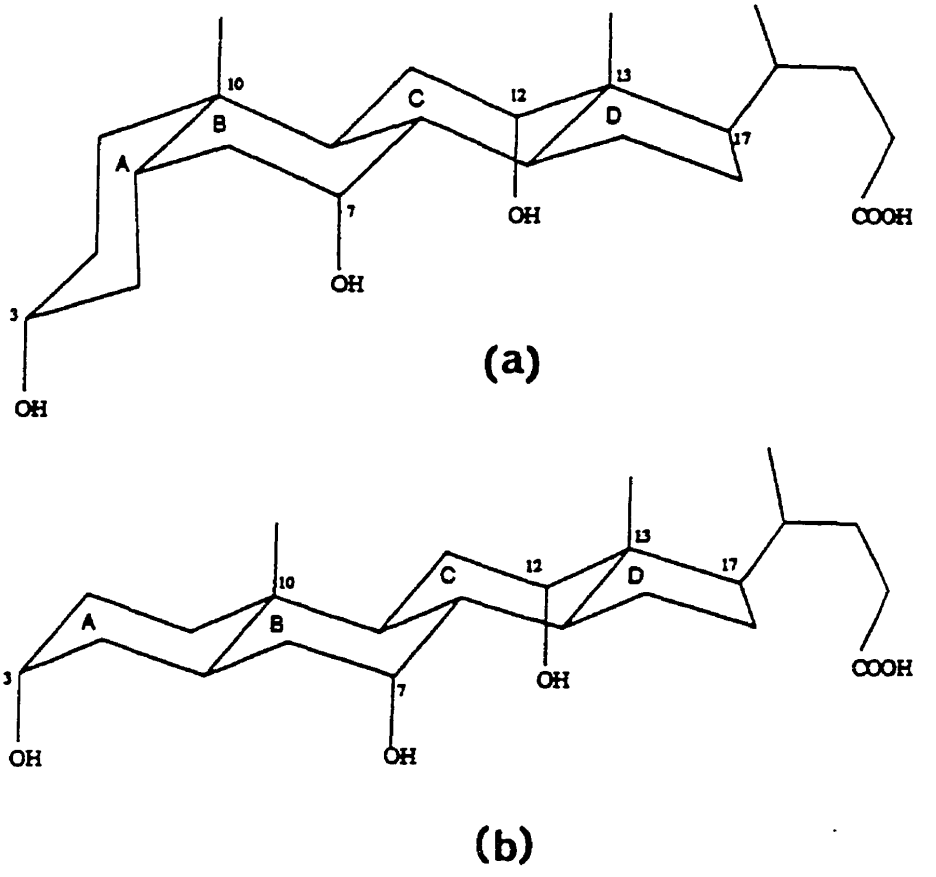

Figure 3.3 The chemical configuration of cholic acid: (a) the commonly occuring 5ß-configuration; (b) the *allo* or 5α-configuarion.

carbons 3/12. Lithocholic acid has only one hydroxyl group, attached to carbon 3. The hydroxyl groups are all in α- or equatorial positions. The carboxyl group is also equatorially oriented. Hence, the hydrophillic groups, i.e., the hydroxyl and carboxyl groups, are all located beneath the plane of the steroid skeleton, while the amphiphilic methyl groups lie on the other side of the skeleton (Figure 3.3). This planar polarity of the molecules is important in the physico-chemical properties of bile salts.

According to Carey,[2] the apparent pK_a values of the free (i.e., unconjugated) bile acids are higher than those of the conjugated bile acids, ranging from 5 to 6.5. The pK_a values of the glycine conjugates fall in the range of 4 to 5. The taurine conjugates have been estimated to dissociate at a much lower pH of -1.5 to 1.5. Other values have also been reported.[3,4] A recent study by NMR titration has assigned a pK_a of 4.6 to cholic acid.[4] At pH values above the pK_a, bile acids are unprotonated and exist in their salt form, usually with sodium or potassium as the counterion. This allows them to form organized molecular assemblies termed *micelles* above a certain concentration termed the *critical micelle concentration* (CMC).

3.2.2 Bile Acids and the Enterohepatic Circulation

Bile acids are produced in the liver and stored in the gallbladder as a component of bile. The major bile acids present in human bile are the glycine and taurine conjugates. During digestion, the gallbladder contracts and excretes bile into the small intestine (duodenum). Since intestinal pH is close to 7,[5] the bile acids exist in their salt form and are present as micelles in equilibrium with their monomers. Bile salt micelles possess a hydrophilic exterior and hydrophobic interior which allows for solubilization of substances with low solubility in water (e.g., fats). They thus serve to emulsify ingested fats and thereby promote digestion. After participating in the absorption of fats in the jejunum, the bile salts pass down to the ileum where they are absorbed and returned to the liver via hepatic portal veins. This circulation of bile salts between the intestine and the liver is termed the *enterohepatic circulation* (Figure 3.4). The enterohepatic circulation is thus an important mechanism in facilitating the excretion of sterols and the digestion of dietary lipids. Failure of the enterohepatic circulation of the bile salts results in malabsorption of lipids and of the fat-soluble vitamins.

The re-absorption of bile acids in the ileum depends on several factors, such as gallbladder emptying, interdigestive mobility,[7] the physical state of the intestinal contents, and the structure of the bile acid molecules after modification by intestinal bacteria. In the lower ileum and colon some bile salts undergo deconjugation and 7α-dehydroxylation under the action of enzymes of the intestinal flora. Overall though,

the enterohepatic circulation is a very efficient process. Each day the bile pool, which contains about 3-5 grams of bile acids, can be cycled 6 to 10 times with only a small loss of bile salts, as little as 500 mg per day or a 1% loss per cycle.

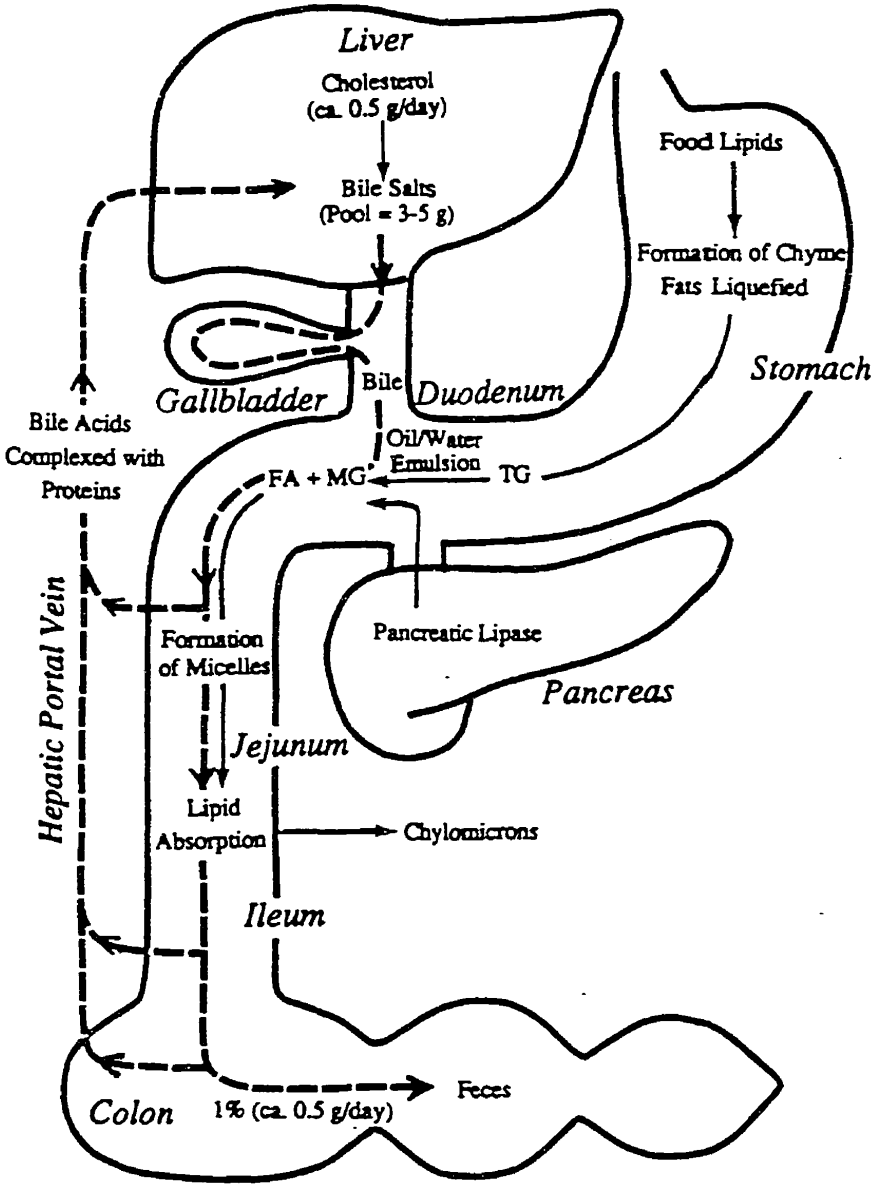

Figure 3.4 The enterohepatic circulation of bile acids and the digestion of lipids (modified from reference 6). The dashes indicate the route of circulation; TG: triacylglycerol; MG: monoacylglycerol; FA: long-chain fatty acid.

3.2.3 Synthesis of Bile Acids From Cholesterol

Under normal conditions, bile acids are synthesized from cholesterol by the liver at about the same rate as bile acids are lost in the feces. This represents the only major route for elimination of cholesterol from the body, and maintains the necessary pool of bile acids. The conversion of cholesterol to the individual bile salts involves introduction of one or two additional hydroxyl groups, all in the α-configuration, and the partial oxidation of the aliphatic side chain to introduce a carboxyl group.

The bile salts not only require cholesterol in their formation, but they can also form molecular complexes with unchanged cholesterol; in so doing, they facilitate the excretion of still more cholesterol through the bile.[8] If the molecular complex between the bile salts and cholesterol becomes dissociated in the gallbladder, as sometimes happens during infectious processes, the cholesterol can deposit about some microscopic nidus to form gallstones, which may grow to the size of large marbles, and which often contain 60 to 99 percent cholesterol by weight.

3.2.4 Bile Acid Sequestrants and Cholesterol Reduction

From the preceding discussion it is evident that any mechanism that can reduce the amount of bile acids in circulation will stimulate the oxidation of cholesterol to bile acid in the liver in order to restore the bile acid pool. The ability to invoke this mechanism could therefore serve as a means for lowering cholesterol levels and limiting the progress of atherosclerosis. This is commonly achieved through the use of bile acid sequestrants.

The use of bile acid sequestering agents is indicated as adjunctive therapy to diet and exercise for the reduction of elevated serum cholesterol in patients with primary hypercholesterolemia.[9] These agents are typically non-absorbable resins which bind bile salts in the gut, interrupting the enterohepatic circulation and increasing fecal bile acid excretion. The resulting decrease in the bile acid pool stimulates the liver to oxidize cholesterol to bile acid, thereby lowering serum cholesterol levels.[10-14]

Among the bile acid sequestering agents, cholestyramine is the most widely studied and used. It is commercially available as the active ingredient in a powder for

oral suspension.[15] Many reports have demonstrated the utility of this resin in lowering serum cholesterol levels and in reducing the risks of coronary heart disease and myocardial infarction.[16-19] In addition to *in vivo* studies, many *in vitro* studies have been carried out to investigate the cholestyramine - bile acid binding process. Both types of studies have demonstrated the superior affinity of this resin for bile salt anions compared with natural fibers[20-22] and other resins.[23-25]

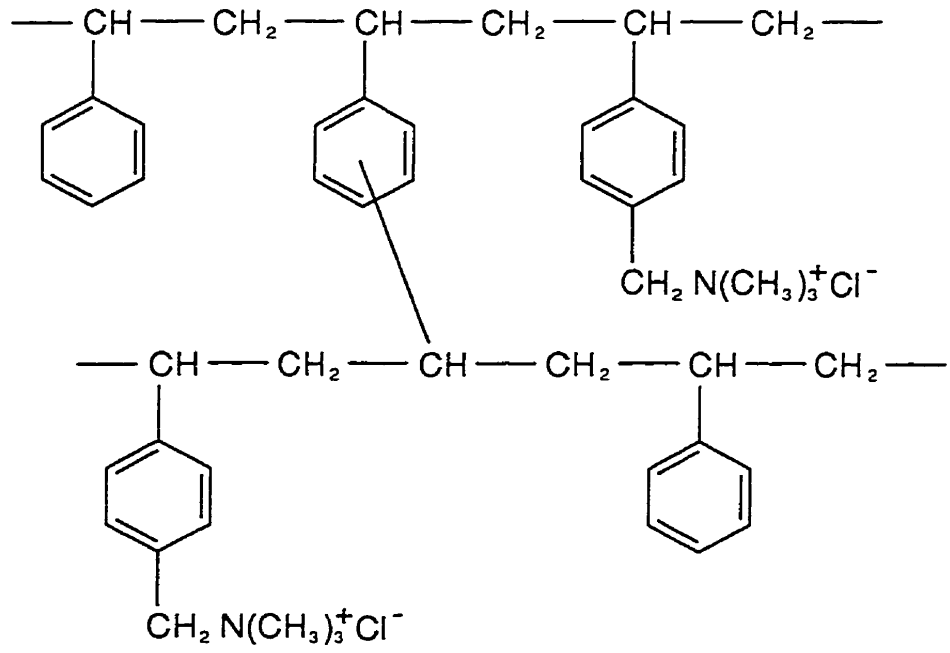

Figure 3.5 Structure of cholestyramine.

Cholestyramine is a styrene-divinylbenzene copolymer bearing quaternary ammonium groups (Figure 3.5). Its bile acid sequestering ability has been proposed to operate mainly through the ionic interaction of the positively charged ammonium group and the negative charge on the ionized form of the bile acid, i.e., ion-exchange.[26,27] However, several reports have also indicated that hydrophobic interactions may also be important.[24,28-30]

3.3 A TSM Sensor for Bile Acids

The potential utility of cholestyramine as a TSM acoustic wave sensor coating was investigated. The interest in the use of this sequestrant resin as a coating material was two-fold. First, use of this coating could allow for a simple and direct method of investigating the cholestyramine - bile salt interaction, an interaction which is of significance to millions of people who use cholestyramine for treatment of hypercholesterolemia. Second, the interaction between bile salts and the coating could serve as the foundation for a novel bile acid sensor. Initial studies indicated that the coating could be easily immobilized, and frequency changes were observed upon introduction of bile salts into a buffered solution to which the coated crystal was exposed. The full characterization of the sensor system was then undertaken.

3.3.1 Materials

Cholestyramine resin was purchased from ICN Biochemicals (Cleveland, OH). The listed mesh size for the resin is 50-100, with an average particle size of 150 μm. The sodium salts of cholic acid, glycocholic acid, taurocholic acid and taurodeoxycholic acid were purchased from Sigma. HPLC-grade methanol (Fisher) was used in coating regeneration. All reagents were used as received. Stock buffer solution was prepared with $NaH_2PO_4 \cdot H_2O$ and sodium hydroxide to give a 0.005 M phosphate buffer of pH 7.2 (unless otherwise indicated, all references to buffer used in the experiments refer to this buffer). Stock analyte solutions (0.01 M) were made for all four bile salts in both buffer and water. All water used was doubly distilled, deionized, and passed through an organic filter cartridge.

3.3.2 Apparatus

The sensor system has already been described in Chapter 2 and illustrated in Figures 2.3 - 2.6. This housing unit exposes only one crystal face (having the coated electrode) to the solution chamber (volume 400 μL). 10-MHz AT-cut quartz crystals were purchased from International Crystal Manufacturing Co. (Oklahoma City, OK) with unpolished electrodes on both sides consisting of 1000 Å Au with a 50 Å Cr underlayer. The specified finish of the electrodes is 3-5 micron. Frequency data were

recorded either manually or collected automatically by software controlling a GPIB bus connected to the counter (see Appendix 1 for software routine). All assays were performed at ambient temperature (~ 22 °C).

3.3.3 Coating Procedure

A concentrated aqueous suspension of cholestyramine resin was made and a 500-µL syringe was used to apply two drops of this suspension to the circular electrode region on one side of the crystal. Each drop was spread to cover the central ~ 95%, and the first drop was allowed to air-dry before applying the second drop. Although some sensor response is lost since coating is not applied to 100% of the piezoelectrically active region (i.e., the electrode), this contribution is likely insignificant since it has been shown that the mass sensitivity exhibits a Gaussian distribution and is greatest at the center of the electrode, decreasing monotonically toward the electrode edge.[31,32] After the second drop had dried, the crystal was submerged in a small beaker of water and sonicated for 10s to shake off loose resin particles. Omission of the sonication step resulted in frequency increases over the first several assays, due to bile salt binding to and detaching loose particles of resin.

3.3.4 Determination of Frequency Response

After stabilization of the frequency in 400 µl of water or buffer for a period of 5-10 minutes, an aliquot (5-80 µL) of the bile salt solution is injected into the chamber. Immediately after injection the chamber solution was manually agitated for about 3s using the syringe, and then the syringe was withdrawn.

The time profile of the frequency decrease proved dependent on the extent of agitation. To improve the precision in replicate measurements, the following procedure was adopted for all experiments. First, upon injection and initial agitation, the chamber solution was left alone and binding was allowed to proceed for a period of 10 minutes (minimum) or until the frequency decrease was ≤ 4 Hz/minute for two consecutive minutes. At this point, the syringe was again used to agitate the solution for 2s, and if necessary frequency readings continued to be recorded until the frequency decrease was ≤ 4 Hz/min for two consecutive minutes. Frequency readings are recorded once

per minute before and after injection.

The frequency response is calculated as the last reading before injection minus the lowest reading after injection. In all assays, any drift observed during the initial stabilization period was calculated in terms of Hz/min and applied as a correction according to the number of minutes involved in the assay following bile salt injection. In most cases the drift was negligible or was steady at between 0.3 - 0.6 Hz/min. Also, based on injections of buffer alone into buffer, a blank correction of -3 Hz/10 µL is applied to correct for small frequency increases that result from an increase in the pressure of the chamber solution on the crystal.

After each assay, the bile salt was removed from the cholestyramine coating using a series of sequential washes with various solutions. The coating was allowed to equilibrate with each 400-µL wash for a period of one minute. Hundreds of regeneration assays employing a constant injected amount of bile salt were performed, probing the effects of wash solution type, number and order (discussed later). When not in use the sensor crystal was stored in 1 M NaCl.

3.3.5 Basic Operation

A typical response to the injection of a 40-µL aliquot of buffered sodium glycocholate into buffer is shown in Figure 3.6. In curve A, the frequency is monitored for 10 minutes prior to injection, and a 4 Hz upward drift is observed during this period. Immediately following the last baseline reading, 40 µL of 0.01 M sodium glycocholate is injected and the syringe is briefly agitated. The frequency is observed to drop quickly, with over half of the frequency decrease occurring within the first minute. The frequency in this case equilibrated within 7 minutes. After 10 minutes the syringe is again used to briefly agitate the solution, and a slight increase is observed. According to the established protocol (see Experimental section), the frequency response is calculated as 989910 - 989719 + 4 = 195 Hz. The blank-corrected response is 195 - 12 = 183 Hz. Control experiments with an uncoated crystal showed no response to injection of bile acid.

The importance of agitation is illustrated in Figure 3.6B. Here, the bile salt is injected slowly with no agitation, resulting in minimal disruption of the solution, and

the frequency drops slowly during the first ten minutes. At 10 minutes, the syringe is used to briefly agitate the solution, producing a final (drift/blank-corrected) frequency decrease of 188 Hz. The protocol represented in Figure 3.6A was thus used for all experiments, since this method required shorter analysis times.

In most cases the second agitation produced either no frequency change, or a small rise (5-20 Hz). In some cases however it produced an additional frequency decrease (15-50 Hz) which was necessary to include in order to bring the final reading within 5-15 Hz of values observed in cases when the second agitation produced no frequency decrease. This is a result of the difficulty involved in applying the exact same degree of agitation following manual injection. The use of a magnetic stirring bar was ruled out since experiments performed with constant (manual) agitation during the first 10 minutes of binding showed that continuous disruption of the solution delayed or prevented attaining the maximum frequency decrease. The protocol

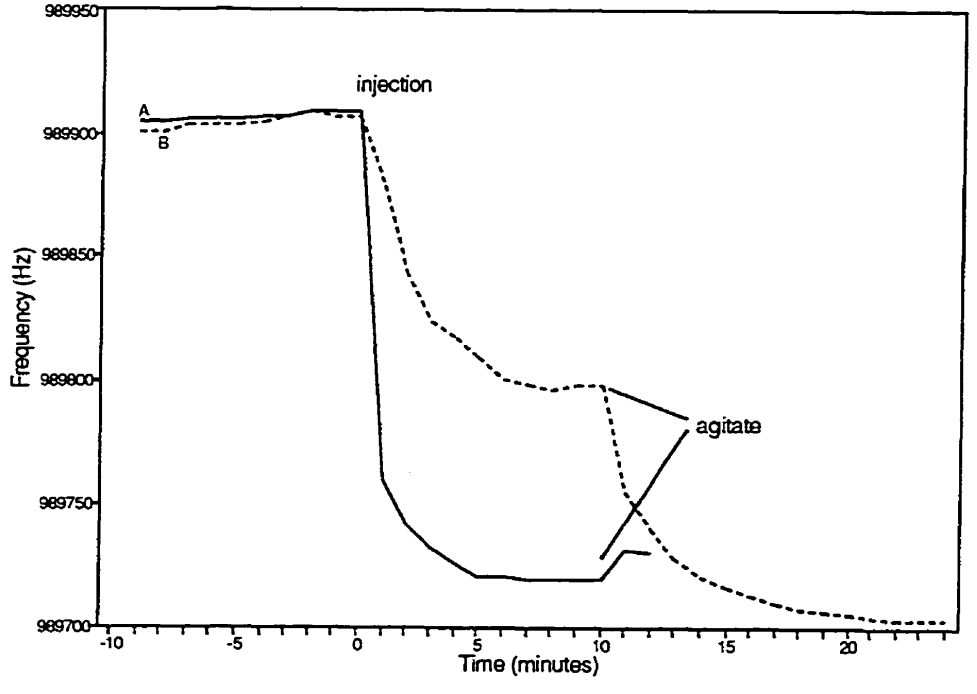

Figure 3.6 Typical response to 1 mM sodium glycocholate in buffer with (A) and without (B) agitation at time of injection. The solution is also agitated at t = 10 min.

described in section 3.3.4 for determining the final frequency decrease in each binding experiment resulted in improved precision in replicate measurements without unduly long assay times.

3.3.6 Nernst Film Model of System

The effect of agitation noted here is consistent with the model of a thin film, called the Nernst film, surrounding the resin particles.[33] In this model, the external solution forms a thin stagnant film on the resin particles with the result that exchange of ions between the resin and the bulk solution is limited by diffusion through this layer. Johns and Bates,[34] performing studies in which cholestyramine resin and bile salt were agitated together in a flask with a 3-blade propeller at different rates, observed that the binding rate constant for both glycocholate and glycodeoxycholate increased with increasing agitation intensity. They concluded that the rate of binding was dependant on the rate of diffusion through the Nernst layer, and that as the speed of agitation of the medium is increased the thickness of this film is reduced. Similarly, in our studies the brief but moderately vigorous manual syringe agitation immediately following injection likely eliminates or at least reduces the thickness of the Nernst film that was built up during the stabilization period.

3.3.7 Comparison of Sensor Response with Previous Reports

Equilibration times between bile anions and cholestyramine have also been examined by other researchers. Benson *et al.*[35] found that with continuous stirring the binding of glycocholic acid, taurocholic acid and taurochenodeoxycholic acid was essentially complete within 6 minutes, with most of the binding occurring within the first couple of minutes. Whiteside *et al.*[36] observed that when sodium cholate was shaken mechanically with cholestyramine most of the binding occurred within one minute, and after 20 minutes binding of cholate was not further increased. De Simone *et al.*[23] also found that maximal binding of sodium cholate with cholestyramine occurred within 20 minutes. Our results also indicate that the binding of all four bile acids studied was > 90% complete within 10 minutes in most cases, with most of the binding occurring within the first minute.

The observation of the binding process in real time is the first such report to our knowledge. *In vitro* studies that have examined the time-profile of the cholestyramine - bile salt binding process have typically involved (i) aliquots of bile salt solution being withdrawn at specified time intervals from a single reaction vessel,[30,34,35] or (ii) aliquots of bile salt solution being withdrawn from a series of vessels that have equilibrated a fixed amount of bile salt and resin for different periods of time.[36] These procedures are more time-consuming, requiring an additional filtration step to separate the resin from the bile salt solution before analysis.

The observation of the negligible or small frequency increase usually observed upon agitation when final binding equilibrium had been attained (e.g., Fig 3.6A at 10 min.) is significant. It indicates that physical motion/disruption in itself has a limited effect on desorbing bound bile salt anions, which is of relevance to the *in vivo* therapeutic action of this resin. This is in agreement with other *in vitro* experiments (mentioned earlier) which demonstrate that even under conditions of continuous agitation, significant (near-saturation) levels of adsorption take place within 20 minutes.[35,36] Also noteworthy is the finding that the binding process is essentially the same at 25°C and 37°C.[28,37] As well, the phosphate buffer concentration employed (5 mM) is within the 1-10 mM range estimated to be present in the small intestine.[38] Thus the present sensor system, even though it operates at room temperature under static conditions, may still be useful for predicting *in vivo* behavior.

In terms of the frequency response, it is likely that in addition to simple mass effects the frequency is influenced by changes in the viscoelasticity of the resin coating layer. For example, when an uncoated crystal is rinsed with water, the water disperses from the gold electrode surface quickly (onto the surrounding quartz). However, when a cholestyramine-coated crystal is rinsed with water, a visible wetting of the coating takes place, and several minutes are required for the coating to dry. Thus rather than having a "tight" uniform structure, the coating appears to have an open-pore sponge-like structure, and the sequestration of bile acid is likely to have some influence on the viscoelastic properties of the coating. The importance of such influences on the frequency response has been noted by others.[39,40]

3.3.8 Coating Regeneration

The ability to remove bound analyte and regenerate the coating is of central importance in the development of acoustic wave chemical sensors. In the case of the present sensor system, a number of defining criteria may be established in the evaluation of a regenerative protocol. First, the protocol should remove a maximum amount of bile anions and leave the resin in a state ready to produce a maximum signal upon subsequent introduction of bile salt. Second, it should do so quickly and reproducibly. And third, a steady frequency reading should be attained immediately upon the completion of the protocol. To this end, many experiments were conducted to study the effects of reagent type, concentration, sequence and duration on coating regeneration.

A sampling of these studies is provided in Table 3.1. Twenty-five sequential injections of a constant amount of sodium cholate were performed with the same coating. Between each injection the coating was regenerated with a 7-minute wash cycle consisting of seven 1-minute incubations with various solutions. Each protocol was repeated 5 times before proceeding to the next protocol. In all protocols the final 3 washes used were phosphate buffer in order to ensure a constant injection medium.

The most effective regeneration protocol in Table 3.1 was number 2, and involved seven 1-minute incubations of the crystal with various solutions (400 μL each), including two initial washes with 1 M sodium chloride, followed by two washes with concentrated (0.5 M) phosphate buffer, and finally three washes with regular phosphate buffer. Other protocols, in which the sodium chloride or concentrated buffer washes were omitted or replaced with water or regular buffer washes, resulted in either (i) lower but relatively constant $-\Delta F$ values for injection of bile acid, or (ii) progressively lower and lower $-\Delta F$ values for injection of bile acid. A one-minute duration for each wash was adopted since most of the effect of each wash occurred within this time interval.

The requirement for solutions of high ionic strength in the displacement of bound bile salts was evident in our studies. For example, when the regeneration protocol consists of seven sequential washes with phosphate buffer, each one minute in duration (protocol 4 in Table 3.1), there is a progressive decrease in the frequency

Table 3.1 Regeneration and Precision Data for 1 mM Sodium Cholate[a]

	Regeneration Protocol				
	1	2	3	4	5
	NaCl[b]	NaCl	T	buffer	NaCl
	NaCl	NaCl	T	buffer	NaCl
	H_2O	T[c]	buffer	buffer	NaCl
	H_2O	T[d]	buffer	buffer	NaCl
	buffer	buffer	buffer	buffer	buffer
	buffer	buffer	buffer	buffer	buffer
	buffer	buffer	buffer	buffer	buffer
-ΔF	153	185	196	140	156
	163	185	190	134	171
	156	197	180	124	161
	152	179	169	119	154
	159	182	157	100	160
mean	157	186	178	123	160
STD	4.5	6.8	15.8	15.5	6.6
RSD (%)	2.9	3.7	8.8	12.5	4.1

[a]44 µL of 0.01 M sodium cholate in buffer injected into 400 µL of buffer. Buffer is 0.005 M phosphate pH 7.2. [b]1 M. [c]T=0.5 M phosphate buffer pH 7.2. All values expressed in Hz before blank correction. [d] See text.

response to injection of bile acid (-ΔF decreases about 10 Hz from one assay to the next). However the use of more concentrated ionic solutions (such as 1 M sodium chloride) considerably improves the coating regeneration. The importance of such mass-action processes has been noted before[27] and is of relevance to the *in vivo* conditions in the human gut. Since the buffer washes are the same as the injection medium, this regeneration protocol (buffer only) represents a simple shifting of bile anion equilibrium away from the resin. This situation is similar to that observed in the terminal ileum where an active transport mechanism continuously removes bile salts from the gut.[41] Our observations here support the view that based on equilibrium effects alone (i.e., not considering other interfering anions), the ileal uptake mechanism may result in a significant but not complete removal of cholestyramine-

bound bile anions. This mechanism has been suggested by others as a main cause of the low *in vivo* capacity of cholestyramine for bile salts (i.e., capacity per gram of resin).[27,35]

The strength of the resin - phosphate interaction is illustrated by at least two comparisons of data in Table 3.1. The first involves a comparison of protocols 1 and 2. It was noted that the mean frequency prior to injection in the last two assays of protocol 1 was 989055 ± 10 Hz, whereas the corresponding value for the first two assays in protocol 2 was 989227 ± 10 Hz (data not shown). That is, protocol 2 immediately produces a baseline about 170 Hz higher. It is uncertain as to why the frequency response to 1 mM sodium cholate only increases about 30 Hz (mean value for 5 replicate injections increases from 157 to 186 Hz), whereas the baseline increases 170 Hz in protocol 2. However, it is likely that concentrated buffer (T) is more effective than water in displacing both chloride ions (from the first two washes) and bile anions (still remaining after the first two washes). Thus the improvement in frequency response expected from greater removal of bile anions may be offset by the presence of a greater extent of monovalent and especially divalent phosphate ($H_2PO_4^-$ /HPO_4^{2-}, pK_2=7.2) counterions (vs. chloride) which are less easily displaced when bile salt is injected. The greater ionic bond strength that would exist between the positive quaternary ammonium groups of cholestyramine and the divalent phosphate anions supports this suggestion. The displacement of chloride by phosphate is confirmed by other experiments that were performed in which injections of chloride produced moderate frequency decreases with coatings treated by protocol 2. These latter experiments prove that the resin could not possibly be exclusively in the chloride form (since exchange of chloride for chloride would not affect the frequency), and also are consistent with the presence of a certain percentage of chloride counterions (after protocol 1) producing a lower baseline frequency.

The strength of the resin - phosphate interaction is also evident from a comparison between protocols 2 and 5. The lower response to cholate in the protocol 5 assays vs. those of protocol 2 implies that concentrated phosphate buffer is more effective than concentrated sodium chloride in displacing bile anions (compare washes 3/4 in both protocols). Again, the greater ionic bond strength between the resin and

a divalent counterion is certainly the causative factor. However, judging from protocol 3, certainly only two T washes are not sufficient in removing bile anions since while the mean frequency response for 5 assays was fairly good, the data indicated a slow drop in response from one assay to the next, indicating that bile anions are progressively accumulating on the regenerated resin.

In later experiments it was found that when the fourth wash in protocol 2 (indicated by footnote d) was changed to 2:1 water:methanol (which shall be referred to as protocol 2A), the frequency response to injected bile salt increased further (i.e., -ΔF was slightly larger), with a similar RSD. A detailed examination of the frequency

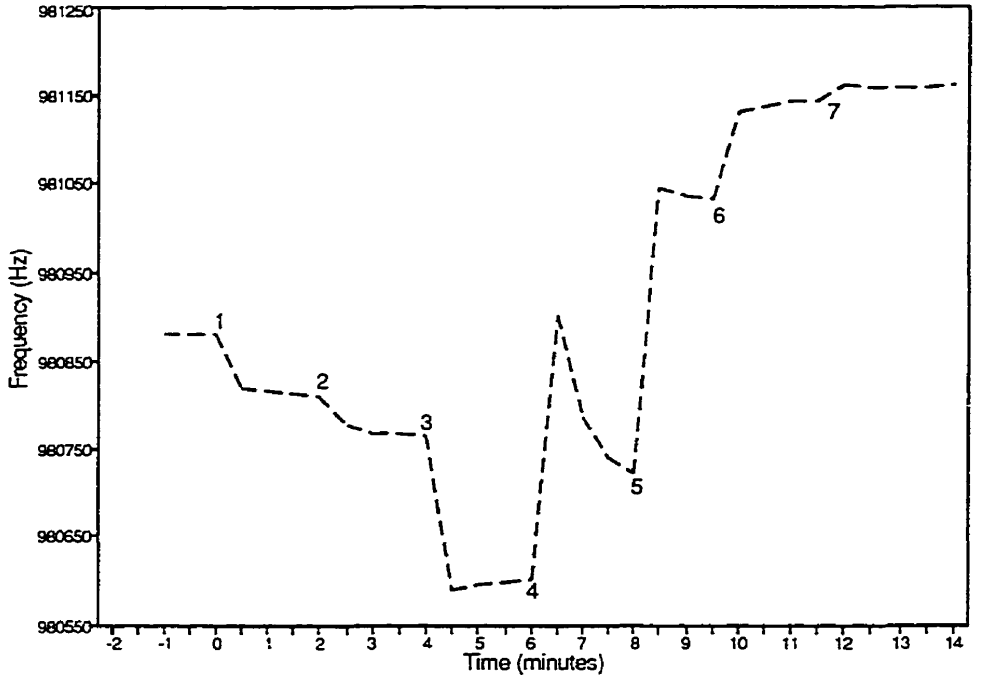

Figure 3.7 Frequency changes during the regeneration protocol. In this particular regeneration (only), the duration of each wash was increased from 1 to 2 min in order to better observe the effect of each wash. Note that the overall effect of the regeneration is to remove bile anions from the coating, which increases the resonant frequency back to its initial level. Washes: 1 M NaCl (1, 2), 0.5 M phosphate buffer pH 7.2 (3), 2:1 water/methanol (4), 0.005 M phosphate buffer pH 7.2 (5-7).

changes observed with protocol 2A is shown in Figure 3.7. The improvement here may be due to increased removal of bile anions and/or an increased resin swelling effect. This protocol enabled the coating to be reused in excess of 400 times over a period of 3 months with only a ≈ 20% drop in response, and this particular coated crystal, along with protocol 2A, was used in the acquisition of all calibration and interference data reported later in this chapter. Defining a lifetime as the point at which the response to 1 mM cholate drops below 100 Hz, other coated crystals had lifetimes ranging from 50-300 assays with other regeneration protocols.

Previous attempts at coating renewal with TSM acoustic wave sensors have only been moderately successful. These include immunosensors for human albumin,[42] *Salmonella typhimurium*,[43] herbicides,[44] and human IgG[45] reusable for 5, 6, 9 and 10 times, respectively. A reusable immunosensor for herpes viruses was developed by König and Grätzel[46] which could be used at least 18 times and was stable for 8 weeks. In some cases the coating itself has had limited stability in solution, being stable only for as little as a few hours.[47] In other applications either the coating is usable for only one assay,[48,49] the number of replicate measurements is not specified[50-52] or simply no attempt is made to regenerate the coating.[40,53] The best example to our knowledge of a reusable acoustic wave sensor is a surface transverse wave (STW) atrazine immunosensor demonstrated by Tom-Moy *et al.*[54] which was used for 100 repeated measurements. However, a 30% decrease in response was observed for 48 assays performed over 10 h, and the lifetime of the coating was not specified. Certainly, the cholestyramine coating described here lacks the specificity which operates in immunological-based TSM sensors. However, this type of coating is well-suited for reusable sensors since it is extremely stable,[55] insoluble in most solvents, and binds to analytes by non-covalent means, which facilitates regeneration. It is therefore proposed that ion-exchange resins such as cholestyramine may be of significant interest in the development of future TSM sensor applications where ionic and/or hydrophobic interactions can be exploited.

3.3.9 Calibration Curves

The four bile acids selected for study were cholic, glycocholic, taurocholic and

taurodeoxycholic acid (in the form of their sodium salts). These four were chosen in order to determine the effects of conjugation and number of hydroxy substituents on the sensor response. Their structures have been described in Section 3.2.1. These four bile acids are also commonly present in man, with the relative proportions depending on the kind of sample (serum, bile, etc).

All four bile acids exhibited an essentially linear response which plateaus at sufficiently high concentration. Calibration curves for experiments both with buffer and with water as the injection medium are shown in Figures 3.8 - 3.11. Correlation coefficients were generally good and support the use of a linear fit over the indicated working range (Table 3.2). The lower r-values observed in some cases can be attributed to two factors: (i) the reduced precision inherent in the manual operation of the sensor, and (ii) the fact that the calibration curves were established by changing the standard from one assay to the next. These factors combined to produce RSD values up to 10-20%, resulting in lowered correlation coefficients. However in Table 3.1 it is seen that RSD values for replicate sequential injections are generally much better (< 10%). Thus for future applications, if standards and samples are measured in replicate (n=3-4) before changing the standard/sample, RSD values should generally be no worse than 10%. Automation of the injection and regeneration steps may also improve precision.

The use of distilled, deionized water as the injection medium improved the sensitivity in all cases, and typically reduced detection limits by half compared to the use of buffer as injection medium. For these studies, protocol 2A was modified so that washes 5-7 were water instead of buffer. In water, ionic competition for binding sites is reduced, and the lower dielectric constant is expected to increase the attraction between the resin binding sites and the bile salt anions. As well, in water the resin counterion population is probably shifted from monovalent and divalent phosphate to monovalent phosphate and monovalent hydroxide. Since the pH of the water ($\approx$ 6.5) was less than that of the buffer (7.2), washes 5-7 shift the phosphate counterion equilibrium from the divalent to the monovalent, and each sequential water wash also increases the hydroxide/phosphate ratio in the bulk solution. Thus increased removal of divalent phosphate and the greater ease of displacement of hydroxide and

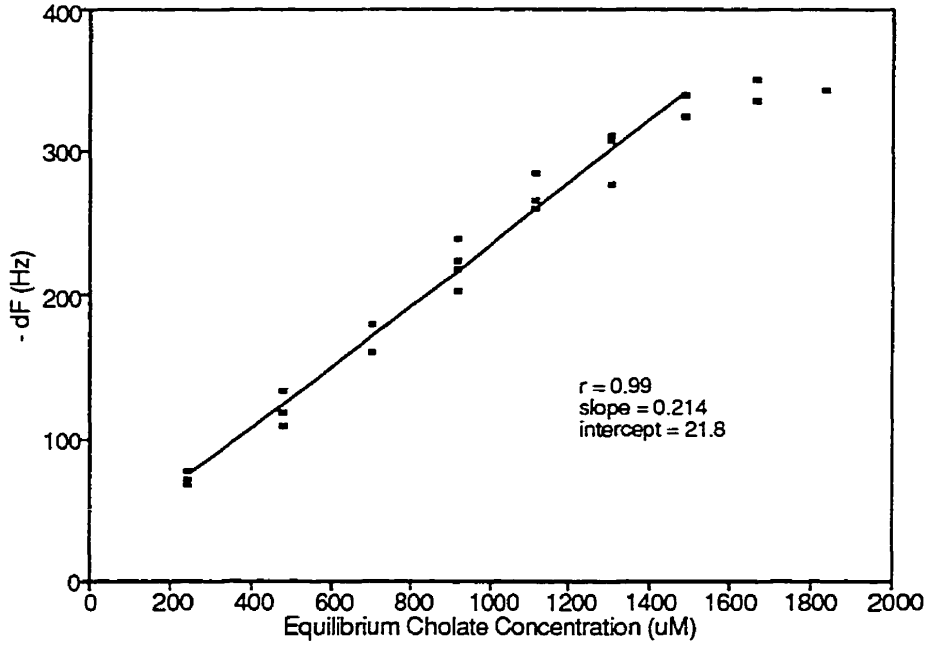

(a)

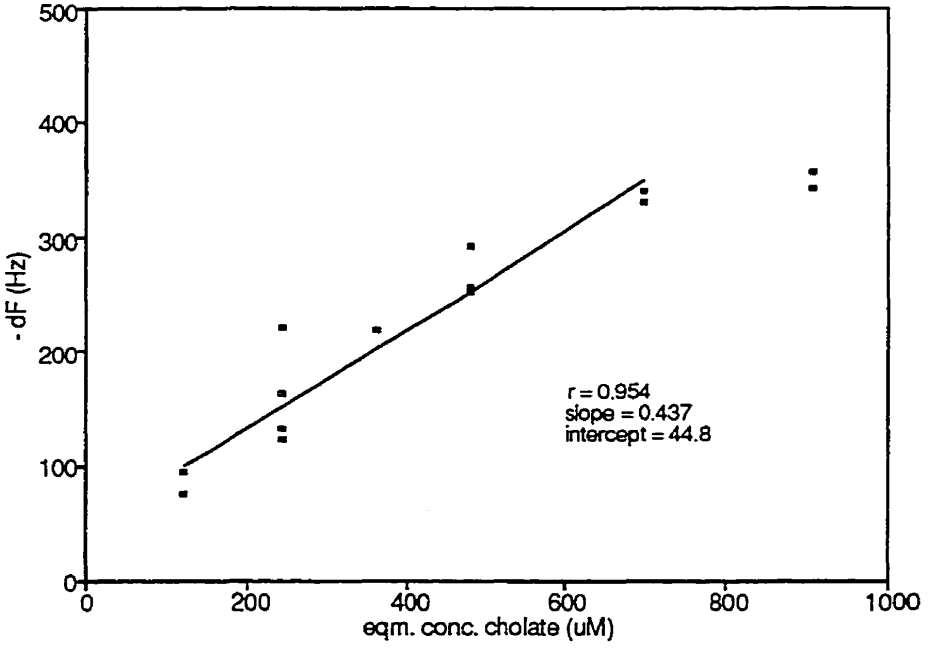

(b)

Figure 3.8 Scatterplots of frequency response to sodium cholate in buffer (a) and water (b). The least-squares regression line is shown for the working range, along with the calculated values for the slope and intercept. The response plateaus at sufficiently high concentrations.

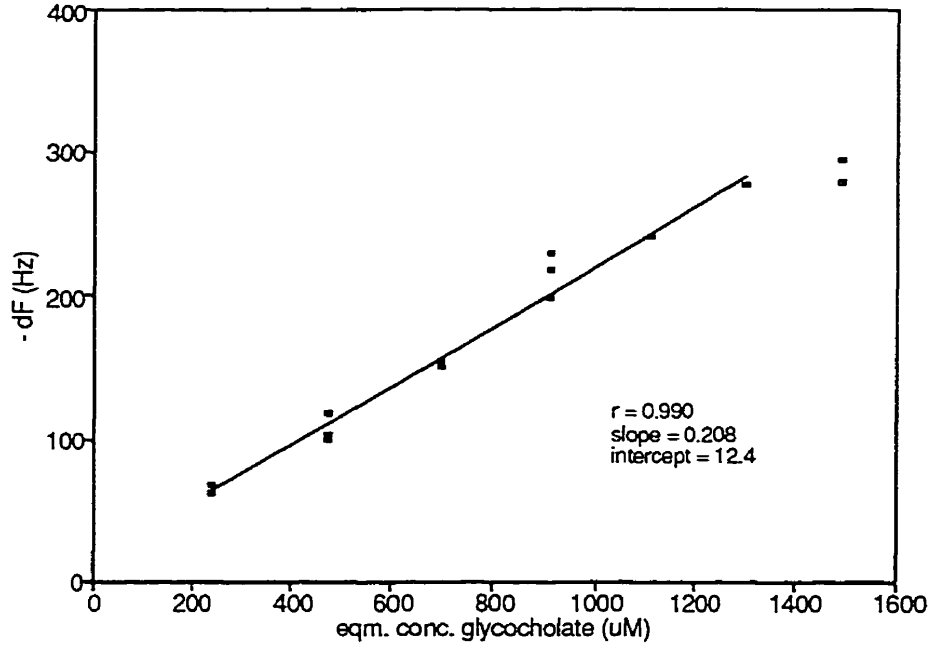

(a)

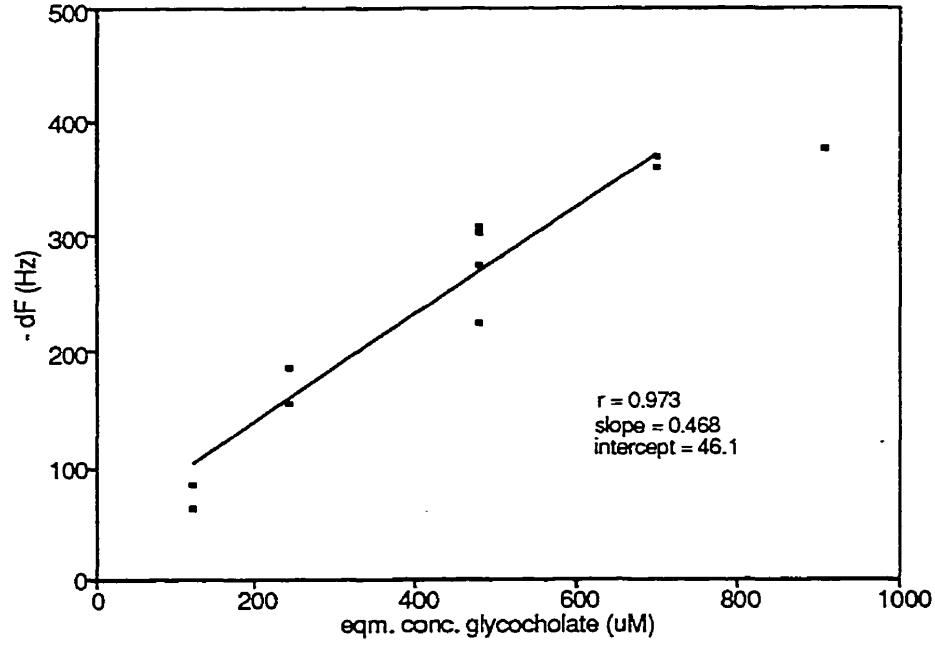

(b)

Figure 3.9 Scatterplots of frequency response to sodium glycocholate in buffer (a) and water (b). The least-squares regression line is shown for the working range, along with the calculated values for the slope and intercept. The response plateaus at sufficiently high concentrations.

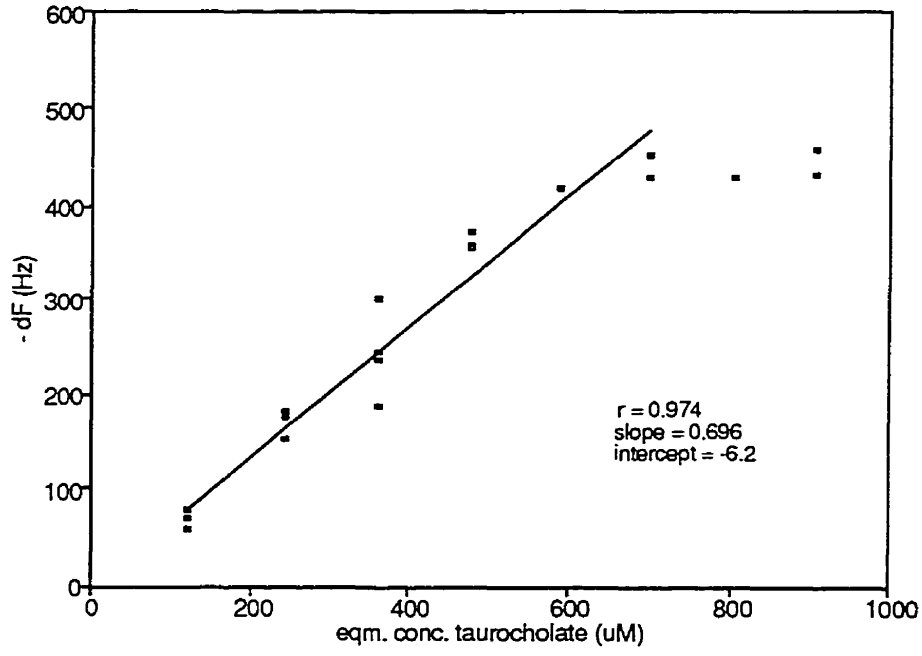

(a)

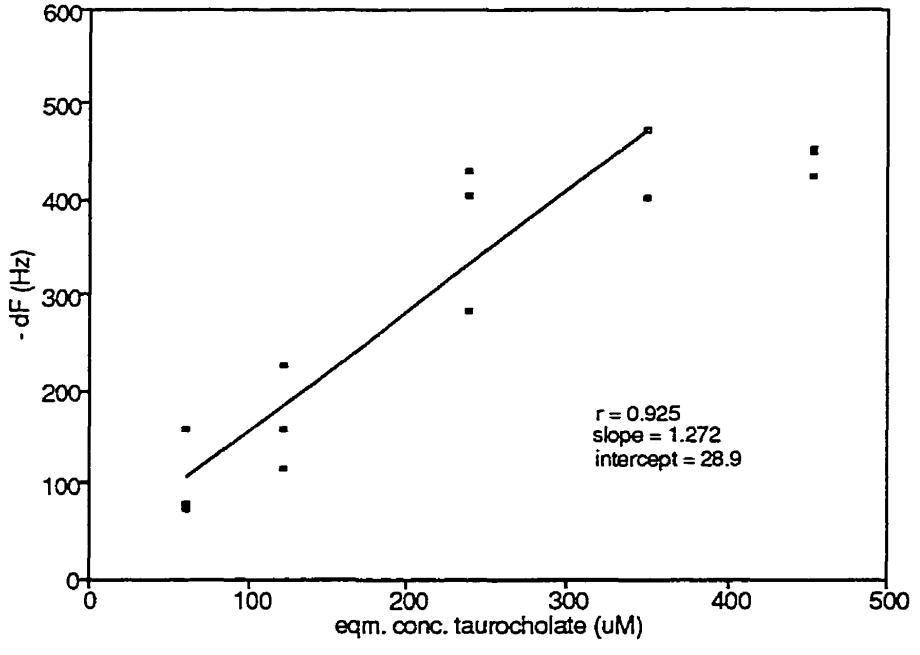

(b)

Figure 3.10 Scatterplots of frequency response to sodium taurocholate in buffer (a) and water (b). The least-squares regression line is shown for the working range, along with the calculated values for the slope and intercept. The response plateaus at sufficiently high concentrations.

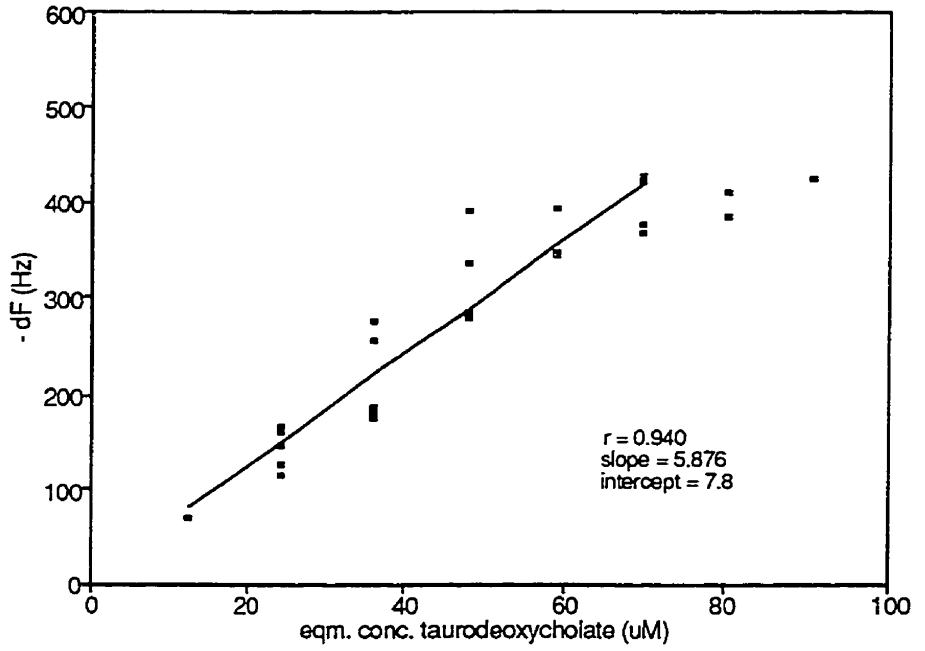

(a)

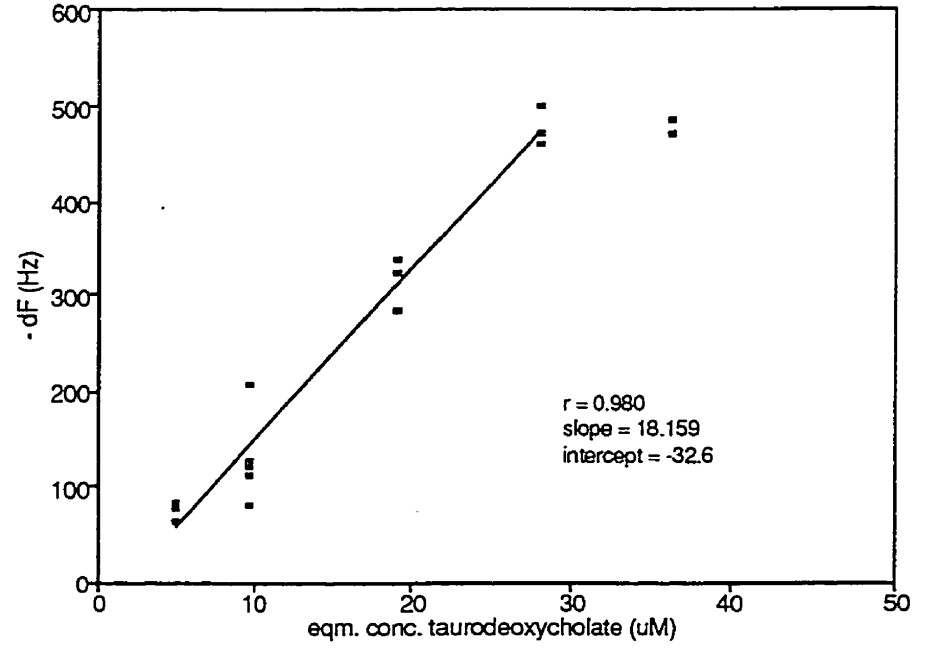

(b)

Figure 3.11 Scatterplots of frequency response to sodium taurodeoxycholate in buffer (a) and water (b). The least-squares regression line is shown for the working range, along with the calculated values for the slope and intercept. The response plateaus at sufficiently high concentrations.

Table 3.2 Sensor Response for Four Bile Acids[a]

Bile Acid	Working Range (μM)	r	Sensitivity (Hz/μM)	Detection Limit μM	Detection Limit nmol
buffer as injection medium					
cholate	140 - 1500	0.99	0.21	42	20
glycocholate	145 - 1300	0.99	0.21	44	21
taurocholate	44 - 700	0.97	0.70	13	6
taurodeoxycholate	5 - 70	0.94	5.88	1.5	0.7
water as injection medium					
cholate	69 - 700	0.95	0.44	21	9
glycocholate	64 - 700	0.97	0.47	20	9
taurocholate	24 - 350	0.94	1.27	7	3
taurodeoxycholate	1.7 - 28	0.98	18.16	0.5	0.2

[a] Figures of merit established as follows: detection limit (DL) = 3σ, σ=S.D. of blank injection of 44 μL (≈ 3 Hz); sensitivity = slope of linear regression line; r=correlation coefficient; lower working range limit = 10σ; upper working range limit by inspection. For each bile salt, $n \geq 3$ experiments were typically performed at each of $n \geq 5$ concentrations.

monovalent phosphate counterions by bile salt anions are likely also responsible for the enhanced sensitivity observed in water. All of these conclusions are in agreement with the ionic bond strength considerations of Coulomb's law. Increased binding of bile salts in solutions of decreasing ionic strength has also been noted in other *in vitro* studies.[27,56]

The sensitivity of the frequency response increases in the order cholate ≈ glycocholate < taurocholate << taurodeoxycholate. The approximately equal affinity of cholestyramine for the trihydroxy bile acids has been observed in previous studies,[30] although a slight increase in affinity for taurocholate has also been noted.[25,28,35,57-59] The high sensitivity observed for the dihydroxy bile acid taurodeoxycholate is attributed to the much greater hydrophobicity of this molecule compared to the trihydroxy bile acids, and is direct evidence of the importance of hydrophobic interactions in addition to the ionic interaction. The increased affinity of cholestyramine for dihydroxy bile acids has also been confirmed in other studies.[22,28,29,34,35,58,59] In both injection media the pH and equilibrium bile salt concentrations are above the pK_a and below the CMC values for all four bile acids.[60] Thus the predominant interactions should be between the resin coating and ionized monomers, although a certain degree of non-critical self association of bile salts may exist (e.g., dimer formation).[61]

The detection limits for the sensor system are generally in the low nanomole range, and depend on the structure of the bile salt as well as the injection medium. These detection limits are already sufficient for analyses of certain biological samples but require improvement for others (see section 3.5).

3.3.10 Interferences

While a thorough examination of all potential interferences was beyond the scope of this work, a selected number of compounds were examined for their ability to bind to the cholestyramine coating. At an equilibrium concentration of 1 mM (in buffer), the following compounds produced responses below the detection limit (< 9 Hz): ascorbic acid, caffeine, glucose, lysine, sodium acetate, uric acid (0.0025 M, satd. solution) and urea. In addition, when 1 mM sodium cholate was introduced following each test compound, the response was within 20 Hz of the response for sodium

cholate alone (≈ 180 Hz). This demonstrates that none of the test compounds hinder the binding of bile salt when present at equimolar concentrations.

A number of conclusions may be drawn from the above interference data. First, the response to glucose is relevant to *Questran*, a hypocholesteremic prescription drug. Each 9g packet (1 dose) of this drug contains 4 g of anhydrous cholestyramine and 3.8 g of sucrose. According to our experiments, sucrose would not be expected to interfere in the binding of bile salts to cholestyramine, at least at comparable concentrations. Second, the presence of small amounts of urea and uric acid remaining in bile salt extractions from urine and feces should not interfere in the assay. And third, the lack of response from sodium acetate, which like sodium cholate has an ionized carboxyl group but lacks the alicyclic skeleton, provides evidence of the importance of hydrophobic interactions in the ability of bile salts to displace counterions and occupy binding sites on the resin. While we do not know whether acetate actually displaces the phosphate counterions, this conclusion may still be established as follows. If acetate does not displace phosphate, then the ability of cholate to do so must be attributed to the presence of the hydrophobic skeleton. And if acetate does displace phosphate, this implies that since cholate evidently displaces bound acetate at equimolar concentrations, it must have a higher affinity for the resin and this must be attributed to the hydrophobic skeleton.

Sodium citrate was the one exception that demonstrated significant interference in the binding of cholate (Figure 3.12). In curve (i), an 44-μL injection of buffered citrate to an equilibrium concentration of 1 mM gives a blank-corrected response (15 Hz) only slightly above the DL. At t = 23 min, the response to a similar injection of cholate then gives a corrected response of ~ 80 Hz. In curve (ii), a decrease of 170 Hz (183 - 13 Hz blank correction) is obtained when cholate is injected first. But when citrate is then injected at the same concentration (t = 27 min), the frequency *increases* ~ 70 Hz. Thus it is observed that citrate has the ability to both prevent binding of bile anions to cholestyramine, and to displace bile anions already bound to the resin. As in the regeneration studies, we again invoke Coulomb's law and attribute this effect to the greater strength of ionic interaction of the resin with trivalent (citrate) vs. monovalent (cholate) anions. Kos *et al.*[30] have also observed, in indirect competitive

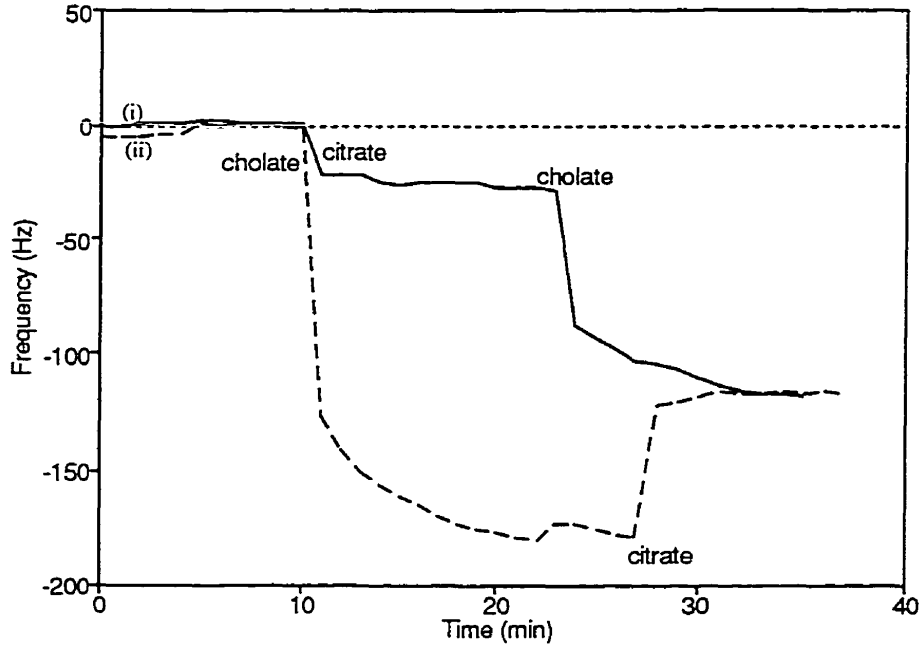

Figure 3.12 Frequency response profiles showing interference from citrate in buffer (see text for description). The small increase at t = 22 min in (ii) resulted from agitating the solution to ensure maximum binding of cholate. The y-axis scale is reset to zero to facilitate interpretation.

binding studies, the ability of citrate to reduce the amount of binding to cholate, but noted that there was still preferential binding of cholate over citrate. Based on the frequency changes in Figure 3.12, it is estimated that at equimolar concentrations citrate reduces the amount of bound cholate by about 40%, indicating a slight preference of cholestyramine for cholate over citrate.

The low frequency response from citrate provides evidence that the alicyclic bile salt skeleton adsorbs to or penetrates into the resin. Since the MW of the citrate anion is about 40% that of the cholate anion, a response of 0.40(170 Hz) ≈ 70 Hz is expected from 1 mM citrate if a simple surface-confined ionic bond is the sole means of acoustic shear coupling. Since the response to citrate is only 15 Hz, this implies that the ionic bond has a limited effect on the frequency response and that the much greater frequency response from cholate must be due to a different mode of coupling

(e.g., mass coupling from surface adsorption of the hydrophobic alicyclic skeleton, and/or changes in the viscoelastic properties of the coating produced by partial penetration of the bile salts molecules into the resin film).

3.3.11 Implications of Citrate Interference on Action of Cholestyramine

The interference observed with sodium citrate is relevant to the therapeutic action of cholestyramine in sequestering bile salts. Citric acid is both an excipient in *Questran* and *Questran Light* and a major component in many of the foods which are recommended[62] for mixing with the dry powder (applesauce, crushed pineapple, orange juice, etc.). A number of adverse effects are common with the use of this drug, including heartburn, nausea, vomiting, stomach pain and constipation.[9,63,64] Constipation, the most common side effect, is known to be a function of the dosage.[9] In addition, Questran is not efficient in its action since up to 24 g are required daily. Such dosage levels contain many times more cholestyramine than is actually required for effective bile salt fecal excretion based on actual resin capacities.[27,35] It is thus possible that any attempt - dietary or otherwise - to increase the efficiency of cholestyramine formulations may result in lower required doses and fewer side effects. This in turn could result in improved patient compliance. Our *in vitro* studies indicate that avoiding citric acid (citrate) during the ingestion of cholestyramine formulations could significantly improve *in vivo* efficiency.

3.4 Analytical Methods for Bile Acids

A variety of techniques, each with different accuracy and applicability, have been applied for the quantitative analysis of bile acids. These methods have been extensively reviewed elsewhere.[65-70] Bile acid determinations may be made on a number of different biological fluids, including bile, serum, stools, urine and gastric juice. Analytical methods must take into account any sample preparation which may be necessary for the method, as well as the relatively low concentrations of bile acids that are present in certain sample types (e.g., serum, urine). Unless a total bile acids determination is sufficient, some form of separation science must also be applied to

the sample. A very short presentation of these methods is provided here for purposes of comparison with the present TSM acoustic wave sensor method.

3.4.1 Isolation from a Biological Matrix

Since bile acids can vary widely in polarity and may be conjugated in different ways to contain more than one negative charge, it is difficult to develop a procedure that quantitatively extracts all types of bile acids.[65] The method of choice usually depends on the nature of the biological sample. The use of solvents for bile acid extraction was widely used but has now been largely discontinued. Ion-exchange chromatography can exploit the acidic properties of bile acids and allow for an efficient separation of bile acids from neutral steroids and lipids. If group separation such as free bile acids, glycine conjugates, and taurine conjugates is desired, gel chromatography is more effective.

More recently, reverse-phase chromatography employing octadecyl-substituted silica (Sep-Pak C-18) has simplified separation from the matrix. This stationary phase can extract both nonpolar and polar bile acids and steroids from water. Commercially available C-18 solid-phase extraction cartridges (Sep-Pak, Bond-Elut) allow easy and rapid separation of bile acids from the matrix, greatly facilitating the clean-up problem for subsequent bile acid analyses.

3.4.2 Colorimetric Methods

The colorimetric method is essentially a modification of the Pettenkofer reaction.[71] The bile acids normally do not absorb UV-visible light. However, all of the bile acids show absorbance in the UV region after treatment with concentrated sulfuric acid (65-70%). The absorbance of relatively low concentrations of bile acids obeys Beer's law. The advantage of this detection method is that it is simple and does not require advanced instrumentation.

Colorimetry can also be used in conjunction with enzymatic methods for analysis of bile acids. Nicolas *et al.*[72] developed an enzyme cycling method involving alcohol dehydrogenase and diaphorase. The NADH formed is oxidized by diaphorase in the presence of ethanol. The result is the accumulation of a dye, which is measured

colorimetrically. The authors reported good linearity and reproducibility in the range of 2 to 1000 μM. A similar approach is used in a commercially available kit from Sigma (catalog no. 450-A), which relies on the reactions

$$\text{3}\alpha\text{-Hydroxybile Acids} + \text{NAD} \rightarrow \text{3-Oxo Bile Acids} + \text{NADH}$$
$$\text{NADH} + \text{NBT} \rightarrow \text{NAD} + \text{Formazan}$$

where the first reaction is catalyzed by 3α-hydroxysteroid dehydrogenase (3α-HSD) and the second by diaphorase. The intensity of the color produced by the action of the two enzymes is directly proportional to the bile acids concentration in the sample.

3.4.3 Chromatographic Methods

Thin-layer chromatography (TLC) has been used for detection of bile acids, and many solvent systems are available for the efficient separation of the common bile acids.[73-76] Silica gel is the most frequently used adsorbent, and bile acid derivatives can be prepared (e.g., C-24 methyl esters) to improve separation efficiency. Detection can be achieved by the use of sulfuric acid, phosphoric acid, phosphomolybdates, and other stains that produce fluorescent products or colored spots. Densitometry may be used for quantitative estimations.[77,78]

Gas chromatography (GC) may also be used for separation and determination of bile acids. However, bile acids themselves are insufficiently volatile and must therefore be derivatized before injection into the column. Derivatization generally involves methylation of the carboxylic acid into a methyl ester (ME) and subsequent conversion of hydroxyl groups to trimethylsilyl (TMS) or dimethylsilyl (DMS) ethers, acetates, trifluoroacetates or hexafluoroisopropyltrifluoroacetates.[79-82] The advent of capillary columns has facilitated the coupling of GC with mass spectrometry (GC-MS). The ME-TMS ether derivatives give more information than other derivatives, and their ease of preparation and volatility make them the most popular choice for GC-MS.

High performance liquid chromatography (HPLC) is also a sensitive and precise method for bile acid analysis.[83] The main advantage compared with GC is that some bile acid classes (e.g., glycine and taurine conjugates) can be analyzed directly

without preliminary derivatization procedures. Ion exchange columns and C-18 reverse-phase silica columns[84] can be used for the separation of bile acids. Direct separations from biological fluids is also possible.[85,86]

Detection methods with HPLC systems may require precolumn derivatization,[87-93] post-column enzymatic reactions,[94] or ion-pair formation.[95] UV, refractive index, fluorimetric, and electrochemical detectors can be used for detection of bile acids, their derivatives, or enzyme reaction products. Detection limits in the pmol range are not uncommon, and fmol detection limits can be achieved with suitable derivatization and fluorescence detection. In terms of concentration, as an example a 10- to 20-pmol detection limit is equivalent to 0.01 to 0.02 μM when 1 mL of serum is analyzed. HPLC can also be coupled with MS detection for qualitative and quantitative information in bile acid analysis. The development in the early 1980s of the thermospray ionization interface permitted coupling of the HPLC column directly to the MS thereby allowing continuous real-time in-line monitoring of the effluent.[96,97]

3.4.4 Other Methods

Other methods include competitive immunoassays such as radioimmunoassay (RIA) and enzyme-linked immunosorbent assay (ELISA). These methods use polyclonal antibodies produced in rabbits immunized with a bile acid coupled to a protein. The carrier protein, generally bovine serum albumin, is covalently linked by a peptide bond on a C-24 carboxy group. As a consequence, the side chain is completely masked by the protein so that the antibodies produced are specific only for the steroid skeleton. The antibodies are isolated and used in competitive binding experiments for determination of bile acids. Incubation times up to an hour or more may be required. Radiolabelled tag analytes are employed in RIA. These methods are highly specific and sensitive, capable of measuring analytes at picomolar levels. They are suitable for the analysis of bile acids in serum, urine, saliva, and other biological fluids in which bile acids are present in very low concentrations. Commercial kits are available for both RIA and ELISA.

Direct electrochemical detection can also be used for bile acids determination. For example, Albery *et al.*[98] have developed an amperometric enzyme electrode for

free bile acids using 3α-HSD coupled to an *N*-methyl phenazinium tetracyanoquinodimethanide electrode. The response time was less than 5 min and the detection limit was 1 μM.

3.5 Applications for the Present TSM Acoustic Wave Sensor

While other methods have undergone sufficient development to enable sensitive and reproducible bile acid determinations, including total bile acids as well as bile acid profiles, there are still certain drawbacks associated with them. These include requirements for expensive (enzymatic, RIA, ELISA) and hazardous (RIA) reagents, licensing and disposal of hazardous waste (RIA), preliminary derivatization (GC, GC-MS) or high operator skill (GC-MS). As well, all of these methods require expensive equipment such as spectrometers, spectrophotometers, spectrofluorometers and scintillation counters.

As a routine sensor for bile acid analysis, there are certain potential advantages of the TSM acoustic wave device when compared with other methods. The main advantage of the present sensor is in terms of cost, being considerably less expensive than other methods in terms of both reagents and instrumentation. The crystals are commercially available, and since the coating may be reused several hundred times, the cost per analysis is quite low. Operation of the sensor is safe and relatively simple.

Performance with real (biological) samples still needs to be examined. Preliminary solvent or solid-phase extraction of such samples is almost certain to be necessary with the present TSM sensor. Such preliminary steps are almost always required with other methods, however, and may be simplified greatly by the use of solid-phase extraction cartridges such as Sep-Pak C_{18}.[99] Group separation according to number of hydroxyl substituents may also be required to account for the differential sensitivity of the sensor to these groups. Preliminary derivatization, required in GC/GC-MS, is not however required for the TSM sensor. Achievable detection limits are already sufficient for certain types of samples (bile, feces, gastric aspirate) in which bile salts are present at millimolar levels, but may not be fully adequate for other samples (serum, urine) where low micromolar levels are common.[65,67] It should also be recalled that the injection step dilutes the sample by a factor of 10 and that

the detection limits listed in Table 3.2 represent equilibrium (post-injection) concentrations. Sample extraction may improve or worsen pre-injection concentrations. Also, the discussion so far applies to total bile acids analysis; as with enzymatic methods, ELISA and RIA, the TSM sensor is not able to directly determine bile acid profiles. In order to do so, further group separation or the development of an HPLC-TSM system must be investigated. However, a determination of total bile acids is sufficient for many clinical applications.

A number of avenues of investigation are available for improvement of detection limits. One approach would be the use of crystals with a higher resonant frequency (f_o).[100] Since the Sauerbrey equation predicts that the frequency response to a given mass is proportional to f_o^2 (section 1.2.4), the use of crystals with higher resonant frequency may provide a considerable improvement in detection limits. Another approach is the use of an array of several (e.g., 2-5) cholestyramine-coated crystals. Using reversed-phase HPLC with refractive index detection, we confirmed that there is no detectable change in the concentration of the bulk solution when one cholestyramine-coated crystal is equilibrated with 1 mM sodium cholate. This fact indicates that if the analyte solution (even at lower bile salt concentrations) could be exposed to several crystals simultaneously, the response from each crystal is likely to be the same as that from only one crystal. In this case, a higher frequency response would then be obtained upon summation of the individual responses.

The batch-mode TSM acoustic wave sensor is presently suited for other useful applications. Partly due to the afore-mentioned low efficiency (per gram) of cholestyramine in sequestering bile salts, there has been considerable interest in the development of novel bile-salt sequestering agents which are effective at lower dosages.[23,56,101-104] The TSM sensor could serve as an inexpensive and convenient means of monitoring equilibrium bile salt concentrations in experiments where the novel agent and bile salt solution are mixed to determine the efficiency of the agent. Alternatively, if the novel sequestering agent can be successfully immobilized, kinetic information would be obtainable directly.

Perhaps an even more interesting application is in the examination of the interaction of cholestyramine with other drugs. Cholestyramine is known to delay or

reduce the absorption of several drugs including warfarin, tetracycline, phenobarbital, digitalis, and others.[9,63] For this reason, patients taking such drugs concomitant with cholestyramine are usually advised to take the drugs at different time intervals. The TSM acoustic wave sensor is ideally suited to determinations of the kinetics and extent of binding of drugs, dietary components and formulation excipients with cholestyramine as well as other novel bile acid sequestrants.

In terms of *in vitro* binding studies, the real-time operation of the TSM sensor represents a distinct improvement over previous methods, where rate information is obtained only indirectly and in a time-consuming manner.

3.6 Conclusions

In this chapter a novel method for the detection of bile acids using a TSM acoustic wave sensor has been demonstrated. Detection limits are adequate for the analysis of certain types of biological materials but must be improved for other sample types. Suggestions are made for ways to achieve better detection limits. Instrumentation and the cost per assay should be less expensive than other methods, and operation is safe and relatively simple. As well, the sensor provides a real time response for the binding process to cholestyramine, an important hypocholesteremic drug. This feature makes it a convenient sensor for a number of useful *in vitro* studies of clinical interest, including studies aimed at improving the efficiency of the resin as well as studies probing the interference of this resin with other drugs. Finally, the stability and non-covalent mode of interaction with the analyte confers an exceptionally long lifetime on this type of coating and this may be of interest in the development of other acoustic wave sensor applications.

Aside from the purely analytical aspects regarding the present sensor system, it has also been found that, at least *in vitro*, citrate can directly interfere in the ability of cholestyramine to sequester free bile salts. Considering that millions of individuals presently use prescription drugs for hypercholesterolemia in which cholestyramine is the active ingredient, it should be worthwhile to investigate whether the citrate interference also occurs to a significant extent *in vivo*. If so, excipient formulations

and food mixing guidelines for these drugs could be modified to reduce citrate interference, thereby lowering required dosages and improving patient compliance. In a roundabout way, the studies described in this chapter have in fact addressed an issue associated with the process of atherosclerosis.

References

1. Excerpts from Stephen Gislason MD, from Environmed Research Inc. at http://www.environmed.com/artery.htm.
2. M.C. Carey, *Hepatology* **1984**, *4*, 66s.
3. A. Roda and A. Fini, *Hepatology* **1984**, *4*, 72s.
4. D.J. Cabral, J.A. Hamilton and D.M. Small, *J. Lipid Res.* **1986**, *27*, 334.
5. A. White, P. Handler, E.L. Smith, R.L. Hill and I.R. Lehman, *Principles of Biochemistry, 6th Edition*; McGraw-Hill, New York, NY, 1978; p. 424.
6. P.A. Mayes, in *Harper's Review of Biochemistry, 19th Edition*; D.W. Martin, Jr., P.A. Mayes and V.W. Rodwell, Eds.; Lange Medical Publications, Los Altos, CA, 1983; Chap. 41, p.456.
7. T.L. Peeters, G. Vantrappen and J. Janssens, *Gastroenterology* **1980**, *79*, 678.
8. N.W. Tietz, *Fundamentals of Clinical Chemistry, 2nd Edition*; W.B. Saunders Co., Philadelphia, PA, 1976; p. 489.
9. *Compendium of Pharmaceuticals and Specialties*; Canadian Pharmaceutical Association: Ottawa, ONT, 1995; pp. 1137-1138.
10. J.B. Carey Jr. and G. Williams, *JAMA* **1961**, *176(5)*, 432-435.
11. R.B. Moore, C.A. Crane and I.D. Frantz Jr., *J. Clin. Invest.* **1968**, *47*, 1664-1671.
12. J.M. Dietschy and J.D. Wilson, *New Engl. J. Med.* **1970**, *282*, 1128-1138.
13. S.M. Grundy, E.H. Ahrens Jr. and G. Salen, *J. Lab. Clin. Med.* **1971**, *78(1)*, 94-121.
14. A.C. Beynen, *Pharm. Weekbl.* **1985**, *120*, 241-245.
15. *Questran* and *Questran Light* are trademarks of Bristol-Myers Squibb, Inc.
16. W. Insull Jr., N.R. Marquis and M.C. Tsianco, *Am. J. Cardiol.* **1991**, *67(6)*, 501-505.
17. Lipid Research Clinics Program *JAMA* **1984**, *251(3)*, 351-364.
18. Lipid Research Clinics Program *JAMA* **1984**, *251(3)*, 365-374.
19. B.M. Rifkind, *Am. J. Cardiol.* **1984**, *54*, 30C-34C.
20. J.A. Story and D. Kritchevsky, *J. Nutr.* **1976**, *106*, 1292-1294.
21. D. Gallaher and B.O. Schneeman, *Am. J. Physiol. (Gastrointest. Liver Physiol. 13)* **1986**, *250*, G420-G426.
22. G.V. Vahouny, R. Tombes, M.M. Cassidy and D. Kritchevsky, *Lipids* **1980**, *15(12)*, 1012-1018.
23. R. De Simone, F. Conti, M.R. Lovati, M. Sirtori, E. Cocuzza and C.R. Sirtori, *J. Pharm. Sci.* **1978**, *67(12)*, 1695-1698.
24. X.X. Zhu, G.R. Brown and L.E. St-Pierre, *J. Pharm. Sci.* **1992**, *81(1)*, 65-69.
25. M. Thale and O. Faergeman, *Scand. J. Gastroent.* **1978**, *13*, 353-356.
26. J. Blanchard and J.G. Nairn, *J. Phys. Chem.* **1968**, *72(4)*, 1204-1208.
27. P.E. Luner and G.L. Amidon, *Pharm. Res.* **1992**, *9(5)*, 670-676.
28. W.H. Johns and T.R. Bates, *J. Pharm. Sci.* **1969**, *58(2)*, 179-183.
29. W.H. Johns and T.R. Bates, *J. Pharm. Sci.* **1970**, *59(3)*, 329-333.
30. R. Kos, J.L. White, S.L. Hem and M.T. Borin, *Pharm. Res.* **1991**, *8(2)*, 238-241.
31. M.D. Ward and E.J. Delawski, *Anal. Chem.* **1991**, *63(9)*, 886-890.
32. A.C. Hillier and M.D. Ward, *Anal. Chem.* **1992**, *64(21)*, 2539-2554.
33. K. Dorfner, *Ion Exchangers*, 3rd ed.; Ann Arbor Science Publishers: Ann Arbor, MI, 1972; pp. 250-251.
34. W.H. Johns and T.R. Bates, *J. Pharm. Sci.* **1970**, *59(6)*, 788-793.
35. G.M. Benson, C. Haynes, S. Blanchard and D. Ellis, *J. Pharm. Sci.* **1993**, *82(1)*, 80-86.
36. C.H. Whiteside, H.B. Fluckiger and H.P. Sarett, *Proc. Soc. Exp. Biol. Med.* **1966**, *121*, 153-156.
37. D. Léonard, S.D. Clas and G.R. Brown, *React. Polym.* **1993**, *20*, 131-140.
38. H.M. Burt, E.C. Cameron, H. Erber and J.D.E. Price, *J. Pharm. Sci.* **1987**, *76(5)*, 379-383.
39. J.P. Jones and T.J. Lewis, *J. Chem. Soc. Faraday Trans.* **1995**, *91(18)*, 3147-3155.
40. M. Muratsugu, F. Ohta, Y. Miya, T. Hosokawa, S. Kurosawa, N. Kamo and H. Ikeda, *Anal. Chem.*

1993, *65(20)*, 2933-2937.
41. F.A. Wilson, *Am. J. Physiol. (Gastrointest. Liver Physiol. 4)* **1981**, *241*, G83-G92.
42. E. Prusak-Sochaczewski and J.H.T. Luong, *Anal. Lett.* **1990**, *23(3)*, 401-409.
43. J.H.T. Luong, E. Prusak-Sochaczewski, and G.G. Guilbault, G.G. *Ann. N.Y. Acad. Sci.* **1990**, *613*, 439-443.
44. G.G. Guilbault, B. Hock and R. Schmid, *Biosens. Bioelectron.* **1992**, *7*, 411-419.
45. H. Muramatsu, J.M. Dicks, E. Tamiya and I. Karube, *Anal. Chem.* **1987**, *59(23)*, 2760-2763.
46. B. König and M. Grätzel, *Anal. Chem.* **1994**, *66(3)*, 341-344.
47. M.R. Deakin and H. Byrd, *Anal. Chem.* **1989**, *61(4)*, 290-295.
48. M. Plomer, G.G. Guilbault and B. Hock, *Enzyme Microb. Technol.* **1992**, *14*, 230-235.
49. E. Prusak-Sochaczewski and J.H.T. Luong, *Anal. Lett.* **1990**, *23(2)*, 183-194.
50. M. Minunni, P. Skladal and M. Mascini, *Anal. Lett.* **1994**, *27(8)*, 1475-1487.
51. K.A. Davis and T.R. Leary, *Anal. Chem.* **1989**, *61(11)*, 1227-1230.
52. H. Muramatsu, E. Tamiya and I. Karube, *J. Membr. Sci.* **1989**, *41*, 281-290.
53. C. Köblinger, S. Drost, F. Aberl, H. Wolf, S. Koch and P. Woias, *Biosens. Bioelectron.* **1992**, *7*, 397-404.
54. M. Tom-Moy, R.L. Baer, D. Spira-Solomon and T.P. Doherty, *Anal. Chem.* **1995**, *67(9)*, 1510-1516.
55. Ref. 33, p.20.
56. X.X. Zhu, G.R. Brown and L.E. St-Pierre, *J. Macromol. Sci. - Pure Appl. Chem.* **1992**, *A29(9)*, 711-721.
57. M.M. Cassidy, F.G. Lightfoot, L.E. Grau, T. Roy, J.A. Story, D. Kritchevsky and G.V. Vahouny, *Dig. Dis. Sci.* **1980**, *25(7)*, 504-512.
58. L.M. Hagerman, D.A. Cook and D.L. Schneider, *Proc. Soc. Exp. Biol. Med.* **1972**, *139(1)*, 248-253.
59. K.W. Heaton, S.T. Heaton and R.E. Barry, *Scand. J. Gastroenterol.* **1971**, *6(3)*, 281-286.
60. M.C. Carey and D.M. Small, *Arch. Intern. Med.* **1972**, *130*, 506-527.
61. M.C. Carey, In *Sterols and Bile Acids*; H. Danielsson and J. Sjövall, Eds.; Elsevier Science Publishers B.V. (Biomedical Division): Amsterdam, Netherlands, 1985; p.380.
62. Mixing guidelines information included with *Questran* and *Questran Light*.
63. *United States Pharmacopoeia*; The United States Pharmacopoeial Convention: Rockville, MD, 1995; pp. 538-540.
64. P.O. Kwiterovich, J.H. Zavoral, S.D. Kafonek, F. Bullemer and B. Kittner, *Curr. Ther. Res.* **1992**, *52(2)*, 330-337.
65. A. Roda, P. Simoni, C. Cerre, C. Polimeni and A. Cipolla, In *Methods in Biliary Research*; M. Muraca, Ed.; CRC Press: Boca Raton, FL, 1995; pp. 123-139.
66. A. Roda, D. Festi, C. Armanino, R. Rizzoli, P. Simoni, A. Minutello and E. Roda, *Prog. Clin. Biochem. Med.* **1989**, *8*, 129-173.
67. K.D.R. Setchell, D. Kritchevsky and P.P. Nair, Eds. *The Bile Acids, Vol.4: Methods and Applications*; Plenum Press: New York, 1988.
68. J.M. Street and K.D.R. Setchell, *Biomed. Chromatogr.* **1988**, *2(6)*, 229-241.
69. J.M. Street, *Proc. Int. Symp. Bile Acids Hepatobiliary Gastrointest. Dis., 1st*; Meeting Date 1983; IRL Press: Oxford, England, 1984; pp. 9-23.
70. J.M. Street, D.J.H. Trafford and H.L.J. Makin, *J. Lipid Res.* **1983**, *24*, 491.
71. P. Metais, H. Deiss and J. Warter, *Bull. Soc. Chim. Biol.* **1957**, *39*, 321.
72. J.C. Nicolas, J. Chaintreuil, B. Descompos, and A. Crastes de Paulet, *Anal. Biochem.* **1980**, *103*, 170.
73. P. Eneroth, *J. Lipid Res.* **1963**, *4*, 11.
74. R. Beke, G.A. De Weerdt, J. Parijs, W. Huybrechts and F. Barbier, *Clin. Chim. Acta* **1976**, *70*, 197.
75. M.N. Chavez and L.C. Krone, *J. Lipid Res.* **1976**, *17*, 545.
76. C.T.L. Huang and B.L. Nichols, *J. Chromatogr.* **1975**, *109*, 427.

77. T. Arnfred and L. Pedersen, *Scand. J. Gastroenterol.* **1976**, *11*, 497.
78. G. Semenuk and W.T. Beher, *J. Chromatogr.* **1966**, *21*, 27.
79. M. Makita and W.W. Wells, *Anal. Biochem.* **1963**, *5*, 523.
80. R.E. Roovers, E. Evrard and H. Vanderhaeghe, *Clin. Chim. Acta* **1968**, *19*, 449.
81. A. Kuksus and B.A. Gordon, *Can. J. Biochem. Physiol.* **1963**, *41*, 1355.
82. H. Miyazaki, M. Ishibashi and K. Yamashita, *Biomed. Mass Spectrom.* **1978**, *5*, 469.
83. W.H. Elliot and R. Shaw, in *Steroid Analysis by HPLC*, M.P. Kautsky, Ed., Dekker, N.Y., 1981, p.1.
84. F. Nakayama and M. Nakagaki, *J. Chromatogr.* **1981**, *183*, 287.
85. C.N. Carducci, M. Matejka, H. Erguven, N. Labonia and A. Mamianetti, *J. Chromatogr.* **1985**, *337*, 91.
86. M. Hayashi, *J. Chromatogr.* **1985**, *338*, 195.
87. F. Stellard, D.J. Hachey and P.D. Klein, *Anal. Biochem.* **1978**, *87*, 359.
88. S. Okuyama, D. Uemura and Y. Hirata, *Chem. Lett.* **1979**, 461.
89. K. Shimada, Y. Komine and T. Oe, *J. Liq. Chromatogr.* **1989**, *12*, 491.
90. S.C. Andreolini and M. Novotny, *J. High. Resolut. Chromatogr. Commun.* **1988**, *11*, 20.
91. S. Kamada, M. Maeda and A. Tsuji, *J. Chromatogr.* **1983**, *272*, 29.
92. S. Ikawa, M. Miyaka, T. Mura and M. Ikeguchi, *J. Chromatogr.* **1987**, *400*, 149.
93. S. Allenmark, M. Chelminska-Bertilsson and R.A. Thompson, *Anal. Biochem.* **1990**, *185*, 279.
94. S. Itoh, S. Onishi, K. Isobe, M. Manabe and K. Inukai, *Biochem. J.* **1982**, *204*, 141.
95. H.J. Wildgrube, U. Fussel, H. Laurer and H. Stockhausen, *J. Chromatogr.* **1983**, *282*, 603.
96. C.R. Blakley and M.L. Vestal, *Anal. Chem.* **1983**, *55(4)*, 750.
97. M.L. Vestal, *J. Lipid Res.* **1989**, *30*, 1459.
98. W.J. Albery, R.B. Lennox, E. Magner, G. Rao, D. Armstrong, R.H. Dowling and G.M. Murphy, *Anal. Chim. Acta* **1993**, *281*, 655.
99. Ref. 67, chapter 1.
100. Z. Lin, C.M. Yip, I.S. Joseph and M.D. Ward, *Anal. Chem.* **1993**, *65(11)*, 1546-1551.
101. H. Toda, K. Kihara, M. Hashimoto and S. Mizogami, *J. Pharm. Sci.* **1988**, *77(6)*, 531-533.
102. S.-D. Clas, *J. Pharm. Sci.* **1991**, *80(9)*, 891-894.
103. E.W. Thomas, M.M. Cudahy, C.H. Spilman, D.M. Dinh, T.L. Watkins and T.J. Vidmar, *J. Med. Chem.* **1992**, *35(7)*, 1233-1245.
104. G.M. Benson, D.R. Alston, B.C. Bond, A.N. Gee, A. Glen, C. Haynes, D.M.B. Hickey, S. Iqbal and B. Jackson, *Atherosclerosis* **1993**, *101(1)*, 51-60.

4 Functional Group Reactions at Stable Coatings

4.1 Introduction

The work that is presented in this chapter, as in the case of the work presented in the previous chapter, had its start with the conceptual idea of building a TSM sensor system to study mass-change processes associated with atherosclerosis. As previously mentioned, one of the foundations of such a system would involve some sort of an initial coating on the crystal electrode. As an early attempt in this direction, we thus attempted to immobilize cholesterol on a crystal with gold electrodes. While these attempts failed, they were instrumental in gaining a larger appreciation of the application of sensor coatings and of limitations inherent in the sensor technique itself. Ongoing reviews of the literature also reaffirmed our initial impressions about the field of liquid-phase TSM sensor applications - that this was an incredibly fertile field, with many potential bridges to other fields of research waiting to be developed. As new ideas presented themselves, many of which appeared to involve systems much more readily suited to investigation by the TSM sensor, the direction of our efforts invariably evolved.

This chapter starts with a presentation of criteria that are necessary or desirable in examining functional group reactions at crystal-immobilized coatings. Some of the attempts to immobilize cholesterol are then briefly presented in order to illustrate some of these criteria. This is followed by work that was done on examining functional group reactions using peptide coupling reagents. The limited success achieved with both of these projects prompted the work that is presented at the end of this chapter - a systematic investigation of stability and reactivity of functionalized coatings. The sequence of studies presented in the chapter illustrates what might be a simple but

universal maxim of scientific research: *one thing leads to another.*

4.2 Criteria for TSM Sensor Functional Group Reactions

In the most general case we are considering reactions in which the terminal functional groups (X) of an initial coating (R) on the crystal metal electrode (M) are reacted in solution with functional groups (Y) of a target molecule (R') that is involved in the sensing application:

$$M\text{—}R\text{—}X \;+\; Y\text{—}R' \;\rightarrow\; M\text{—}R\text{—}(XY)\text{—}R' \;+\; Z \qquad (4.1)$$

where Z represents any byproducts produced from the covalent coupling of X and Y to form (XY). In the case where Y is a functional group which can bond directly with the metal electrode (e.g., Y=SH and M=Au) then the initial coating is not necessary. In the studies reported in this chapter, the metal electrode material is that which is most commonly used with TSM crystal sensors - gold.

Ideal criteria for the covalent reaction are listed in Table 4.1. The first requirement is that the initial coating be stable and not desorb under the reaction conditions employed; evidently this is essential if proper interpretation of frequency changes is to be made. Quick reactions (e.g., < 10 min.) are desirable since assay

Table 4.1 Ideal Criteria for TSM Sensor Functional Group Reactions

1.	stable initial coating
2.	quick reaction
3.	complete reaction of immobilized functional groups
4.	reaction at room temperature
5.	additional reagents not required
6.	irreversible bond formation if attached molecule is not the analyte; reversible bond formation if attached molecule is analyte

times are shortened and interference from instrumental drift is minimized. A complete reaction of the immobilized functional groups (X) allows for the maximum amount of mass (target molecule) to be attached to the coating and hence produces greater frequency shifts. If the spacing of the X groups is less than the binding cross section of the target molecule, then not all of the X groups will be able to react. In either case, the maximum amount of target molecule attachment is preferred. Reactions at room temperature are greatly preferred since the use of reflux or other heating systems will likely introduce excessive noise which would preclude real-time frequency monitoring and may also compromise the integrity of the initial coating. The use of additional reagents (e.g., catalysts) is also not desired since they may introduce frequency changes which interfere with the signal associated with the covalent reaction of interest (Eqn. 4.1). The frequency changes may be from direct adsorption of the additional reagent itself or through other means including destabilizing the initial coating or etching exposed portions of the electrode or metal flags. Finally, if the attached molecule (R') is to serve as a coating for further sensing, it is desirable that it be essentially irreversibly attached to the initial coating and not prone to dissociation under the conditions used for further sensing. Conversely, if R' *is* the analyte and there is no further sensing involved, it would be advantageous that there could exist a simple method of dissociating R' from the initial coating in order to reuse the initial coating for multiple assays.

Evidently there are many factors that may need to be considered and evaluated for accurate interpretation of frequency changes resulting from performing reactions at thin film coatings immobilized on TSM sensor crystal electrodes. Many of these might not even be readily apparent in the beginning, and this underlines the importance of performing proper control experiments. In the following sections a number of these factors are illustrated.

4.3 Attempts to Immobilize Cholesterol on a Gold TSM Electrode

As mentioned in section 4.1, in keeping with the idea of constructing a sensor system for studying processes associated with atherosclerosis, it was decided that as

an initial exercise we would attempt to form a thin coating of cholesterol on the sensor electrode. The structure of cholesterol was given in Fig. 3.2, where it is seen that only two functional groups exist where chemistry might be performed: the hydroxyl group at the 3 position and the carbon-carbon double bond at the 5/6 position. Since we were not aware of any interaction which might allow strong bonds to be formed between either of these two groups and a metal surface, an initial coating was deemed necessary. This initial coating would need to be bifunctional, having a functional group at one end for attachment to the crystal electrode, and a functional group on the opposite end for reaction with cholesterol.

4.3.1 Choice of Reaction

Since hydroxyl groups are generally much easier to react than carbon-carbon double bonds, this group was chosen for coupling to an initial coating. An examination of the chemical reactivity of hydroxyl groups in organic textbooks[1,2] reveals that hydroxyl groups may be involved in two broad classes of reactions: reactions which couple the —OH group to a second molecule, and reactions that modify the —OH group without coupling (e.g., conversion to an alkyl halide, dehydration to an alkene or oxidation to a carbonyl group). Within the first set of reactions, which involve coupling to a second molecule, ester formation was seen as a potential candidate for immobilization of cholesterol. In particular, we proceeded to attempt to form an ester linkage between cholesterol and the terminal carboxylic acid groups of a monolayer of either 16-mercaptohexadecanoic acid (MHA) or 3-mercaptopropionic acid (MPA).

In this scenario, MHA or MPA would serve as the initial coating and gold would be used as the electrode material. Many mercaptan derivatives are known to undergo self-assembly to form thin monolayer films on gold surfaces.[3,4] The monolayers formed by these molecules are attracted to the surface by a combination of adsorption and organizational free energies; if the n-alkyl chain is sufficiently long, the adsorbed monolayer is extremely robust. The gold - sulfur interaction is believed to involve a formal dissociative adsorption of the S-H bond to form a gold surface thiolate (RS—Au or RS^-—Au^+).[4,5]

$$RCOOH + R'OH \overset{H^+}{\rightleftharpoons} RCOOR' + H_2O \quad (4.2)$$

$$RCOOH \xrightarrow{SOCl_2} RCOCl \xrightarrow{R'OH} RCOOR' \quad (4.3)$$

The reaction of an alcohol and a carboxylic acid to form an ester can proceed in two ways. A carboxylic acid is converted directly into an ester when heated with an alcohol in the presence of a little mineral acid, usually sulfuric acid or dry hydrogen chloride (Eqn. 4.2). This reaction is reversible and generally reaches equilibrium when there are appreciable quantities of both reactants and products present. Equation 4.3 shows the use of thionyl chloride ($SOCl_2$) which initially converts the carboxylic acid into an acid chloride, which then reacts with the alcohol to form the ester. The advantage of this method is that both steps are essentially irreversible and go to completion. Since the mineral acid method does not go to completion, the thionyl chloride method was selected for attempts at cholesterol immobilization.

4.3.2 TSM Sensor Studies

The use of thionyl chloride and an initial monolayer coating of either MHA or MPA for immobilization of cholesterol via ester formation is illustrated in the plots in Fig. 4.1. For these studies, the full-immersion design using the jiffy jack (Figure 2.7) was employed (however, the third crystal (C3) was not used in these studies). The working crystal was always of 10-MHz resonant frequency. Before use, the crystals were cleaned according to the following procedure. The crystal electrodes were exposed to piranha solution (2:1 sulfuric acid:hydrogen peroxide) for a few minutes, and then the crystal was rinsed twice with water and then once with absolute ethanol. The studies shown in Figure 4.1 represent a subset of a broader selection of related studies that were done, and are only meant to be qualitative in nature.

Figure 4.1a represents two simple experiments done to verify that thiols form an adsorbate on the gold crystal electrodes. The crystal was cleaned and then fully submersed in 10 mL of absolute ethanol. Frequency readings were taken once per minute for several minutes to establish the baseline noise. Then 1-dodecanethiol (Aldrich, 98%) or MHA (≈ 20 mM solution in absolute ethanol, gift from the lab of Dr. Lennox) were injected. The upper plot is the experiment with MHA, where 50-μL were injected (first arrow), time was allowed for equilibrium to be reached, and then another 50-μL were injected (second arrow). The lower plot is a separate experiment with 1-dodecanethiol, where 50-μL were injected (at the arrow). As expected, frequency decreases were observed upon injection of both thiols. Injection of ethanol alone (in small volumes) does not cause frequency changes. These preliminary experiments thus verified that the thiols adsorb to the gold electrodes and that the TSM sensor as configured responds to these mass changes. It should be noted that there were a few occasions when the sensor did *not* provide observable frequency decreases upon injection of thiol. This originally was a cause for some confusion. However, subsequent work (described later in this chapter) revealed that one likely cause for such ambiguous results was related to the cleaning procedure of the crystal. It was found that after cleaning with piranha solution and rinsing, reproducibility improves if the crystals are allowed to oscillate in two sequential volumes of the solvent to be used, each immersion preferably for ≥ 10 minutes. Since piranha solution not only removes organics but also likely etches the gold surface, this treatment allows for a stabilization of the gold surface before application of coatings.

Figure 4.1b shows an experiment where the cleaned, uncoated crystal was fully-immersed in 10 mL of absolute ethanol. Frequency decreases were noted upon injection of MHA (first and second arrows). Then the jiffy jack was lowered and the beaker of ethanol was replaced with a beaker of fresh absolute ethanol (at the asterisk). Injection of thionyl chloride (50-μL, third arrow) then resulted in a very large decrease (≈ 800 Hz) in the frequency of oscillation. The purpose of this study was to use the solvent itself as the alcohol for ester formation with the MHA coating. This allows the alcohol to be present in very large (maximum) excess and should favor ester formation. The frequency decrease would seem to indicate that ester

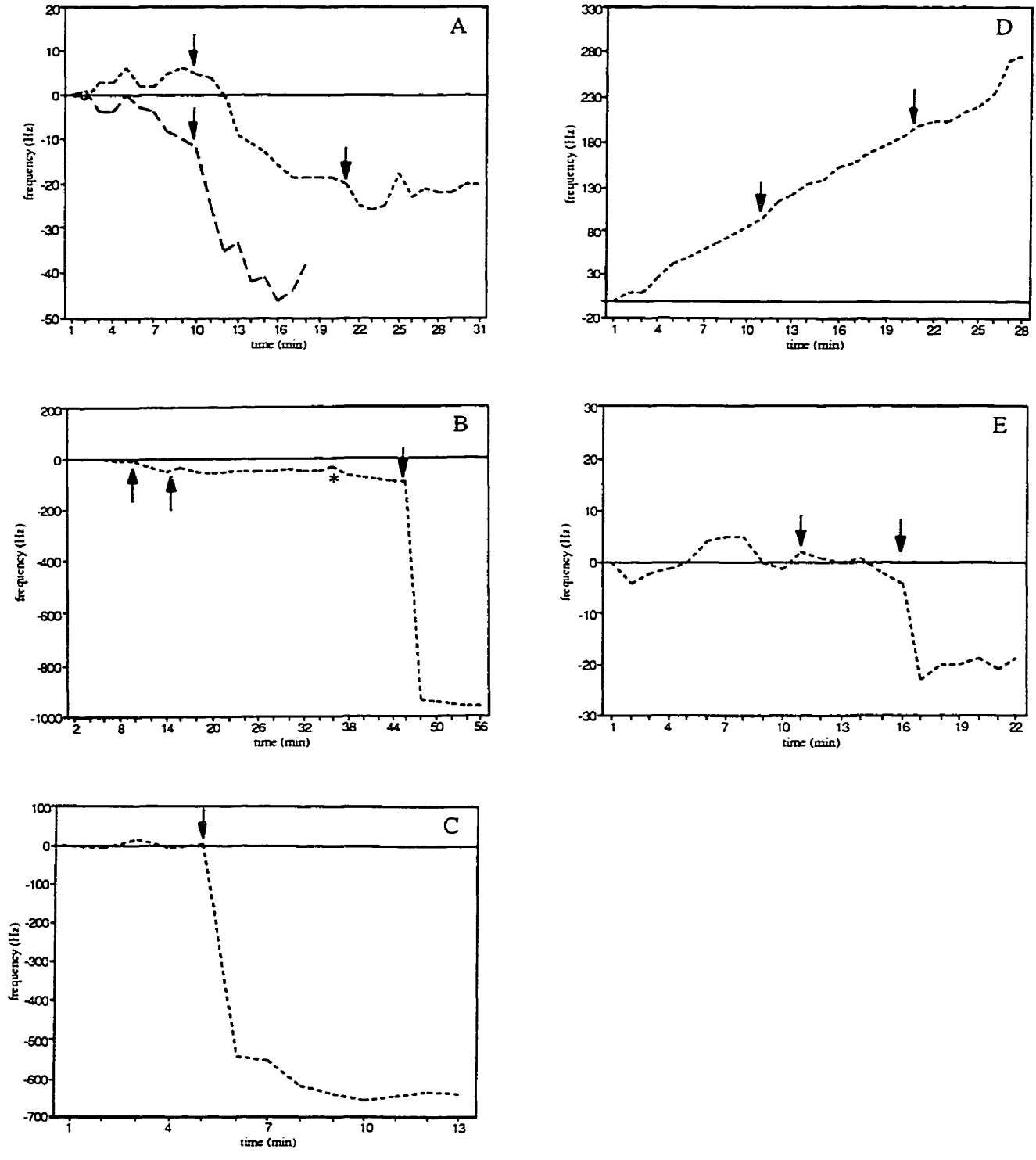

Figure 4.1 Studies examining the use of a thiol as an initial coating for the immobilization of cholesterol via ester formation using thionyl chloride. The y-axis frequency has been normalized to zero to facilitate interpretation. The arrows represent points of injection (see text for further descriptions).

formation was taking place; however the magnitude of the frequency decrease far exceeds what would be expected based solely on the mass of an attached —O—CH_2CH_3 moiety.

Figure 4.1c shows an experiment with a cleaned, uncoated crystal fully-immersed in 10 mL of absolute ethanol. Injection of thionyl chloride (40-µL, at the arrow) produces a frequency decrease of ≈ 650 Hz. This result was unexpected since there was no coating present to form an ester or any kind of bond with. Thus, this control experiment reveals that the thionyl chloride itself causes a major shift in frequency, possibly as a result of coordination of the metal surface with thionyl chloride, or by reaction with the ethanol itself which would produce HCl as a reaction byproduct. The HCl could in turn influence the frequency by etching the electrodes, flags and/or wire leads of the crystal holder which are exposed to solution. Therefore, thionyl chloride cannot be used at the same time as the alcohol for using the TSM sensor to look at the ester formation reaction itself.

An experiment was then performed where it was attempted to form the acid chloride first, and then transfer the crystal to a solution of n-hexane for reaction with cholesterol. A crystal was cleaned and then immersed in 1 mM MHA in absolute ethanol for 30 min, rinsed with ethanol and then allowed to air-dry. The crystal was then immersed in 10 mL of nitrogen-purged n-hexane with 50-µL thionyl chloride added for another 30 min, followed by rinsing with n-hexane. Immediately after the n-hexane rinse, the crystal was transferred to a beaker of fresh n-hexane. This was done quickly so as to minimize hydrolysis of the acid chloride. Monitoring of the frequency while immersed in n-hexane (Figure 4.1d) indicates a substantial amount of upward drift. Injection of 50-µL of cholesterol in n-hexane (first arrow) does not affect the slope of the drift, which indicates that little or no ester formation is taking place. A subsequent injection of 100-µL of cholesterol (second arrow) produces a small decrease in the slope of the drift, which perhaps indicates a small amount of ester formation. One reason for the evident lack of ester formation could be that the acid chloride had simply reverted back to the carboxylic acid due to exposure to moisture. Another reason could be an insufficient amount of cholesterol being injected due to the limited solubility of cholesterol in the solvent. The extent of drift here is

undesirable and may be due to solvent evaporation and on-going hydrolysis of the acid chloride due to traces of water in the solvent.

Finally, Figure 4.1e shows an experiment performed in a less-volatile, non-alcohol containing solvent, DMF (b.p. 153 °C). The crystal was first cleaned and rinsed, and a coating of 3-mercaptopropionic acid (MPA) (Aldrich, 99+ %) was deposited by applying drops of this thiol directly to the crystal electrode surfaces. The purpose of switching from MHA to MPA was to ensure the identity of a carboxylic acid-functionalized thiol, since MHA had been obtained from a non-commercial source. After coating and rinsing with ethanol, conversion to the acid chloride was attempted by immersion in DMF/thionyl chloride for 5 min. The crystal was then transferred to a solution of fresh DMF, presumably with the acid chloride still intact. Stable oscillation in DMF was obtained, and upon injection of cholesterol in DMF at arrow 1 (100-μL) and arrow 2 (200 additional μL), a small frequency decrease was observed. While this is a possible indication of ester formation with cholesterol, the frequency change is nevertheless considerably smaller than would be expected for a complete surface reaction, given the MW of cholesterol.

4.3.3 Assessment of Results and Direction of Efforts

The preceding set of experiments were selected from a larger set of experiments that were performed in an attempt to immobilize cholesterol on a crystal electrode. They illustrate a number of the factors which must be brought into consideration when attempting surface immobilizations with the TSM sensor. These include using solvents which are non-volatile (relative to the time course of the immobilization) and to which the wire leads of the crystal holder are not overly sensitive; using additional reagents which do not themselves influence the frequency; and using additional reagents which allow the reaction to proceed quickly and smoothly without concern for loss of reactive intermediates (e.g., acid chlorides) due to certain factors (e.g., exposure to moisture). In retrospect, better results might have been obtained if more attention had been paid to establishing strictly anhydrous conditions throughout, but this would perhaps have necessitated the use of a dry glove-box since the crystal must be transferred from the solution which contains

thionyl chloride to a solution of fresh solvent which does or will contain the cholesterol. It is also possible that at room temperature, the rate of acid chloride formation was very slow. Although heating or refluxing can be used to increase the rate of reaction, the use of heating with the TSM sensor is ruled out as discussed in the previous section. In all cases, although for sensing applications the frequency response itself is sufficient, independent surface analysis techniques would be helpful in order to confirm the chemistry that is actually occurring at the crystal electrode surface.

It was during this time that our thinking gradually shifted from the atherosclerosis application to the broader issue of performing functional group coupling reactions on TSM sensor crystals, regardless of the application. The appeal here was that if one could identify the conditions (e.g., coatings, reagents) under which functional group coupling reactions could readily be performed, then this could serve as the basis for using the TSM sensor in the mode of a functional group sensor. Using the TSM sensor in this manner could then allow for a tremendous range of molecular binding investigations, with the sensing depending only on the presence of a particular functional group in the target molecule/sample.

4.4 Experiments Using Peptide Coupling Agents

As just mentioned, as a result of the problems and concerns that were brought up in the attempts to immobilize cholesterol, interest shifted to the broader issue of investigating functional group coupling reactions which can occur under such conditions that the coupling can be monitored in real-time with the TSM sensor. Such reactions should conform as closely as possible to the conditions outlined in Table 4.1. Although a tremendous literature database exists in organic chemistry for functional group reactions, the vast majority of these reactions require conditions (e.g., heating, reflux or long reaction time) which are unsuitable for TSM sensor monitoring. However one area which does appear almost ideally suitable for TSM sensor monitoring involves functional group reactions which employ a particular class of coupling agent: *peptide coupling agents*.

4.4.1 Peptide Synthetic Route Using Coupling Agents

Peptide coupling agents, as the name implies, are molecules which are used to couple or join amino acids together to form peptides or polypeptides. Due to protein instability at elevated temperatures, a vast literature constituting several thousand papers has been developed in which these agents perform this function under mild conditions at room (or even cooler) temperature. The role of the coupling agent is illustrated in Figure 4.2. Here, the coupling agent Z is used to activate the carboxylic acid group of an amino acid, which then is reacted with the primary amine group of a second amino acid. The activation of the carboxylic acid allows the peptide coupling to occur at a much faster rate than normal. As well, the primary amine group on the first amino acid is protected so that it will not react with the activated carboxylic acid. In this manner, a peptide chain can be built up by sequentially reacting the terminal amino acid with the next desired amino acid to be added to the chain. Afterwards the protecting group on the first amino acid is removed to generate the final product.

A polymer support can be used to anchor the first (and subsequent) amino acid, and then at the end of the entire procedure the peptide is cleaved from the solid support. This procedure is known as *solid-phase peptide synthesis*, an important area which owes its existence in large part to the work of R.B. Merrifield starting in 1962,

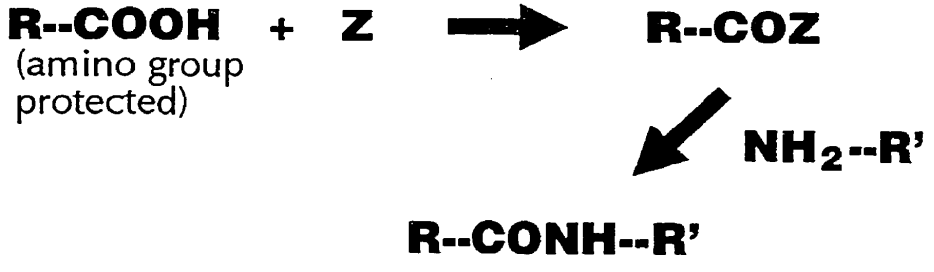

Figure 4.2 Role of coupling agent (Z) in amide bond formation.

for which he was awarded the Nobel Prize in 1984.[6,7] Figure 4.3 provides an illustration of the overall synthetic route involved in solid-phase peptide synthesis. Several instruments are commercially available which perform all of these steps sequentially for automated peptide synthesis.

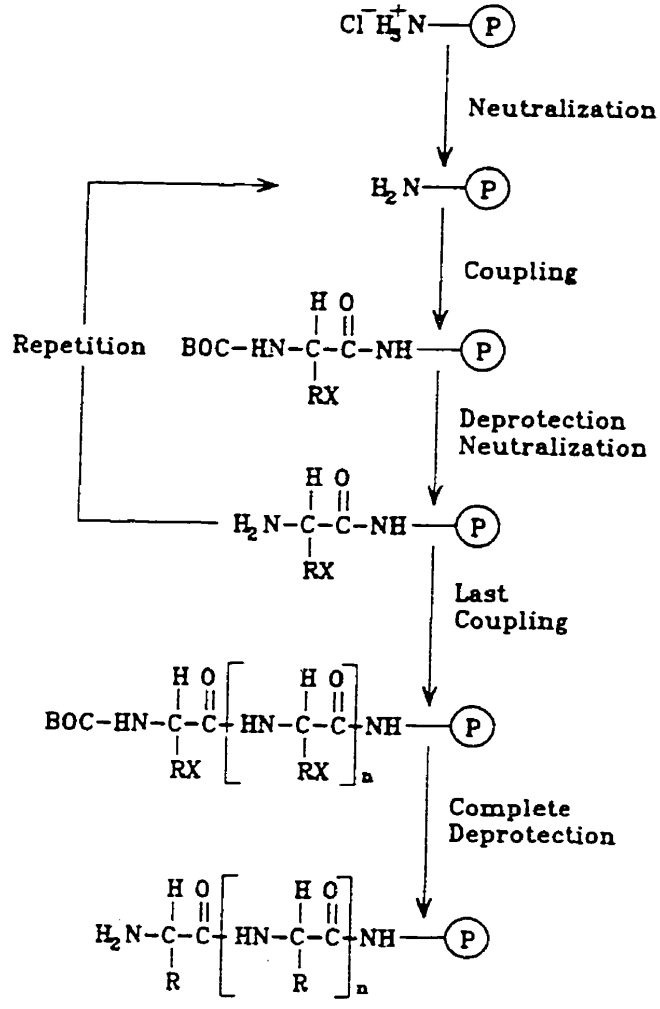

Figure 4.3 Flow chart for solid-phase peptide synthesis using Merrifield resin as the solid support (P = polymer). The first coupling is the step of interest for examination with the TSM sensor.

4.4.2 Advantages For Use With The TSM Sensor

In theory, it should be possible to exploit this functional group coupling method with the TSM sensor by first immobilizing a coating with one of the functional groups involved (i.e., amine or carboxylic acid). The coated crystal would then be exposed to an organic solvent containing activating agent and a target molecule with the complementary functional group. The appeal for examining this type of functional group coupling with the TSM sensor arises from a number of considerations. These include: (1) the coating would in effect be simulating the solid support often used in solid-phase peptide synthesis; (2) under suitable conditions these reactions can proceed relatively quickly and at room temperature; (3) the functional groups involved are commonly found in many molecules and thus many TSM sensing applications might be made possible; (4) the method is simple experimentally; and (5) since an organic solvent is used, both crystal sides can be used which increases the sensitivity. In addition, the use of peptide coupling agents with the TSM sensor is an area which has not yet been investigated. In fact there appears to be a complete absence of any reports in the literature that deal with functional group reactions in organic solvents using the TSM acoustic wave sensor. The lack of investigation into this general area prompted the studies described in this section as well as those described in the remainder of this chapter.

4.4.3 Selection of Alternate Analytical Method for Examining Coatings

It was decided that the sensor-immobilized functional group should be the primary amine group, since it seemed likely that the activation step should proceed more smoothly if both coupling agent and carboxylic acid were free in solution. Before proceeding with the coupling experiments however, it was also decided that it would be desirable to use an alternative method (other than TSM sensor frequency changes) to confirm the stability of the selected coating materials on the gold crystal electrodes when immersed in the solvents to be used. A number of possible analytical methods were initially considered.

The scanning electron microscopy - energy dispersive x-rays (SEM-EDX) facilities in the Dept. of Metallurgy were used to examine an organic thiol coating

applied on a sensor crystal with gold electrode an a chromium underlayer. The SEM-EDX method bombards the sample surface with 15.0 keV electrons under ultra-high vacuum (UHV) conditions, which knocks out inner shell electrons. Electrons in higher orbitals then fall down to replace these lost electrons, with concomitant emission of x-rays characteristic of the elements present. The resulting plot of counts vs. x-ray energy revealed peaks for oxygen, silicon, gold, and chromium. Unfortunately however, peaks (e.g., sulfur) corresponding to the organic thiol were not observed, likely since the amount of coating material present was simply below the detection limit of the method.

The use of external reflectance or grazing-angle infrared spectroscopy was also investigated. This method has also been used by other workers for examination of thioalkyl monolayers on gold surfaces.[5,8-10] However, most of these studies have examined *long-chain* thiol monolayers, where from 8 to 15 repeating methylene units are present in the thiol. This allows for an increase in intensity of the methylene stretch (ca. 2920 cm^{-1}),[8] which is used to monitor the presence of the monolayer. Using the Bruker IFS-88 FTIR instrument in the department, a thick smear of glutaraldehyde on a gold slide was used for initial testing. An excellent spectrum was obtained which confirmed that the instrument optics, detector, computer software and choice of grazing angle (~86°) were all operational. However, since long-chain thiols with terminal primary amine groups were not commercially available, we were limited to using short-chain alkyl- or aryl-thiols, and despite many efforts it was not possible to distinguish the presence of these coatings relative to the noise. Corn et al.[11-13] have constructed a polarization-modulation FTIR instrument which is specifically designed for these types of studies, and have used it to monitor, for example, gas-phase amide formation between a primary amine and an acid chloride. Other research groups in this department have been attempting to obtain a grant for such an instrument for the past several years. Had this instrument been present at the time of these studies, FTIR might then have been a feasible option for the alternative analytical method.

Subsequently, a number of coated and uncoated samples were examined with x-ray photoelectron spectroscopy (XPS), which proved to be an excellent method for confirming the presence or absence of amine-functionalized coatings. In this surface

analysis technique, a sample is bombarded with a source of high-energy X rays which cause the emission from sample atoms of inner shell electrons. The energies of the ejected electrons are characteristic of the element from which they were ejected. In addition, the different photoelectron peaks from the same element may be distinguished (e.g., carbon in a methylene unit vs. carbon in a carboxylic acid) since the energy of the electron, referred to as the binding energy (BE), depends on the particular electronic environment of each atom. Carbon, oxygen and nitrogen were easily identified in the monolayer samples that were examined. Although small amounts of carbon impurity (e.g., arising from the pump oil used to maintain the UHV) could also be detected, levels were significantly lower for uncoated vs. coated samples. Due to the fact that the rectangular sample window that was examined by the detector included the electrode as well as some of the surrounding quartz, photoelectron peaks for Au, Si and O were observed in all samples. However, nitrogen photoelectron peaks were never observed when the coating did not contain nitrogen. Hence, for the examination of sensor crystals with amine-functionalized coatings, XPS was a completely interference-free technique and was thus chosen as the alternative analytical method for examination of coatings.

4.4.4 Verification of Coating Stability Using XPS

An initial selection of compounds with primary amine functional groups were chosen as coating candidates; these included 4-aminothiophenol (4-ATP), 4-aminopyridine (4-AP), 5-amino-1,3,4-thiadiazole-2-thiol (ATT) and 2-aminoethanethiol (AET). The thiol compounds were selected for the reported ability of mercaptan derivatives to self-assemble into organized monolayer systems, as described earlier in section 4.3.1. The choice of 4-AP as an amine-functionalized sensor coating was based on previous reports of the adsorption of pyridine at gold electrode surfaces.[14] All four compounds were purchased from Aldrich and used as received. 5-10 mM solutions in absolute ethanol were freshly prepared, and piranha solution-cleaned crystals were immersed in the thiol solution for 4-6 hours, after which they were rinsed with fresh absolute ethanol. Half of the crystals were set aside for XPS analysis, and the other half were sequentially mounted in the circuit socket for oscillation in organic solvent.

The purpose of these experiments was to confirm that the monolayers did not desorb due to immersion and oscillation in the organic solvents that were to be used for the peptide coupling experiments. The two solvents that were examined were dimethylformamide (DMF) and dichloromethane (DCM), which are two of the most commonly employed solvents used in peptide synthesis. After mounting the coated crystal in the oscillator, the jiffy jack (cf. Figure 2.7) was used to raise a 10-mL beaker containing pure solvent and thereby immerse the coated crystal. Oscillation was then allowed to proceed for a period of 30 minutes, after which the beaker was lowered and the solvent allowed to evaporate from the crystal. When DMF was the solvent (but not with DCM, which has a very low boiling point), the crystal was also briefly rinsed with absolute ethanol to facilitate complete removal of solvent.

Photoelectron spectra were obtained with a VG ESCALAB MKII spectrometer, located at the École Polytechnique of the Université de Montréal. The instrument used MgKα radiation (E = 1253.6 eV, 280 W) at an angle of 50° from the sample surface normal. The pressure in the instrument chamber was ca. 2×10^{-9} torr. Each sample was first subject to a full (survey) scan which examines the entire range of detectable elements. Element intensities from the full scan are multiplied by an elemental sensitivity factor, after which the various atomic percentages present in the sample are calculated. A representative spectrum for a monolayer of 4-ATP on a gold sensor electrode is shown in Figure 4.4. Selected element windows can then be scanned at high resolution to determine exact binding energies. The N 1s photoelectron peak from a 4-ATP sample is shown in Figure 4.5.

The results of the solvent immersion studies are given in Table 4.2. Signals from gold, carbon, nitrogen, oxygen, silicon and sulfur are observed where expected. The presence of the coating is most readily verified by following the N 1s signal, where it is observed that for all coatings, nitrogen generally constituted approx. 2 - 5 atomic percent of the sample. The possible loss of coating after oscillation in organic solvent can be followed not only with the N 1s signal itself but also by following the Au/N and C/N atomic ratios. Overall, there were no sharp reductions in the nitrogen content for any of the coatings after immersion in either solvent. Although a larger data set (i.e., more samples examined) could have allowed for a statistical determination

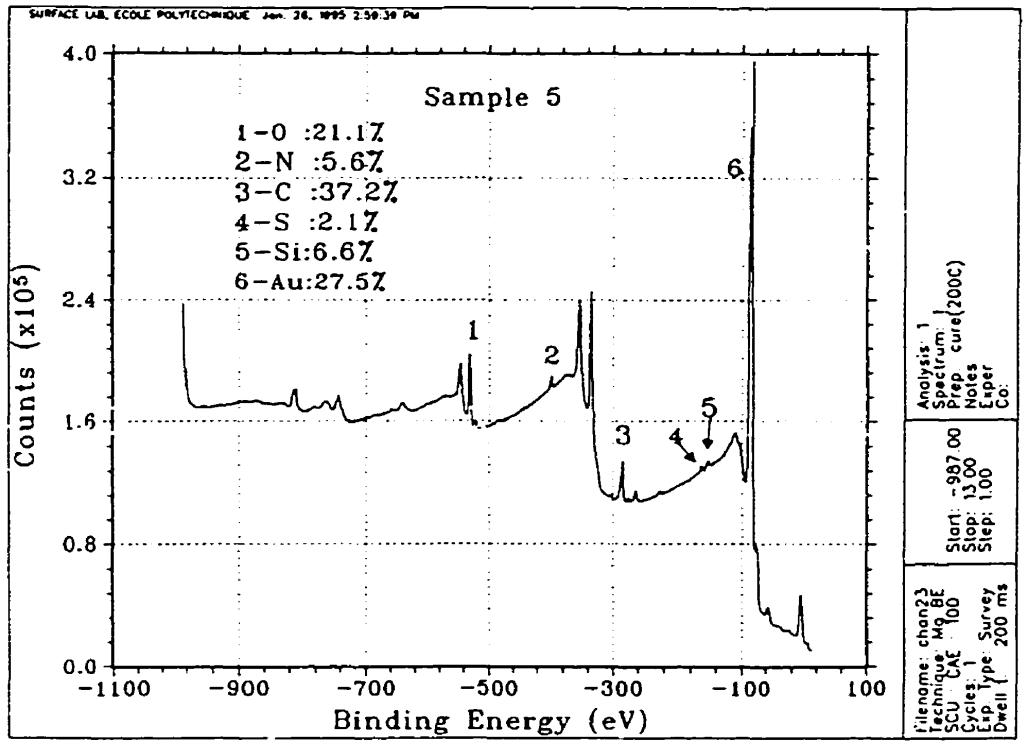

Figure 4.4 XPS survey scan for a coating of 4-ATP on a gold crystal electrode.

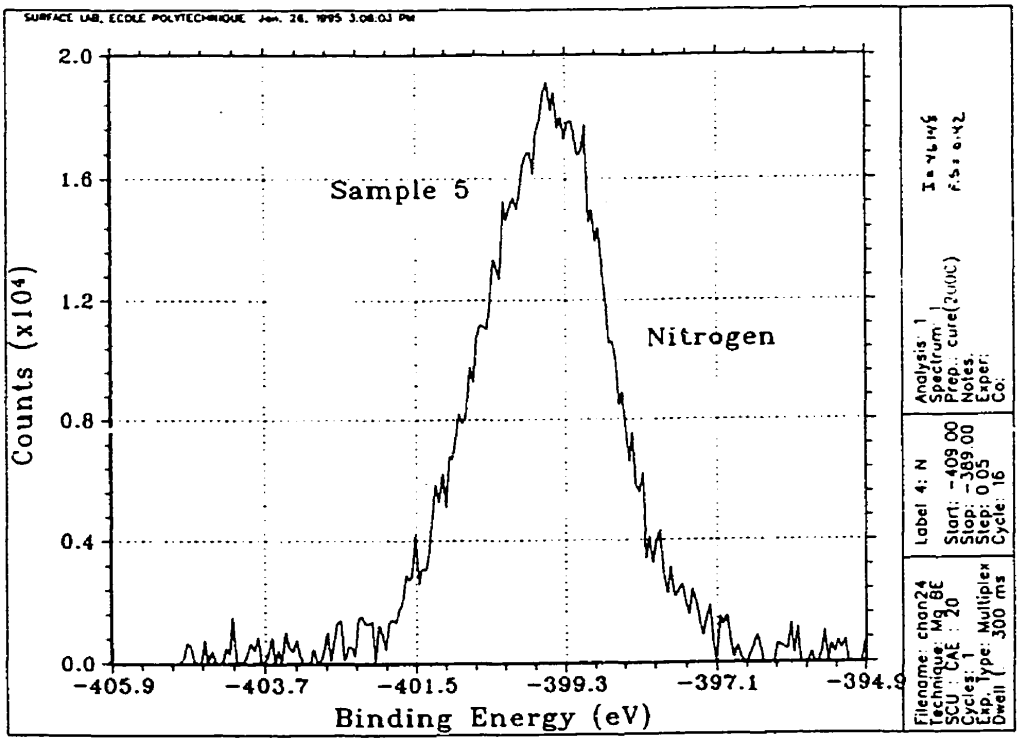

Figure 4.5 High-resolution N 1s spectrum from a sample coated with 4-ATP.

Table 4.2 XPS Results for Monolayer Stability in DMF and DCM[a]

Sample	Description	Au	C	N	O	Si	S[b]	Au/N	C/N
1	uncoated	23.1	26.0	--	32.6	18.3	--	--	--
2	uncoated	26.1	51.2	--	18.0	4.8	--	--	--
3	uncoated	48.1	23.7	--	21.8	5.6	--	--	--
4	4-ATP	11.3	23.0	3.3	42.1	20.3	*	3.4	7.0
5	4-ATP	27.5	37.2	5.6	21.1	6.6	2.1	4.9	6.6
6	4-ATP	16.5	38.6	3.4	31.4	5.7	3.6	4.9	11.4
7	4-ATP	8.8	48.2	3.6	27.9	10.4	*	2.4	13.4
8	4-ATP, DMF	13.1	20.8	2.0	42.5	20.0	*	6.9	10.9
9	4-ATP, DCM	12.7	22.6	2.5	41.0	20.8	*	5.1	9.0
10	4-AP	13.7	22.3	1.9	43.1	17.6	*	7.2	11.7
11	4-AP, DMF	14.9	19.0	3.0	41.5	20.2	*	5.0	6.3
12	4-AP, DCM	14.5	20.5	2.0	42.1	19.9	*	7.3	10.3
13	AET	20.6	23.4	3.1	35.7	15.2	*	6.6	7.5
14	AET, DMF	16.8	21.1	2.6	40.6	17.0	*	6.5	8.1
15	AET, DCM	20.7	23.7	2.8	36.7	14.6	*	7.4	8.5
16	ATT	22.3	14.1	2.9	39.8	19.9	*	7.7	4.9
17	ATT, DMF	20.6	18.7	3.0	38.6	17.6	*	6.9	6.2
18	ATT, DCM	20.9	16.4	3.9	37.9	20.2	*	5.4	4.2

[a] Some of the variation in atomic percentages is due to variation in the positioning of the sample relative to the detector window from sample to sample. [b] The asterisks refer to S < 1.0 %.

of possible partial coating losses, the intent of the XPS studies for the time being was a quick qualitative check to ensure that the coatings were not being significantly removed from the sensor electrode after oscillation in the organic solvent. 4-ATP has been reported to be a successful coating material on gold surfaces for pH-dependant electrostatic binding of charged species in solution[15] and was thus chosen for the first set of experiments using coupling agents.

4.4.5 Procedure for Peptide Coupling Agent Experiments

The peptide coupling agents that were tested were benzotriazol-1-yloxytris(dimethylamino)phosphonium hexafluorophosphate (BOP), 1,1'-carbonyldiimidazole (CDI), and dicyclohexylcarbodiimide (DCC). All were obtained from Aldrich and used as received. The use of peptide coupling agents has already been extensively reviewed elsewhere.[16-18]

The results of a number of studies performed with the TSM sensor are presented in Table 4.3. The general experimental procedure was as follows.

1. Application of coating. A 10-MHz sensor crystal was cleaned with piranha solution, rinsed with water (twice) and then ethanol. The crystal was then immersed in a fresh 5-10 mM solution of the coating compound in absolute ethanol. For all studies in Table 4.3 the coating compound was 4-ATP, except study 9 where the coating was 4-AP. After overnight incubation, the crystal was removed from the coating solution and rinsed with fresh absolute ethanol.

2. Preparation of activated carboxylic acid. The coupling agent and the carboxylic acid were combined in the indicated solvent and allowed to stand at room temperature for a period of 0.5 - 1 hr. The purpose here was to produce the activated form of the carboxylic acid before the actual coupling step. The equilibrium concentrations of the coupling agent and the carboxylic acid varied in certain studies but were usually in the vicinity of 0.01 M. In some experiments, triethylamine (TEA) was added as a base in order to help ensure that the amine groups were not protonated during the coupling step. It was verified that TEA did not itself cause changes in the TSM sensor frequency.

3. Examination of coupling step with the TSM sensor. The apparatus described in section 2.5 was used, but without the third crystal. The coated crystal was mounted in the oscillator circuit and allowed to oscillate for several minutes. The frequency of the dry crystal was recorded. The jiffy jack was then used to raise a 10-mL beaker of the indicated solvent and thereby fully immerse the crystal. The crystal was allowed to oscillate until a stable baseline was achieved. An aliquot of the coupling agent/carboxylic acid was injected at least once, and on some occasions a second and third aliquot were also injected, each injection spaced by a period of 5-10 minutes. Often, the first injection produced only a small frequency change and subsequent injections were responsible for the majority of the total frequency change. Injections were typically 100 or 200 µL and were made with a 500-µL syringe. The crystal frequency was recorded once per minute. In most studies (except #1 and #6) the jiffy jack was lowered and the crystal allowed to evaporate. Studies done with DMF as the solvent were also rinsed with absolute ethanol at this time. When the solvent had evaporated and a stable frequency of oscillation was achieved, the dry frequency of the crystal was again recorded.

4.4.6 Results for Peptide Coupling Agent Experiments

For simplicity in this section, the previously prepared mixture of coupling agent and carboxylic acid is referred to as "M" (for mixture). For comparison, in several other experiments it was noted that application of coatings derived from self-assembly of small molecules such as those in section 4.4.4, to both sides of the crystal followed by rinsing with ethanol, typically resulted in a decrease in the dry crystal frequency of < 100 Hz (for a 10-MHz crystal). The corresponding *in situ* frequency changes were always less than the dry crystal frequency change. Therefore, it is desirable to monitor the amine - carboxylic acid group coupling not only in real-time (*in-situ*) but also by comparing the dry crystal frequency before and after the experiment. In the present experiments the expected frequency decreases for covalent attachment of the target molecules listed in Table 4.3 (except cholic acid) to all terminal amine groups would also be in the range of -50 to -200 Hz (dry) or less (*in situ*).

Table 4.3 Peptide Coupling Agent Experiments Using the TSM Sensor[a]

	Coupling Agent	Target	Solvent	ΔF_{liq} (Hz)	ΔF_{dry} (Hz)
1	BOP	3-BPA	DMF/TEA	-470	--
2	BOP	3-BPA	DMF/TEA	-550	+15
3	BOP	benzoic acid	DMF/TEA	-15	+70
4	BOP	cholic acid	DMF/TEA	+15	+75
5	BOP	palmitic acid	DMF/TEA	-50	+70
6	BOP	--	DMF	-250	--
7	BOP	palmitic acid	DCM	-200	-100
8	BOP	palmitic acid	DCM	-260	-950
9	BOP	palmitic acid	DCM	-310	-670
10	BOP	--	DCM	-240	-670
11	CDI	palmitic acid	DMF	+40	+90
12	CDI	palmitic acid	DCM	+15	+80
13	DCC	3-BPA	DMF	0	+20
14	DCC	palmitic acid	DMF/TEA	+15	+15
15	DCC	palmitic acid	DCM	-10	-60

[a] All studies involved a coating of 4-ATP, except study 9 for which the coating was 4-AP.

The majority of the experiments were done with benzotriazol-1-yloxytris(dimethylamino)phosphonium hexafluorophosphate (BOP) as the coupling agent. BOP reacts with the carboxylic acid group to form a symmetrical anhydride, an activation process which has been shown to take only a few minutes.[19] Experiments #1 and #2 (and also #13) were done with 3-bromopropionic acid (3-BPA) as the carboxylic acid. The rationale for selection of this compound was that covalent attachment to the sensor coating might be readily verified by using XPS to check for bromine after the experiment. Injection of M produced large frequency decreases (-470 and -550 Hz). The post-experiment dry crystal frequency (study #2), compared with the dry crystal frequency before the experiment, indicated a slight increase in resonant frequency. This is unexpected since the large frequency decrease observed while the crystal was in the solvent hinted at the possible successful covalent attachment of the

acid. The conclusion for these two studies is that the coating did interact with the activated acid, but it is not clear whether the interaction represented covalent attachment or not. It is possible that the activated complex or the coupling agent alone physisorbed to the coating (which was then removed by the ethanol rinse) or that covalent attachment did occur, but the rinsing step removed most of the coupled coating/acid complex. As expected from the TSM sensor results, bromine was absent when these crystals were subject to analysis by XPS. The TSM sensor results are less than ideal, since in an ideal experiment the coupling of mass would be indicated by both *in situ* and dry crystal frequency decreases.

Experiments #3 and #4 employed benzoic acid and cholic acid, respectively, as the carboxylic acid. For both acids, the non-zero change in frequency upon injection of M indicates a slight interaction of the contents of M with the coating (in the case of cholic acid, the interaction may be removing some of the coating). The only explanation for the increases in the dry crystal frequency (+70 and +75 Hz) is removal of coating material.

Experiments #5, #7, #8 and #9 involved the use of palmitic acid, CH_3—$(CH_2)_{14}$—COOH, as the carboxylic acid. The *in situ* frequency changes are all indicative of interaction -- covalent attachment and/or physisorption -- of the contents of M with the coating. When DMF was the solvent, the dry frequency change was +70, indicating that interaction with M and rinsing with ethanol again removed coating material. When DCM was the solvent, the dry frequency change ranged from -100 to -950 Hz, indicating significant accumulation of mass on the sensor crystal (note: study #9 used 4-AP instead of 4-ATP as the coating material). These frequency decreases are much larger than expected for simple covalent attachment of palmitic acid, and indicate that the activated acid and/or free BOP adsorbs significantly to the sensor surface when DCM is the solvent. In retrospect, it would have been worthwhile to rinse the crystal with ethanol after the experiment, as was done with the DMF experiments. Nevertheless, the situation is less than ideal since the frequency changes are indicative of non-specific adsorption. The absence of carboxylic acid in experiments #6 and #10 confirm that BOP itself interferes with the experiment by adsorbing to the sensor surface, regardless of the solvent.

Experiments #11 and #12 were done using carbonyldiimidazole (CDI) as the coupling agent and palmitic acid as the carboxylic acid. CDI has been shown to form an imidazolide with carboxylic acids, which in turn reacts with amines to form the amide bond.[18] In both solvents, the conclusion from the *in situ* and the dry crystal frequency changes is that there is an interaction with the coating and the contents of M, and that this results in loss of coating material.

Experiments #13 - #15 used dicyclohexylcarbodiimide (DCC) as the coupling agent. When DMF was the solvent, there is no indication of successful coupling, but there is evidence for some loss of coating material. When DCM was the solvent, both *in situ* and dry crystal frequency changes indicate adsorption of mass on the sensor surface. Although the TSM sensor itself cannot definitively tell us whether this represents successful covalent coupling of palmitic acid to the 4-ATP monolayer, experiment #15 is the first (and only) experiment in Table 4.3 in which the respective frequency changes correspond roughly to the theoretical prediction.

In retrospect the experimental procedure adopted for the peptide coupling agent experiments just described may have had some shortcomings. One shortcoming is that before each experiment, the coated crystals should have been rinsed with the organic solvent (DMF or DCM) by immersing the crystal in the solvent, removing the crystal and allowing the crystal to dry (followed by re-immersion in fresh solvent). The adopted procedure of rinsing the coated crystal with absolute ethanol (see section 4.4.5) was the procedure typically employed in the literature for fabrication of thiol monolayers on gold slides. However in separate studies it was observed that if the coated crystal was also rinsed with DMF or DCM, an increase in dry crystal frequency would sometimes occur which would indicate some removal of coating material. This observation was not always consistent however; at times there would be no change in dry crystal frequency. In addition, it is recalled that the XPS experiments performed in section 4.4.4 show that immersion in the organic solvent does not completely remove the coating either. The likely explanation here is that insufficient attention was paid to the ethanol rinse immediately after coating the crystal. In particular, this step was not always performed in the exact same fashion, and it is possible that in some cases multilayer material still remained on the crystal

after this rinse, and that this multilayer material (but not monolayer material) was subsequently removed upon immersion in DMF or DCM. This is significant since in the peptide coupling agent experiments just described, the dry crystal frequency change (but not the *in situ* frequency change) would be obscured. The recommendation for future studies is that before commencing a functional group reaction experiment, the coated crystal should be subject to two sequential immersions in the solvent used for the coating material (e.g., absolute ethanol), then an immersion in the solvent used for the reaction (e.g., DMF or DCM), followed by removal and drying of the crystal.

The other shortcoming in the experimental procedure is that, for the experiments done in DCM, it would have been preferable to rinse the crystal with ethanol at the end. This was done for the experiments performed in DMF in order to facilitate solvent evaporation, but was not done with DCM since it has a very low boiling point (40° C) and evaporated off the crystal within seconds of being removed from the reaction beaker. This quick and complete evaporation evidently does not allow remaining traces of solvent to interfere with the reading of the dry crystal frequency. However in retrospect it is possible that physically adsorbed material which had accumulated on the sensor surface *in situ* may have remained there after removing the crystal from the DCM. This is a minor issue however, since physically adsorbed material (e.g., BOP), which interferes with the *in situ* frequency response as well, is not desired in the first place.

Despite some possible shortcomings in the planning and execution of the peptide coupling agent experiments, there are nevertheless a number of things that have been learned from them. It is clear that coating stability is a critical issue. Three conditions must be met for an ideal coating material: the coating must undergo a sufficiently rigorous rinsing cycle in both coating solvent and reaction solvent in order to remove possible multilayer material; the resulting monolayer coating must not be removed by the reaction solvent; and the resulting monolayer coating must not be removed by chemical or physical interaction with the components in the injection mixture.

It is also important that the primary amine group be sufficiently nucleophilic

for quick reaction with the activated acid. The choice of 4-ATP had been based primarily on the perceived stability it might offer owing to its successful use in a previous (non-acoustic wave sensor) report.[15] However, in this compound the amino group is adjacent to a benzene ring which allows for a partial delocalization of charge, making the nitrogen lone pair less available for nucleophilic attack on the activated acid. Such amino groups might therefore be expected to require much longer reaction times than more nucleophilic amines. The more nucleophilic amine 2-AET, which was also seen to be stable to oscillation in both DMF and DCM (section 4.4.4), might have been a better choice for the peptide coupling agent experiments.

What we have been trying to do since the beginning of this chapter is make some inroads into using the TSM acoustic wave sensor to monitor functional group reactions in organic solvents. Based on literature consultation, an appreciation of the constraints involved (cf., Table 4.1), and a subsequent quasi-educated "trial and error" approach, a set of experiments were then performed in order to probe their potential. The lack of success to this point has however been accompanied by an deepened appreciation of *how* to go about doing such experiments and what factors need to be given careful consideration.

4.5 Systematic Evaluation of Amine-Functionalized Coatings

In this section we essentially take a step back again, to adopt a "ground — up" approach to the effort to use the TSM acoustic wave sensor to examine functional group reactions in organic solvents. With the insight gained from the work described in previous sections, a systematic investigation of both coating stability and reactivity was conducted.

A systematic, comparative investigation of coatings also addresses a void in the literature. Most of the TSM sensor literature consists of individual, isolated reports in which only one coating protocol is employed, and relatively little work has been done involving comparative testing of different coating materials. For example, in the development of an acoustic wave sensing strategy that calls for the immobilization of a particular functional group on the sensor surface, it would be desirable to know

beforehand what material, among others, might provide the greatest analytical utility in terms of stability in the liquid phase and frequency response resulting from reaction with analyte.

In this section, such a study is presented for the primary amine group, a functional group with a wide range of possible reaction pathways, including the peptide coupling agent application. The criteria for coating stability have already been discussed in section 4.4.6. The reactivity of the amine groups is evaluated by selection of a covalent reaction which is straightforward, occurring quickly and without complication at room temperature. The reaction selected in this case is the reaction of an anhydride with the primary amine group, conducted under strictly anhydrous conditions. The TSM sensor frequency change is the parameter of interest in evaluation, with the goal being to identify a coating which is both stable (according to the conditions outlined in the previous section) and sufficiently nucleophilic/reactive for quick reaction with target molecules.

4.5.1 Experimental

An expanded selection of compounds were examined for their potential as stable and reactive liquid-phase acoustic wave sensor coatings with the primary amine group as the reactive functional group of interest. 4-Aminopyridine (4-AP), 4-aminothiophenol (4-ATP), 2-aminoethanethiol hydrochloride (2-AET or cysteamine), 3-amino-5-mercapto-1,2,4-triazole (AMT), poly(ethyleneimine) (PEI), succinic anhydride and anhydrous dimethylformamide were purchased from Aldrich. 3-Aminopropyltriethoxysilane (APTES) was obtained from Sigma, and anhydrous ethyl alcohol was purchased from Commercial Alcohols, Inc. (Brampton, ON). All chemicals were used as received. Water was doubly distilled, deionized and passed through an organic filter cartridge.

10-MHz AT-cut quartz crystals were purchased from International Crystal Manufacturing Co. (Oklahoma City, OK) with electrodes consisting of 1000-Å Au with a 50-Å Cr underlayer. Both polished and unpolished electrodes were used, with specified surface finishes of $\leq$ 1 and 3-5 μm, respectively. Both electrode finishes yielded similar results. In most cases the crystal flags were cemented to the connecting

metal clips (i.e., "bonded electrodes"), and the crystal remained connected to the circuit at all times. In some cases however, unbonded electrodes were used and the crystal was removed from the clips and immersed in each of the various solutions. Both experimental procedures provided similar frequency changes for all steps, but the latter procedure was sometimes necessary in the case of cysteamine which can react with the metal clips and sometimes caused spurious frequency changes. All data were recorded manually with the crystal oscillating in air at ambient room temperature (≈ 22 °C). The three-crystal design described in section 2.5 was employed to compensate for long-term drift and improve the accuracy of frequency difference measurements.

Prior to coating, the electrode surfaces were cleaned with hot piranha solution (2:1 sulfuric acid:hydrogen peroxide) for several min. and then rinsed with water and ethanol. To establish a stable frequency baseline, it was essential to oscillate the uncoated crystal in the coating solvent (ethanol or water) for several minutes and then allow the crystal to dry. This step was repeated with fresh solvent as necessary. 4-AP, 4-ATP, 2-AET and AMT were freshly prepared as 1-10 mM solutions in absolute ethanol. The working crystal was fully immersed in the ethanolic solution for either 2 or 12 hours, withdrawn, re-immersed in fresh ethanol for 2 min., and withdrawn and allowed to dry in air. APTES was used directly without dilution, and PEI was also used directly as the 50 wt. % solution in water. For APTES and PEI, the working crystal was fully immersed in the solution for about 10 min., withdrawn, re-immersed in water for 2 min., and withdrawn and allowed to dry in air. A Pasteur pipet connected to a vacuum line was used to provide a gentle vacuum to remove excess rinse solutions at the crystal circumference (only) to shorten the time required for air-drying.

To test for stability of the coatings, the sensor crystals were subjected to an additional two-minute immersion in ethanol (thiol- and pyridine-based coatings) or water (APTES and PEI), followed by a two-minute immersion in DMF. After each of these immersions, the crystal was allowed to air-dry and the frequency recorded. Immediately after these rinse cycles, the crystal coating was probed for amino-group reactivity by incubation in a concentrated solution of succinic anhydride in anhydrous DMF for 10 minutes, followed by immersion in fresh DMF for 2 minutes, and finally

air-dried. It was verified that incubation of an uncoated crystal in a solution of succinic anhydride/DMF followed by rinsing does not produce a change in frequency.

4.5.2 Results and Discussion

The structures of the compounds that were examined are given in Figure 4.6, and their performance in the coating, stability and reactivity test cycles are summarized in Table 4.4. Since our primary interest is in identifying good candidates for liquid-phase acoustic wave sensor applications, the most important result parameter is a large signal-to-noise ratio for the anhydride reaction step. While a large sensor frequency decrease for the anhydride reaction is desirable (resulting from attachment

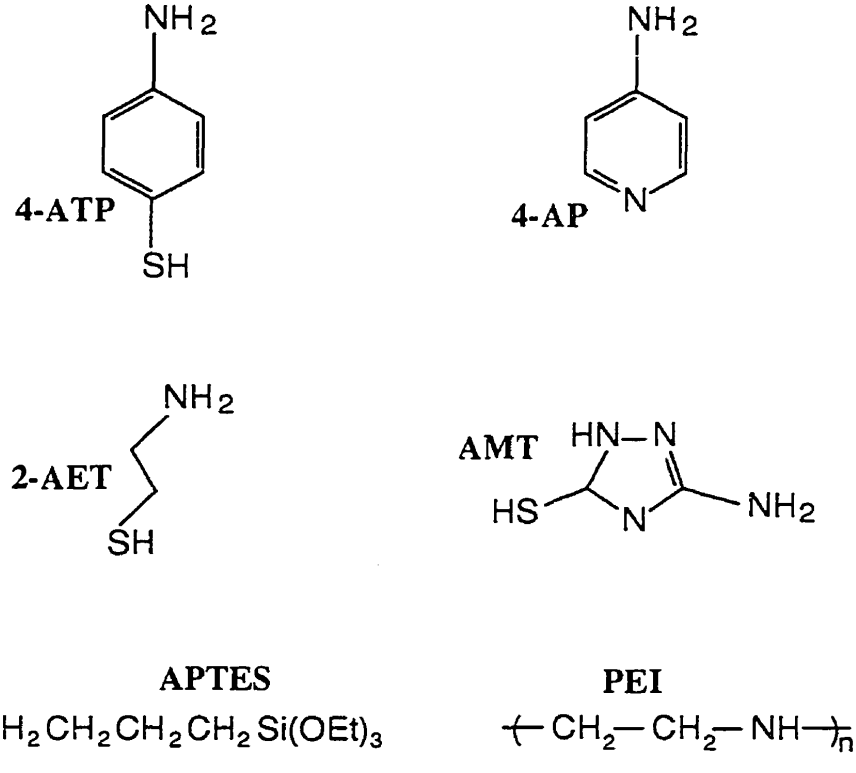

Figure 4.6 Structure of amine-functionalized coating compounds examined.

of mass via amide formation), the frequency must also remain stable after immersing the coated electrode in pure solvent instead of anhydride. Thus after duplicate rinsing with the coating material solvent (ethanol or water), the coated crystal was immersed in the anhydride solvent (i.e., pure anhydrous DMF) a sufficient number of times to achieve a stable coating baseline. These control immersions demonstrated that only one pre-anhydride DMF immersion was necessary; further DMF control immersions produced only small frequency changes of ca. ± 2 Hz, which was taken as the "noise" level for the subsequent anhydride reaction step. With a detection limit (DL) defined by 3σ, a change in frequency of ± 6 Hz is thus necessary to confirm a change in mass associated with the reaction step.

The data in Table 4.4 represents the work of over one hundred experiments performed over several months. Individual plots of frequency vs. time have not been plotted since the only relevant parameter is simply the value of the frequency change in each step. For each coating compound, we analyze the performance data below and also discuss the use of the compound in other literature reports.

The results for 4-aminopyridine (4-AP) may be summarized as follows (refer to Table 4.4). Incubation in 4-AP/ethanol followed by one ethanol rinse results in a decrease in crystal frequency, indicative of the adsorption of mass. Subsequent immersions in ethanol and DMF generally increases the frequency, which corresponds to loss of some of the coating. Finally, reaction with anhydride (10 min) followed by one DMF rinse further increases the frequency by 5-7 Hz. Although this value is near the DL, the inference is that *reaction with anhydride may involve removal of some of the adsorbed 4-AP*. It is also noted that coating for 12 h vs. 2 h results in greater adsorption of 4-AP to the gold electrodes. After reaction with anhydride, the presence of 4-AP is still indicated for crystals coated for 12 h, but the frequency returns to the uncoated baseline for 2 h coated crystals.

The choice of 4-AP as an amine-functionalized sensor coating was based on previous reports of the adsorption of pyridine at gold electrode surfaces. Stolberg *et al.*[14] found that pyridine adsorbs on gold surfaces with a high standard Gibbs energy of adsorption, at a limiting surface concentration of between 3×10^{-10} mol/cm^2 and 7×10^{-10} mol/cm^2, depending on the orientation of the ring. An estimate of the surface

Table 4.4 Frequency data for all steps involved in the coating evaluation.[a]

Compound	Coat time[b] (hrs.)	rinse 1[c] (Hz)	rinse 2 (Hz)	rinse dmf (Hz)	SA+rinse[d] (Hz)	ΔfSA[e] (Hz)
4-AP	2	-16±5	-12±6	-6±5	-1±2	5±6
	12	-42±21	-34±24	-32±18	-25±12	7±8
4-ATP	2	-38±11	-37±11	-31±8	-25±9	6±4
	12	-51±18	-44±12	-44±10	-40±16	4±7
AMT	2	-27±12	-26±9	-25±14	-17±15	7±6
	12	-54±15	-49±13	-41±15	-30±21	10±7
2-AET	2	-37±6	-30±6	-22±11	-22±12	0±6
	12	-60±13	-49±4	-47±5	-38±16	10±12
APTES	0.2	-98±40	-51±23	-44±22	-53±23	-9±2
PEI	0.2	-272±113	-200±72	-161±92	-223±114	-61±34

[a] All frequency values are the difference from a 0 Hz baseline established just prior to the coating step. 4-5 experiments were performed for each system. [b] Number of hours used in the coating step. [c] Rinses 1 and 2 were with either ethanol (first four compounds) or water (APTES and PEI). All rinses (including DMF rinses) involved fully immersing the crystal in the solvent for 2 minutes. [d] The crystal was fully immersed in 0.1 M succinic anhydride (SA) in anhydrous DMF for 10 min, followed by one DMF rinse. [e] Frequency change for the reaction step alone.

concentration in our work can be made using the Sauerbrey equation (Eqn. 1.1). Assuming an average value of 5 x 10^{-10} mol/cm^2 for 4-AP on gold, the theoretical change in frequency with the present 10-MHz sensor, using both sides of the crystal (n = 2), is calculated to be *-22 Hz*. This is in relatively good agreement with the data in Table 4.4, being intermediate between the values observed for 2 and 12 h incubations. The 12 h incubations may thus involve a certain degree of multilayer formation, while the 2 h incubations may produce slightly sub-monolayer coverages. Zhu *et al.*[20] have observed that after soaking a monolayer of 4-AP (immobilized on a superconductor surface via the amino group) that there is a greater surface adsorption of gold colloid particles to the ring nitrogen after 14 h compared with after 2 h. The reproducibility (i.e., standard deviation) in the frequency data does not however presently permit a rigorous quantitative determination of the relative coverages. It is nevertheless clear from the TSM sensor frequency data that while 4-AP does adsorb to the sensor electrodes, it fails in producing an analytically useful signal for reaction with the amino group.

Similar in structure to 4-AP, 4-aminothiophenol (4-ATP) was also examined as a potential amine-functional coating for liquid-phase TSM sensor applications. As mentioned earlier in section 4.3.1, many mercaptan derivatives (RSH) are known to undergo self-assembly to form thin monolayer films at gold surfaces.[3,4] The mechanism involved in the adsorption of thiols on gold surfaces is not completely understood, but is believed to involve a formal dissociative adsorption of the S-H bond to form a gold surface thiolate (RS-Au or RS^-—Au^+).[4,5] 4-ATP generally performed similarly to its pyridine counterpart. There is first an initial adsorption of thiol, followed by some loss after the second ethanol rinse and the DMF rinse. A theoretical 4-ATP monolayer coverage on gold has been estimated at 1.4 x 10^{-9} mol/cm^2,[21] which substituted in Eqn. 1.1 with a thiolate MW of 124.18 gives a predicted frequency change of -78 Hz. This would tend to indicate that both 2- and 12-h immersions produce 4-ATP coatings at sub-monolayer coverage, although the 12-h immersion time again provides for a greater adsorption of mass. The second and third rinses cause the frequency to increase slightly, indicating some removal of mass. Upon incubation with anhydride, the frequency change also tends to indicate further

loss of a small amount of coating material, although the continued presence of 4-ATP is indicated in all cases regardless of the number of hours used in the coating step.

3-Amino-5-mercapto-1,2,4-triazole (AMT) was chosen as a representative heterocyclic primary amine-functionalized thiol, in which the amino group should be sterically accessible for reaction if the molecule is anchored via the thiol group. AMT also contains a secondary amine which may also be reactive with anhydride although this may be precluded by steric crowding in the monolayer. Assuming a packing density similar to 4-ATP, a rough estimate for the expected frequency decrease for an AMT thiolate (MW = 115.07) monolayer is 74 Hz. Within the experimental error, crystals coated for both 2 and 12 h are thus likely at sub-monolayer coverage just before the reaction step (-25±14 and -41±15 Hz, respectively), with the longer coating time again resulting in the stable adsorption of a greater amount of thiol. After reaction with anhydride the frequency rises, once again indicative of some loss of coating.

A third thiol candidate, the straight chain compound cysteamine (2-aminoethanethiol, 2-AET), was also examined. The general trends regarding the coating step are similar to those observed with the other two thiols. In terms of surface coverage, using a value of 21.4 Å^2/thiol used for similar long-chain alkylthiols,[4] the theoretical surface coverage is 0.78 x 10^{-9} mol/cm^2 and the expected frequency change for a cysteamine thiolate ($MW_{thiolate}$ = 76.1) monolayer is -26 Hz. The data in Table 4.4 suggest that, if the assumption of a similar packing density to long-chain thiols on gold is correct, some multilayer formation may be occurring with the 12 h incubation time but that the 2 h incubation time produces approximately monolayer coverage after rinsing. After reaction with anhydride, loss of mass was indicated for 12 h coated crystals (likely due to partial multilayer removal), but *no* mean change in mass (0±6 Hz) was indicated for crystals coated for 2 hours. This latter observation places cysteamine in contrast to 4-AP and the other two thiols (although all reaction step values in question are close to the DL of the protocol).

Of the four compounds examined so far, two have been employed in multiple studies as anchor coatings on gold for subsequent reaction at the amino group. Sun et al.[21] have observed stoichiometric reaction of dimethyloctylchlorosilane at 4-ATP

monolayers on gold using a vapor-phase surface acoustic wave device, and electrostatic binding of anions at a 4-ATP monolayer on gold in aqueous solution by cyclic voltammetry.[15] Kajiya *et al.*[22] modified monolayers of 4-ATP on gold with glutaraldehyde for the successful immobilization of glucose oxidase in aqueous solution. Cysteamine monolayers on gold have been used for attachment of naphthoquinones in ethanol under reflux (3 min),[23] C_{60} in benzene (24 h),[24] and the enzyme diaphorase in aqueous solution (30 min) also via glutaraldehyde coupling.[25] Schlereth *et al.*[26] formed similar monolayers on gold from cystamine (the disulfide analog of cysteamine), but attempts to covalently link the coating to toluidine blue in phosphate buffer (overnight reaction) via glutaraldehyde cross-linking were unsuccessful in this case.

One factor to consider in discussing the results for 4-AP and the thiol compounds is the reactivity of the amine group itself. Although stable adsorption of monolayers (in most cases) is indicated even after rinsing in both ethanol and DMF, none of these four compounds exhibited a decrease in frequency for reaction with anhydride. Using the MW of succinic anhydride (100.07) and the Sauerbrey equation (since frequencies were measured in air and the films should still be thin), modest decreases in frequency are expected for (complete) reaction of the anhydride with the various coatings: -22 Hz (4-AP), -64 Hz (4-ATP, AMT) and -36 Hz (2-AET). Also, a limited number of additional experiments performed with added base (triethylamine) did not alter the results, which helps to exclude possible amine protonation as a causative factor. It is noted however that the amine groups in 4-AP, 4-ATP and AMT are all subject to electron delocalization and hence lowered nucleophilicity. Reaction with anhydrides may still be expected but could require longer reaction times and/or the presence of heating or catalysts. For example, the para-amine group in p-aminobenzamidine (similar to 4-ATP) has been successfully reacted with succinic acid in an anhydrous mixture of DMF and pyridine, but DMAP was also employed as a catalyst and a 1-h reaction time was used to obtain the amide in 88 % yield.[27] In comparison, the alkylamine 2-AET is more nucleophilic and should be more reactive to anhydride; this is possibly reflected in our results by the absence of a frequency increase with crystals coated for 2-h (the positive change in frequency for the 12-h

cysteamine-coated crystals is almost certainly due to multilayer removal). The transferability of solution-phase reactivity to surface reactivity, a question which has been raised previously,[28] may also influence the extent of the present reaction, although successful reaction of anhydrides with surface-confined alkylamine groups has been reported.[29]

A second factor to consider is the stability of the gold-thiolate (or gold-pyridine) bond. Long-chain thioalkyl self-assembled monolayers (SAMs) on gold are generally assumed to be very stable, with negative free energies of adsorption. For example, Karpovich and Blanchard[30] observed a ΔG_{ads} = -4.4 kcal/mol for 1-$C_8H_{17}SH$, although they could not determine the relative contributions of gold-thiolate and interchain interaction energies to this term (the gold-thiolate bond energy is likely the predominant driving force for monolayer formation in the present study). Even larger energies of chemisorption (eg. ~40-45 kcal/mol) have been reported.[4] However, Karpovich and Blanchard also concluded that there was an equilibrium in the adsorption/desorption process which proceeds predominantly between thiolate moieties and free gold sites at the edges of monolayer islands and/or at step edges and defect sites. The STM work of McCarley *et al.*[31] has also called into question the extent to which these monolayers are "fixed" in place, and has demonstrated that mobile defects can exist in the gold surface and that the Au-S bond is labile. Exchange experiments of various thiols in solution, such as the displacement of thiophenol (similar to 4-ATP) on gold by octadecyl mercaptan,[32] also indicate a reversible RS/Au interaction. Edinger *et al.*[33] observed that after adsorption of n-alkanethiols, new morphological features are observed which can be shown to originate from a removal of 30-50% of a monolayer of Au atoms from the surface into solution. Using a 5.9 MHz TSM sensor, McCarley *et al.*[34] observed frequency increases of 12 ± 3 Hz after exposure of one gold crystal electrode to aqueous sulfide (HS^-) for 20-30 min and drying. Noting that blank rinses or soakings in high-purity water did not produce such increases, they concluded that the decrease in mass was due to loss of 20-30% of a monolayer of Au atoms.

In the absence of other supporting experimental work (such as atomic absorption analyses for gold), we offer the following interpretation of the data in

Table 4.4 for the thiol compounds and 4-AP. First, the frequency decreases observed after the coating and rinse steps are indicative of stable adsorption of material without significant loss of gold atoms from the electrode surface. Second, the small frequency increases observed after the anhydride reaction and rinse steps may represent a balance between mass gain due to amide formation, and loss of mass due to desorption of unreacted thiolate, reacted thiolate and/or reacted thiolate-Au. Loss of multilayer material (where applicable) may also be a contributing factor. Amide formation is a function of amine nucleophilicity and is likely incomplete. Where amide formation does occur, the additional mass attached may increase the instability of the monolayer system. This instability would be greatest at the monolayer edges and could be magnified by the shear-wave mechanical oscillation of the surface, the small size of the gold electrode ($\approx$ 0.2 cm^2) and the immersion-emersion/drying protocol. Evidently many factors may influence the frequency changes (or lack thereof), and further work would be necessary to properly examine their relative contributions. However, in terms of the objective of this work it is clear that the thiol and pyridine amine-functionalized derivatives we have examined, under the present experimental conditions, are not suitable as coatings which can provide analytically useful TSM sensor frequency signals for quick reaction of analyte with the amine group at room temperature.

The silane, 3-aminopropyltriethoxysilane (APTES), has previously been employed in a number of other TSM sensor applications. APTES was used on silver electrodes of AT-cut quartz crystals to successfully provide a reactive amine surface for further chemistry in solution.[34-36] It was claimed that the silane was attached via reaction with a stable hydroxide layer of the silver electrode.[35] It has also been immobilized on aluminum TSM sensor electrodes for vapor-phase reaction with chlorodimethylsilane.[28,38] A frequency decrease of 48 $\pm$ 2 Hz was observed and attributed to the adsorption of approximately one monolayer of APTES. Multilayer formation on oxidized Al electrodes has also been observed.[39] However when gold is used as the electrode material, there is no direct mechanism for APTES to become strongly attached to the electrode. Nevertheless this system has also been tested, and found to yield subsequent frequency decreases with TSM sensors for enterobacteria,[40]

Salmonella typhimurium[41] and anti-2,4-D antibodies.[42] In all three reports the electrode-immobilized silane was subsequently coupled to other molecules via glutaraldehyde cross-linking, and in the first two reports the silane-based immobilization strategy was found to be inferior to other strategies in terms of sensitivity and reproducibility. Notably, in all three reports the authors did not speculate if or how the silane was actually attached to the gold, and not simply to the surrounding quartz. Mechanisms such as field fringing are believed to impart a certain degree of mass sensitivity near electrode edges.[43] In a detailed study examining S/N aspects of TSM and SAW devices, Bodenhöfer *et al.*[44] observed stable coatings of polysiloxanes using TSM crystals with gold electrodes, and although the authors also did not speculate on the mechanism of adsorption, the large frequency shifts observed suggest that there were significant amounts of material on the electrodes. In one elaborate strategy, a circular hole was etched in the gold electrode on an AT-cut crystal in order to silanize the exposed quartz with APTES.[45] Successful oscillation and detection of galactosyltransferase was achieved.

It is seen from Table 4.4 that after a 10 min incubation and rinsing with water there is a considerable decrease in frequency (-98 ± 40 Hz) indicative of the adsorption of mass. Removal of loosely-adsorbed silane occurs after additional rinsing with water and DMF. Upon reaction with the succinic anhydride probe and rinsing the frequency decreases by -9 ± 2 Hz, providing support for reaction of surface amine groups. Improved reproducibility is also seen in the reaction step, compared with the coating step. Despite the variability in the coating step, it is worth noting that the mean frequency decrease here (-44 ± 22 Hz) is quite close to the value of -48 ± 2 Hz observed by Kurth and Bein[38] with APTES on aluminum-plated 9-MHz AT-cut crystals in the gas-phase. We are uncertain however, in our studies using gold electrodes, how much of the frequency decrease is a result of material on the electrode itself vs. on the surrounding quartz. We raise the question here since silanes in general are expected to have a much greater interaction with a quartz surface than with gold. For now we set aside the resolution of this particular question, but state that while APTES may be useful for providing reactive amine groups for subsequent liquid-phase reactions, the frequency changes for analyte reaction (at least in the present study) are

quite small.

The final candidate examined was poly(ethyleneimine)(PEI). PEI is a highly-branched water-soluble polymer with a distribution of primary, secondary and tertiary amino groups in the ratio 1:2:1. It has been used in a wide range of immobilization strategies and has found acceptance in a number of industrial immobilized biosystems.[46] There have also been a few reports[40,41,47,48] on the use of PEI as a stable initial coating on piezoelectric crystals for acoustic wave sensor immunoassays. Here, the polymer forms a stable thin film on the gold electrodes of the crystal, and antibody is then immobilized via glutaraldehyde cross-linking. The results in Table 4.4 also indicate successful use of the polymer; large frequency changes are associated with the deposition of PEI (-272 ± 113 Hz), rinsing removes loosely bound polymer (coating baseline stabilizes at -161 ± 92 Hz), and reaction with anhydride and rinsing produces a mean frequency decrease of -61 ± 34 Hz. The amount of polymer deposited is quite variable and this has been observed previously;[40] however we note that the reproducibility of the reaction signal is improved over that for the coating signal. The large reaction frequency shift is in marked contrast to the results seen with the other coating candidates, and is likely due to a combination of high stability of the adsorbed polymer on gold and a high reactivity (nucleophilicity) of the amine functional groups. In the next section work is described in which XPS was used to confirm covalent attachment of the anhydride, and the thickness of the unreacted and reacted polymer was determined by ellipsometry to be 24±4 Å and 29±4 Å, respectively. The results for all 6 candidates are illustrated graphically in Figure 4.7.

4.5.3 Conclusions

Surface-confined thin films with reactive amine functional groups have numerous potential applications, including study of polymer-drug conjugates, peptide coupling, and immunological studies. In this section a diverse range of potential amine-functionalized coating materials was selected and examined for their liquid-phase stability and reactivity on AT-cut piezoelectric crystals with gold electrodes. The selection was based on previous use with TSM sensor devices, other literature reports which indicated at least some promise for the present application, and

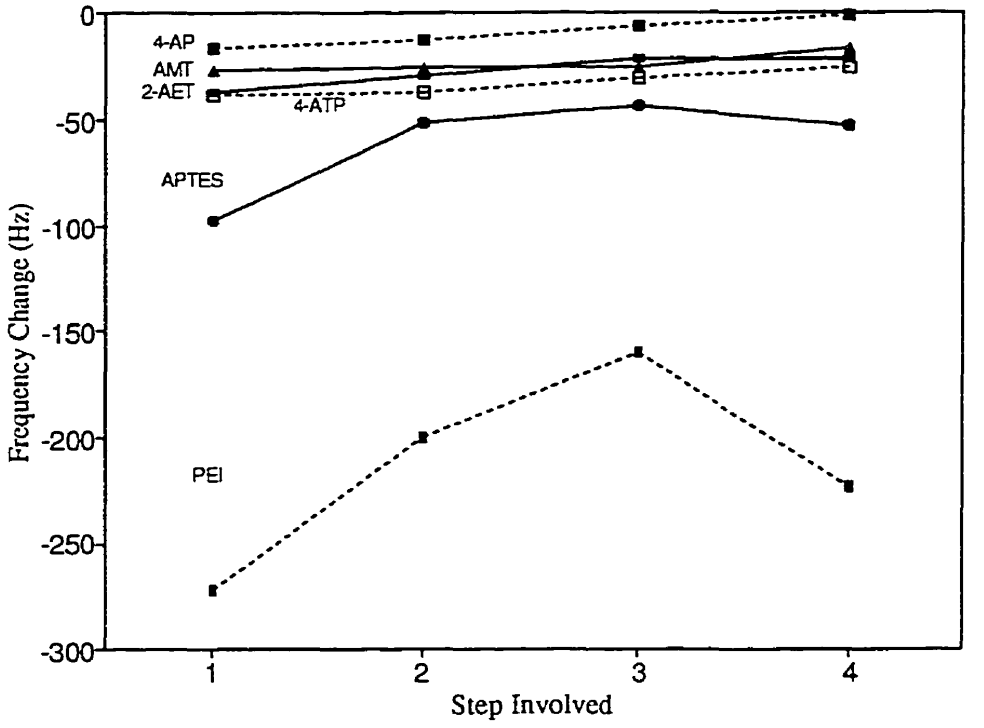

Figure 4.7 Graphical representation of frequency changes for the four steps of coating and one ethanol or water rinse (1), second ethanol or water rinse (2), DMF rinse (3), and anhydride reaction followed by one DMF rinse (4). Two-hour coating data are plotted for 4-AP, AMT, 2-AET and 4-ATP. PEI is shown to be the most analytically useful coating, in terms of the frequency decreases observed for both the coating and the reaction steps.

commercial availability. It is reasonable to assume that the application of thin film systems to TSM devices presents a number of unique experimental considerations concerning stability of the films. First, it should not be forgotten that AT-cut piezoelectric crystals operate via the propagation of acoustic shear waves, which causes the crystal surface to have a definite, high-frequency transverse shear oscillation. Second, when frequency readings are taken dry, strict rinsing procedures are necessary and also the immersion-emersion cycles may introduce a further stress on the thin film system.

In addition to selecting a stable coating material, a high degree of coating functional group reactivity is essential for optimal signal-to-noise enhancement with acoustic wave sensors. While a number of steps may be taken to increase the rate of reaction, they are generally undesirable since they may either increase the degree of

coating instability (e.g., use of heating) or may introduce species which may also adsorb to the coating (e.g., use of catalysts). For liquid-phase acoustic wave sensor applications, an ideal coating will thus be highly stable and will possess functional groups which react quickly at room temperature. The results in this section indicate that for such applications, networked, polymeric thin films may be superior to those formed from discrete, self-assembled molecules. In particular, where amine-functionalized thins films are desired, poly(ethyleneimine) is a superior choice to pyridine-, thiol- and silane-based coatings for providing analytically useful signals with liquid-phase TSM acoustic wave sensor devices.

4.6 Fabrication of Carboxylic Acid Terminated Thin Films Using Poly(ethyleneimine) on a Gold Surface

Thin films with reactive surface functional groups have many potential applications and have been the subject of an increasing number of reports in the literature over the past several years.[28,49,50] Films with primary amine, carboxylic acid or carboxylic acid derivative terminal groups are especially desirable since target molecules can be attached to them by a wide range of methods and they are directly reactive or can be made so easily through activation. When gold is used as the substrate, thiol-based compounds have often been employed to anchor a monolayer to the gold surface. For example, 11-mercaptoundecanoic acid (MUA) has been employed in a number of studies[11,51-61] to provide reactive surface carboxylic acid functional groups.

In view of the fact that reaction of PEI with succinic anhydride should convert the polymer support from an amino-terminated thin film to a carboxylic acid-terminated thin film, obtaining additional evidence for this conversion and probing the resulting film for carboxylic acid reactivity are of interest. The PEI-COOH film might not only offer an alternative to MUA, but might also prove more suitable for sensing applications in light of the polymer — thiol comparison examined in the previous section. The investigation was also of interest since at the time this work was performed, MUA or other long-chain carboxylic acid-terminated alkylthiols were not

commercially available (MUA became commercially available from Aldrich in late 1996).

In this section therefore a more thorough investigation of the film resulting from the reaction of succinic anhydride and poly(ethyleneimine) (PEI) is made. The purpose here is not only to verify that a covalent reaction did occur between the PEI coating and the anhydride, but also to establish that the resulting film can then be used as a platform for probing functional group reactions with the carboxylic acid group as the immobilized functional group of interest. After application of PEI and reaction with succinic anhydride, the formation of reactive COOH groups was tested with a carbodiimide-activated covalent immobilization of dopamine. TSM acoustic wave sensor studies, ellipsometry, and x-ray photoelectron spectroscopy provided support for all steps involved.

4.6.1 Materials and Methods

Poly(ethyleneimine) (50 wt. % solution in water), succinic anhydride, 1-(3-dimethylaminopropyl)-3-ethylcarbodiimide methiodide (DEC), triethylamine and anhydrous dimethylformamide (DMF) were obtained from Aldrich. 3-Hydroxytyramine (dopamine) was purchased from Sigma. All reagents were used as received. Water was doubly distilled, deionized and passed through an organic filter cartridge. AT-cut quartz crystals (10 MHz) were supplied by International Crystal Manufacturing Co. (Oklahoma City, OK). The full-immersion design described in section 2.5 was used (without the use of crystal C3 however). The jiffy jack was employed to raise and lower coating and rinse solutions, allowing the vertically-positioned crystal to remain stationary while connected to the oscillator circuit. All frequency readings were taken dry with both crystal surfaces in contact with ambient air (~ 22 °C).

Photoelectron spectra were obtained with a VG ESCALAB MKII spectrometer using MgKα radiation (E = 1253.6 eV, 280 W) at an angle of 50° from the sample surface normal. Film thickness measurements were taken with a Gaertner L116C ellipsometer (n_f = 1.45), for which polished crystals were required (specified gold electrode surface finish $\leq$ 1 micron). Ellipsometric measurements were performed at

3-4 different positions on each sample. For XPS studies (and also TSM studies), unpolished crystals were used (surface electrode finish 3-5 micron) in order to maximize photoelectron peaks.

4.6.2 Reactions Steps and TSM Sensor Frequency Data

Several steps are involved in the reaction sequence. The first step involves immersing the gold substrate in a dilute aqueous solution of PEI for a few minutes. After rinsing with water (twice) and then anhydrous dimethylformamide (DMF),[62] the polymer-coated substrate is then immersed in a concentrated (0.1 M) solution of succinic anhydride in anhydrous DMF. Here the cyclic anhydride ring is opened, forming a covalent amide bond with primary and secondary amine groups of PEI and generating residual carboxylic acid functionalities (Figure 4.8). We have found this reaction to be quick, reaching completion generally within 5 minutes or so. This is followed by another final rinse with DMF. Application of the polymer to both sides of a 10-MHz AT-cut piezoelectric crystal with unpolished gold electrodes and rinsing generally produced permanent frequency decreases of 100-150 Hz, followed by a further 40-80 Hz decrease after reaction with anhydride and rinsing.[63] The procedure is generally accomplished within twenty minutes.

As a test for the availability of reactive carboxylic acid functional groups, a carbodiimide-activated immobilization of dopamine was then attempted (overnight reaction, see Figure 4.8). Again, after rinsing with DMF a further permanent frequency drop of 100-170 Hz is observed.[64] The frequency changes here are consistently larger than those observed with the anhydride reaction step, which is in keeping with the increased MW of dopamine (189.6) vs. succinic anhydride (100.07), and supports a claim of near-complete reaction of all COOH groups. This is not unexpected since the spacing of amine groups on the polymer support should translate into a roughly equivalent spacing of carboxylic acid groups, which in turn should not pose any significant steric problem for reaction with the relatively small dopamine molecule.

An estimation of surface functional group density may also be obtained from the TSM sensor frequency data. Using the Sauerbrey equation with n = 2 (Eqn. 1.1) and the mean frequency change obtained from the anhydride step (-60 Hz) with 10

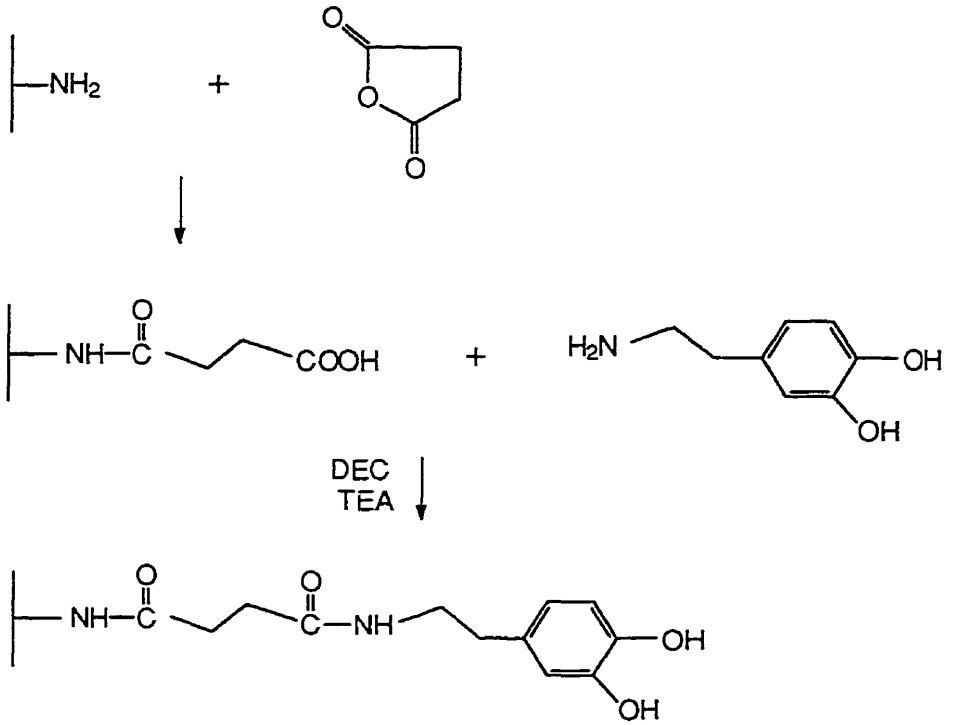

DEC = 1-(3-dimethylaminopropyl)-3-ethylcarbodiimide methiodide
TEA = triethylamine. All reactions in anhydrous DMF.

Figure 4.8 Reaction of poly(ethyleneimine) thin film with succinic anhydride and subsequent reaction with dopamine.

MHz sensor crystals, we calculate (Δm/A)(mol/100.07 g) = 1.32 x 10^{-9} mol/cm^2. For comparison, in long-chain thioalkyl monolayers the spacing of chains is determined by the underlying gold lattice. Taking a typical spacing of 21.4 Å^2 per chain,[4] the COOH functional group density in a monolayer such as MUA would be 0.78 x 10^{-9} mol/cm^2. We caution however that the surface structure afforded by the underlying PEI film is almost certainly considerably more disordered than the organized self-assembled structure of an MUA monolayer; the present film is likely three-dimensional, branched and perhaps coiled to some extent. This suggestion is also supported by the spread in the ellipsometric data (see below). Nevertheless, PEI is reported to have the highest concentration of amino groups per unit among all the synthetic polymers.[46] This high density of primary and secondary alkylamine groups, along with their expected high reactivity with anhydride and the observed frequency

shifts for the reaction, make it plausible to suggest that while the resulting film is disordered it is still relatively rich in COOH functional groups.

4.6.3 Ellipsometric and XPS Data

Further support for the reaction sequence was obtained through ellipsometric and x-ray photoelectron spectroscopy (XPS) measurements. Ellipsometry performed on two separate crystals with polished gold electrodes indicated thicknesses of 32 ± 5 Å (PEI and two water rinses), 24 ± 4 Å (after additional rinse with DMF),[62] 29 ± 4 Å (reaction with succinic anhydride and one DMF rinse), and 40 ± 5 Å (reaction with dopamine and one DMF rinse). The spread in thickness values (up to 11 Å) on each sample was significant and indicates an uneven surface structure caused by the underlying PEI support. Although some impurity was observed in the PEI sample,[65] XPS measurements nevertheless exhibited support for each step as well (Table 4.5). Reaction of succinic anhydride (SA) with PEI introduces C and O peaks characteristic of the COOH group, increases the content of amide C and amide O, increases the content of amide N at the expense of PEI N, increases the C/Au, O/Au and C/N ratios, and decreases the N/O and C/O ratios, all as expected.[66] Reaction with dopamine then introduces alkyl or aromatic C, increases the presence of amide C and amide N, increases the presence of amide/ester O (531.6 eV), decreases the presence of COOH C, and increases the N/Au, C/Au and O/Au ratios, again all as expected. The increase in amide C and amide N contributions, as well as the loss of the 289.2 eV C (acid or ester) supports attachment of dopamine via the amino group. The decrease in the 533.7 eV O represents a balance between the loss of carboxylic acid O and the gain of aromatic O from dopamine. High-resolution photoelectron spectra for the carbon, nitrogen and oxygen regions are shown in Figure 4.9 for qualitative inspection.

4.6.4 Conclusions

The fabrication of carboxylic acid terminated thin films is relevant to several fields including materials science,[67-69] chemical sensor development[55,70] and the investigation of surface-mediated biological phenomena.[71,72] Methods for preparation

Table 4.5 XPS Data for Reaction Steps in Figure 4.8

BE (ev)[a] or ratio	assignment	PEI	PEI +SA[b]	PEI+SA[b] +dopamine
285.2	alkyl/unsubst. aromatic C	---	---	13.1[c]
285.8	PEI C/anhydride alkyl C	32.6	23.6	23.3
288.3	amide C	4.6[d]	5.9	7.0
289.2	COOH	---	3.5	---
400.0	PEI/alkyl N	9.0	4.8	5.2
400.8	amide N	3.2[d]	4.5	6.4
531.6	C=O acid/amide/ester	5.7[d]	7.6	9.8
532.5	quartz O/C-O	6.4[e]	10.8	5.9
533.7	O=C-OH/phenolic O	---	2.0	1.4
N/Au		0.9	0.9	6.5
C/Au		3.9	4.8	31.6
O/Au		0.9	1.8	11.1
C/N		4.2	5.3	4.7
N/O		1.0	0.5	0.6
C/O		4.2	2.7	2.8

[a] All binding energies (BE) referenced to Au $4f_{7/2}$ = 84.0 eV. Spectra were deconvoluted using a 90%/10% Gaussian/Lorentzian peak shape. [b] Data in these two columns represent the average of two crystal samples. [c] For the peak assignments, the value given for each sample represents the % of that peak of the entire elemental composition of all elements. [d] An impurity containing C, O and N was identified in the PEI. [e] The rectangular observation window examined the circular gold electrode on one side of each crystal sample, as well as a small amount of surrounding quartz; in all samples silicon provided between 2-5 % of the total elemental signal.

of such films where gold is the initial substrate have focused on the use of MUA and other[73-78] thioalkyl monolayers. The present method offers an alternative route for preparation of carboxylic acid-terminated thin films. The method is quick and simple, and the films are also sufficiently robust for liquid-phase acoustic wave sensor applications. In particular, the observed stability of these films to multiple rinse cycles and liquid-phase oscillation, as well as the predicted high functional group density, make the present films attractive for maximizing signal-to-noise ratios in acoustic wave sensor devices.

Figure 4.9 Carbon, nitrogen and oxygen high-resolution photoelectron spectra for the reaction sequence depicted in Figure 4.8. (a) C - PEI, (b) C - PEI/SA, (c) C - PEI/SA/dopamine, (d) N - PEI, (e) N - PEI/SA, (f) N - PEI/SA/dopamine, (g) O - PEI, (h) O - PEI/SA, (i) O - PEI/SA/dopamine.

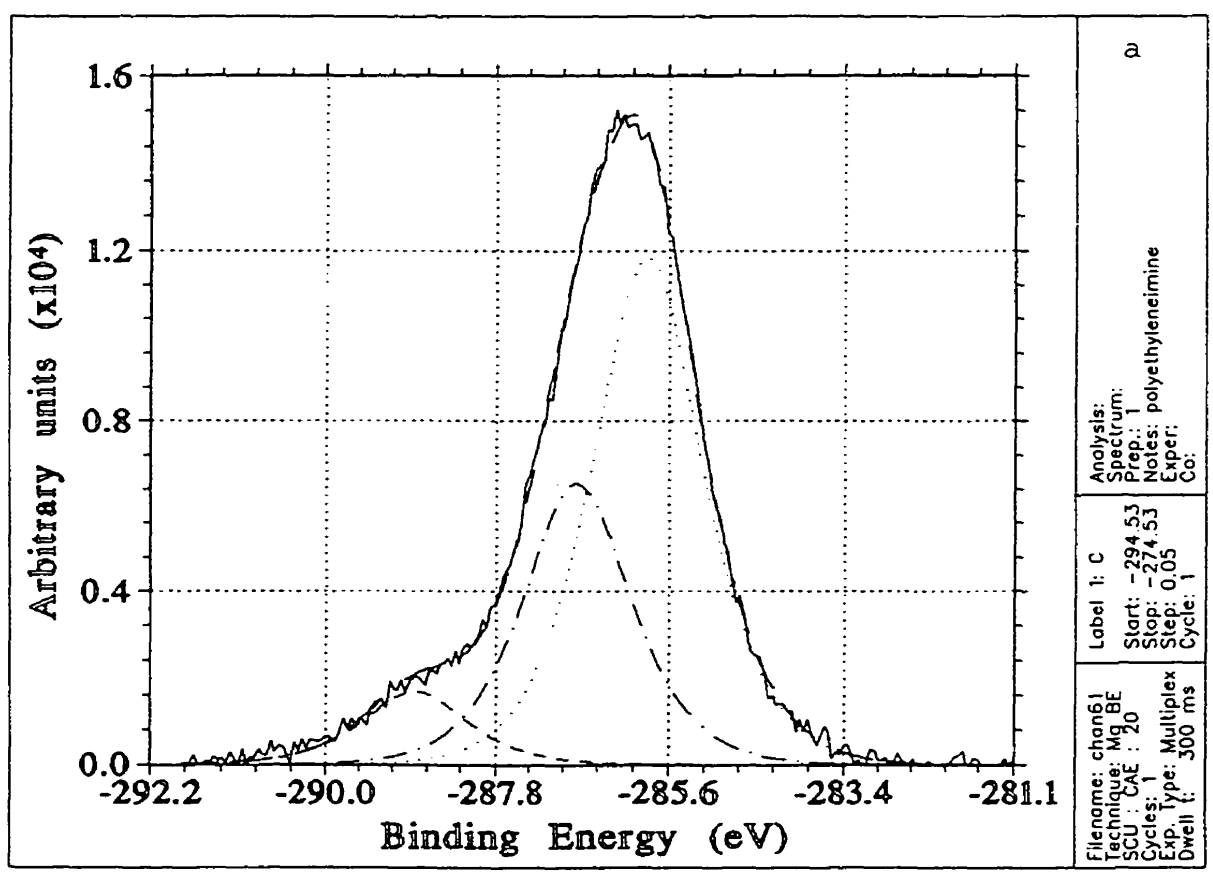

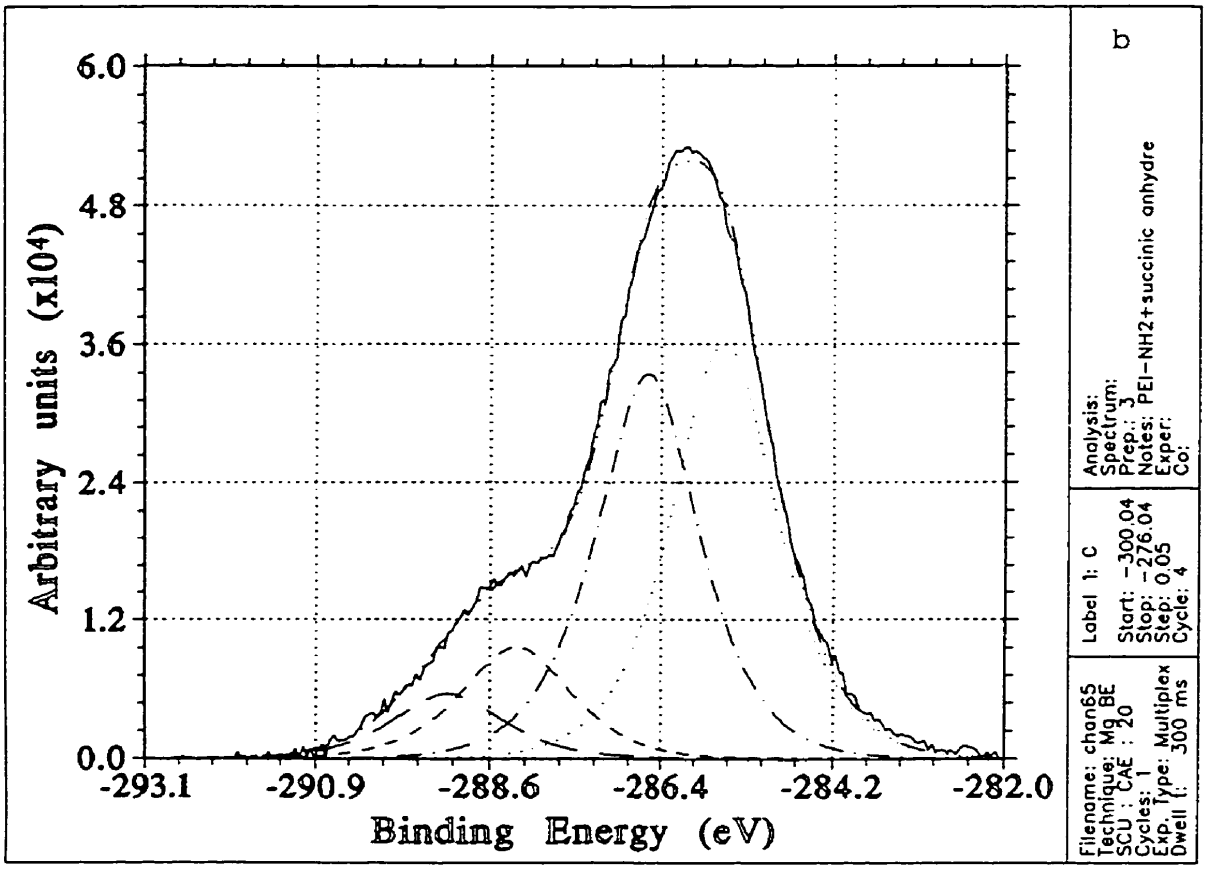
b
Arbitrary units (x104)
6.0
4.8
3.6
2.4
1.2
0.0
-293.1
-290.9
-288.6
-286.4
-284.2
-282.0
Binding Energy (eV)
Analysis:
Spectrum:
Prep.: 3
Notes: PEI-NH2+succinic anhydre
Exper:
Co:
Label 1: C
Start: -300.04
Stop: -276.04
Step: 0.05
Cycle: 4
Filename: chan65
Technique: Mg BE
SCU : CAE : 20
Cycles: 1
Exp. Type: Multiplex
Dwell t: 300 ms

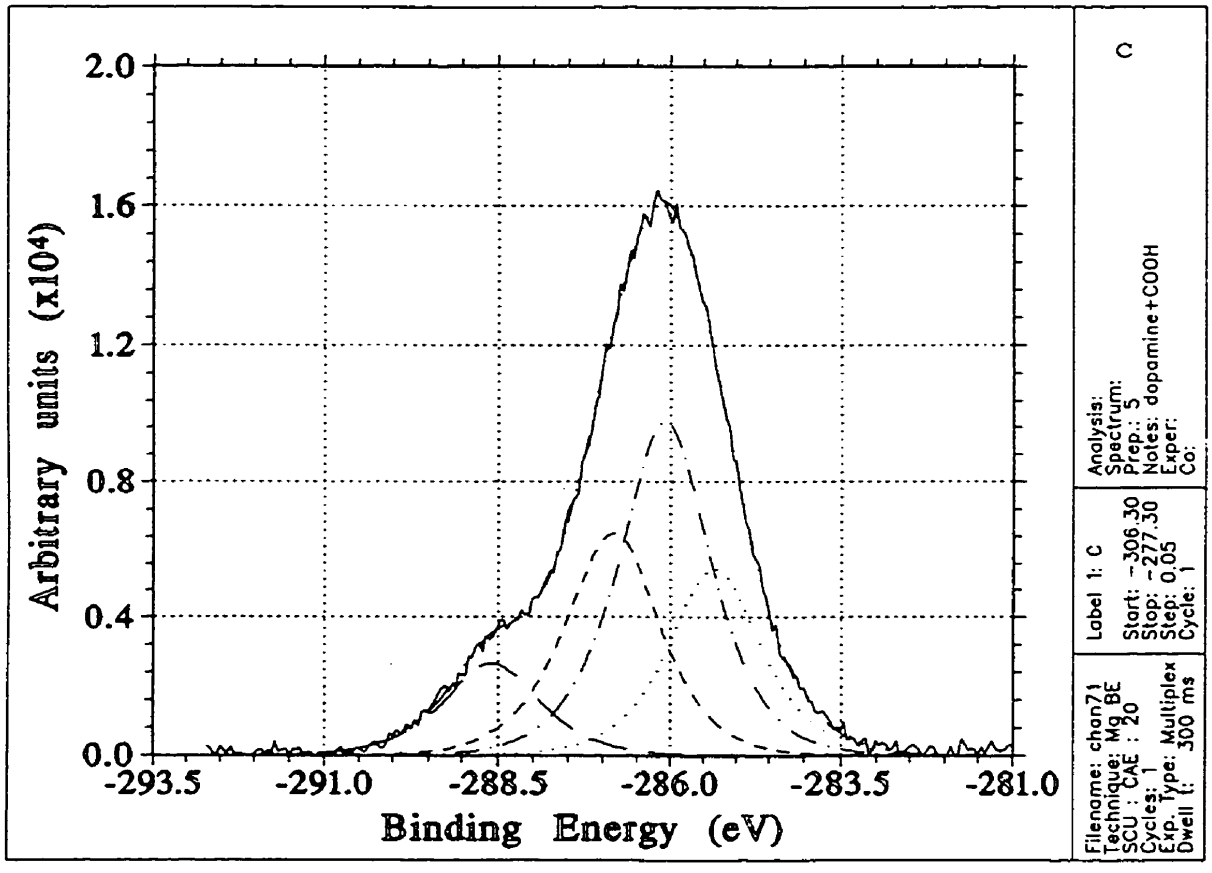
c
Arbitrary units (x104)
2.0
1.6
1.2
0.8
0.4
0.0
-293.5
-291.0
-288.5
-286.0
-283.5
-281.0
Binding Energy (eV)
Analysis:
Spectrum:
Prep.: 5
Notes: dopamine+COOH
Exper:
Co:
Label 1: C
Start: -306.30
Stop: -277.30
Step: 0.05
Cycle: 1
Filename: chan71
Technique: Mg BE
SCU : CAE : 20
Cycles: 1
Exp. Type: Multiplex
Dwell t: 300 ms

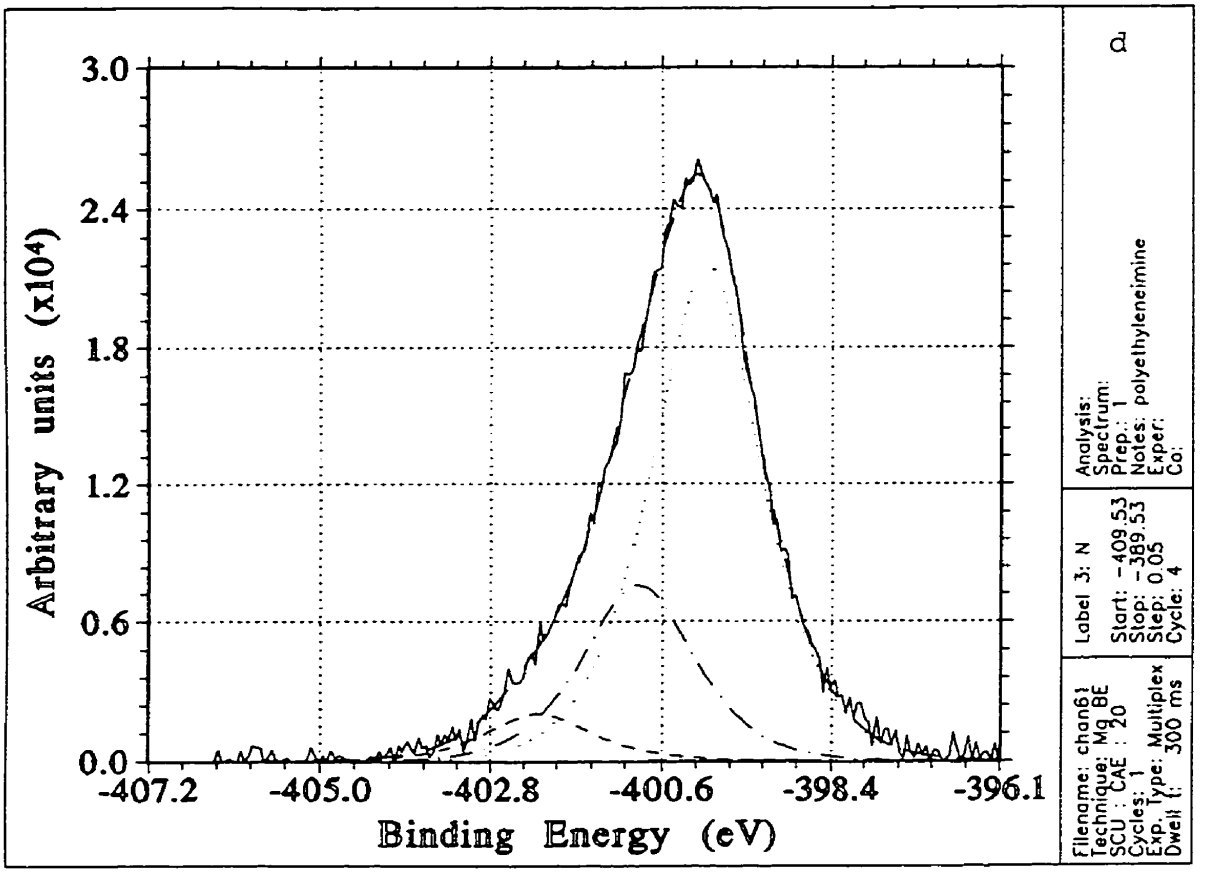
d
3.0
2.4
1.8
1.2
0.6
0.0
Arbitrary units (x10⁴)
-407.2
-405.0
-402.8
-400.6
-398.4
-396.1
Binding Energy (eV)
Analysis:
Spectrum:
Prep.: 1
Notes: polyethyleneimine
Exper:
Co:
Label 3: N
Start: -409.53
Stop: -389.53
Step: 0.05
Cycle: 4
Filename: chan61
Technique: Mg BE
SCU : CAE : 20
Cycles: 1
Exp. Type: Multiplex
Dwell t.: 300 ms

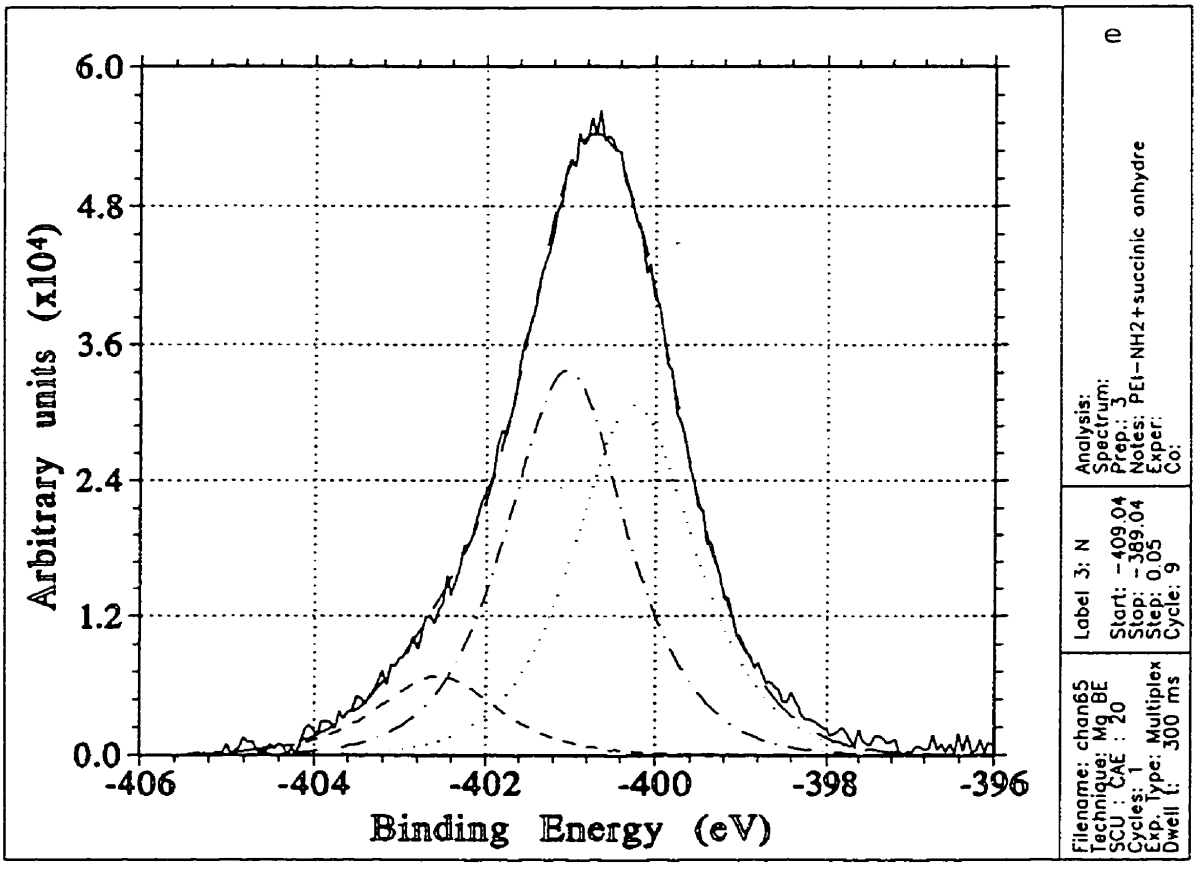
e
6.0
4.8
3.6
2.4
1.2
0.0
Arbitrary units (x10⁴)
-406
-404
-402
-400
-398
-396
Binding Energy (eV)
Analysis:
Spectrum:
Prep.: 3
Notes: PEI-NH2+succinic anhydre
Exper:
Co:
Label 3: N
Start: -409.04
Stop: -389.04
Step: 0.05
Cycle: 9
Filename: chan65
Technique: Mg BE
SCU : CAE : 20
Cycles: 1
Exp. Type: Multiplex
Dwell t.: 300 ms

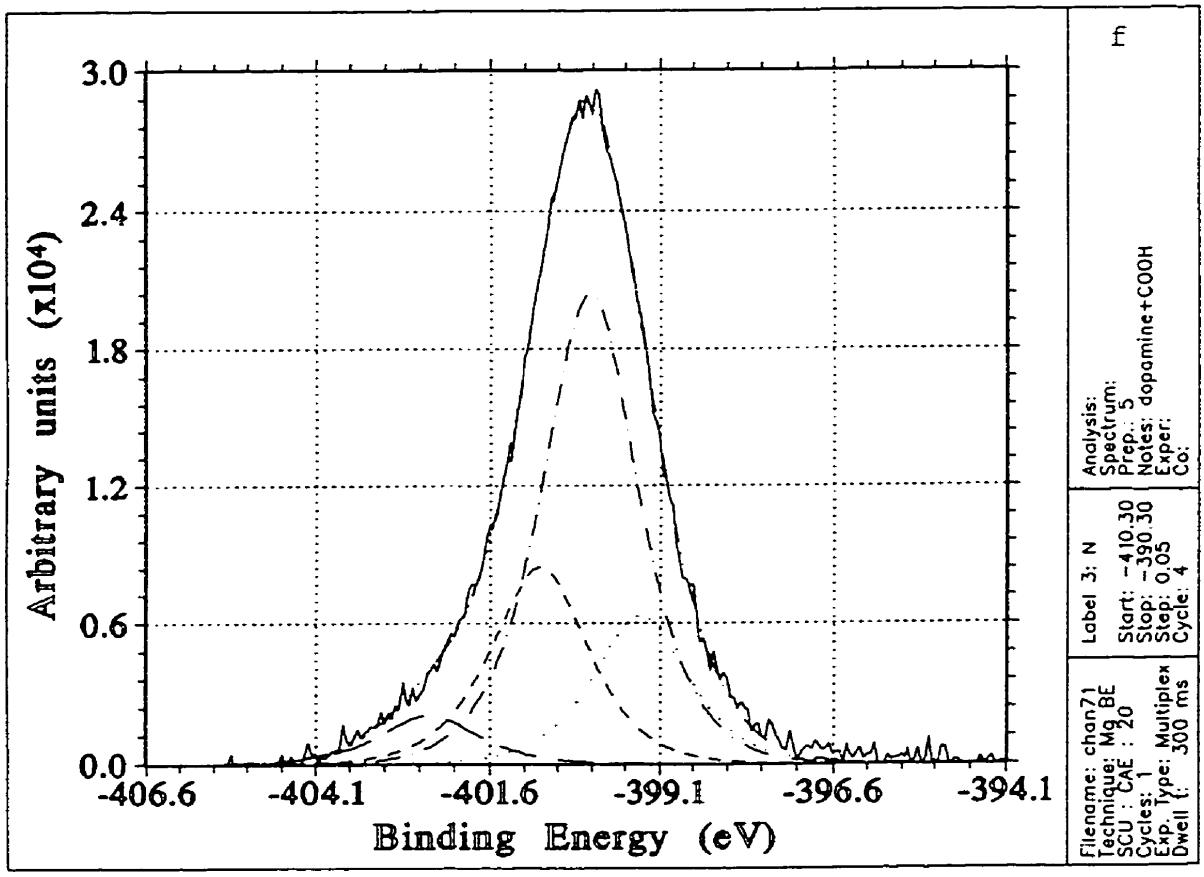
f
3.0
2.4
1.8
1.2
0.6
0.0
Arbitrary units (x10⁴)
-406.6
-404.1
-401.6
-399.1
-396.6
-394.1
Binding Energy (eV)
Filename: chan71
Technique: Mg BE
SCU : CAE : 20
Cycles: 1
Exp. Type: Multiplex
Dwell t: 300 ms
Label 3: N
Start: -410.30
Stop: -390.30
Step: 0.05
Cycle: 4
Analysis:
Spectrum:
Prep.: 5
Notes: dopamine+COOH
Exper:
Co:

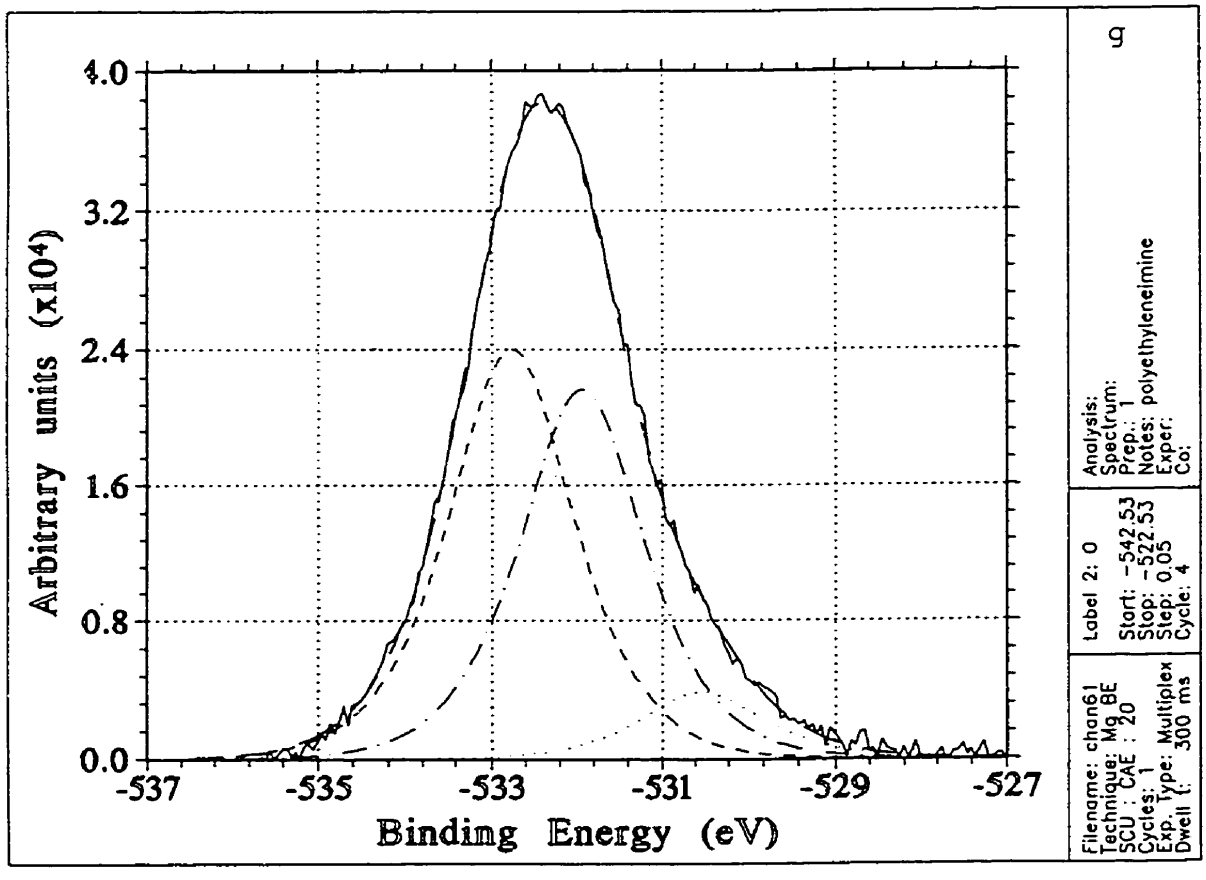
g
4.0
3.2
2.4
1.6
0.8
0.0
Arbitrary units (x10⁴)
-537
-535
-533
-531
-529
-527
Binding Energy (eV)
Filename: chan61
Technique: Mg BE
SCU : CAE : 20
Cycles: 1
Exp. Type: Multiplex
Dwell t: 300 ms
Label 2: O
Start: -542.53
Stop: -522.53
Step: 0.05
Cycle: 4
Analysis:
Spectrum:
Prep.: 1
Notes: polyethyleneimine
Exper:
Co:

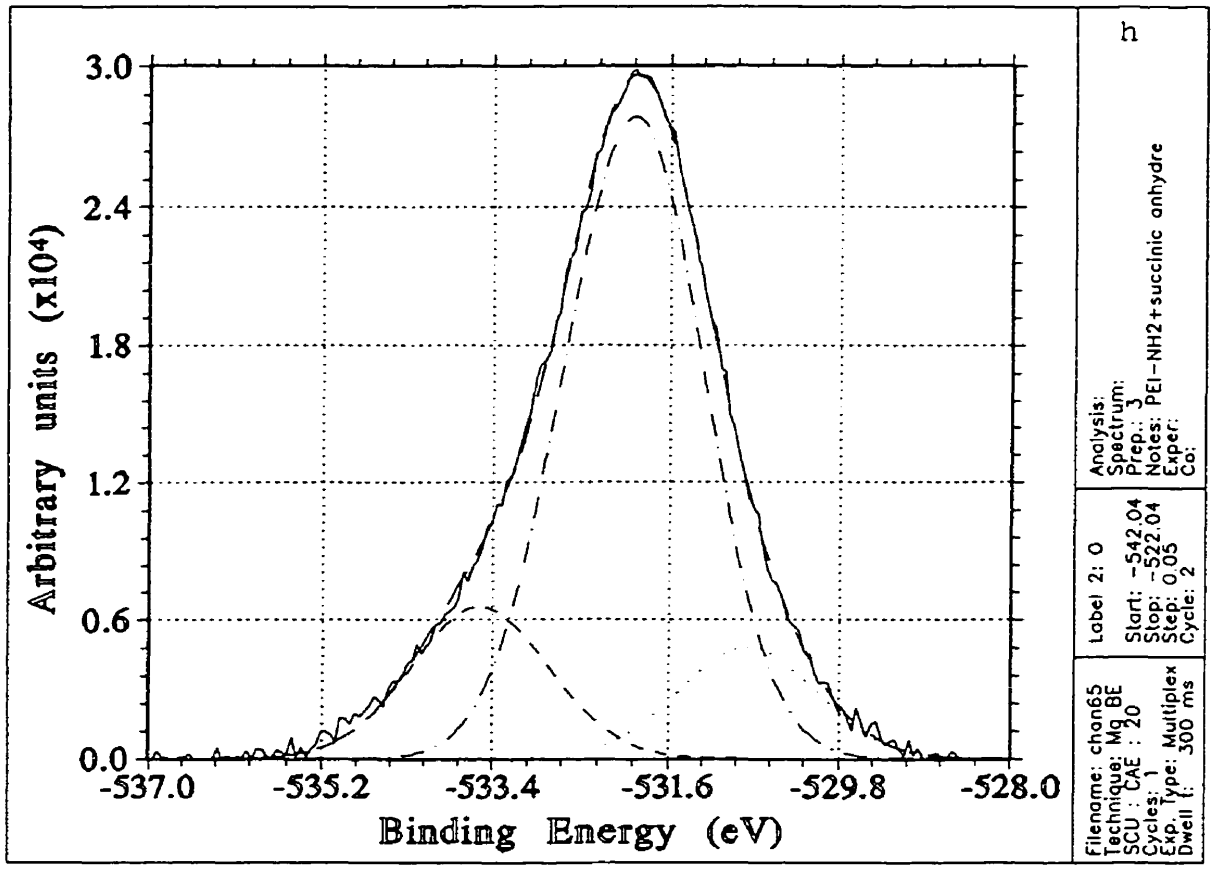
h
3.0
2.4
1.8
1.2
0.6
0.0
Arbitrary units (x10⁴)
-537.0
-535.2
-533.4
-531.6
-529.8
-528.0
Binding Energy (eV)
Analysis:
Spectrum:
Prep.: 3
Notes: PEI-NH2+succinic anhydre
Exper:
Co:
Label 2: 0
Start: -542.04
Stop: -522.04
Step: 0.05
Cycle: 2
Filename: chan65
Technique: Mg BE
SCU : CAE : 20
Cycles: 1
Exp. Type: Multiplex
Dwell t: 300 ms

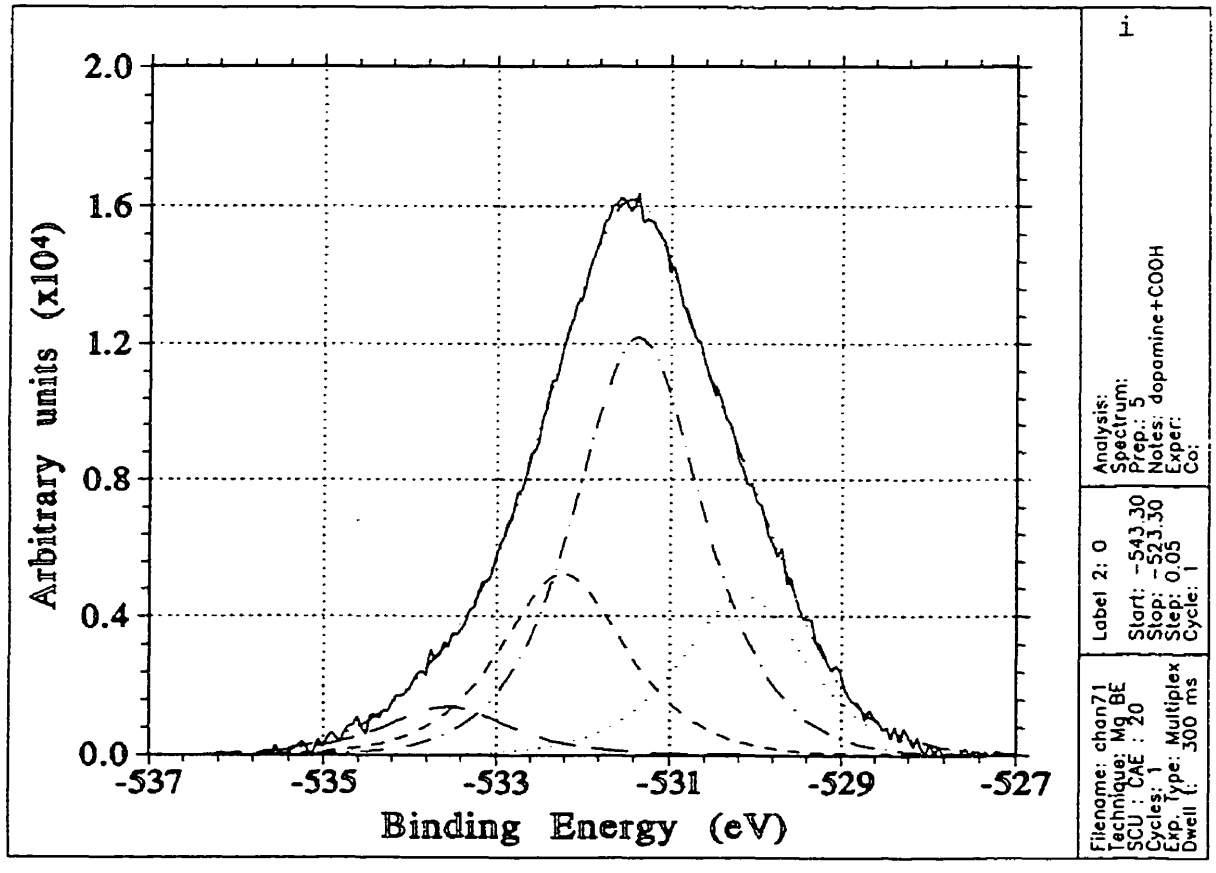
i
2.0
1.6
1.2
0.8
0.4
0.0
Arbitrary units (x10⁴)
-537
-535
-533
-531
-529
-527
Binding Energy (eV)
Analysis:
Spectrum:
Prep.: 5
Notes: dopamine+COOH
Exper:
Co:
Label 2: 0
Start: -543.30
Stop: -523.30
Step: 0.05
Cycle: 1
Filename: chan71
Technique: Mg BE
SCU : CAE : 20
Cycles: 1
Exp. Type: Multiplex
Dwell t: 300 ms

4.7 Chapter Overview

It is evident that many factors must be taken into account when developing a TSM acoustic wave sensor application. Much of the work in this chapter has involved examining and identifying a suitable coating material, which is perhaps most important and certainly the foundation of any sensing application. Probing functional group reactions in organic solvents remains an intriguing area of research, considering that an enormous wealth of functional group reaction chemistry has already been developed and that investigations in this area with the TSM sensor, aside from the work described in this chapter, have not been undertaken. As an example, phosphoramidite derivatives are widely used in nucleoside coupling and are reported to react with hydroxyl groups nearly quantitatively within one minute.[79] Immobilization of such derivatives on a TSM sensor crystal might thus provide for rapid detection of target molecules containing the hydroxyl group. Numerous other examples likely await investigation.

If there is one urgent need in this field of chemical sensors, it is precisely that which has been initiated in this chapter - identifying optimal coating candidates with particular functional groups. Ideal coating candidates would be similar to the cholestyramine coating examined in Chapter 3 in that they would adhere tenaciously to the electrode surface and be insoluble in virtually all solvents. If possible, such coatings might be incorporated into the electrode material itself for improved stability. One might then envision the day when instead of calling the crystal supplier and specifying only the resonant frequency and the electrode metal, one would also specify the functionality. The researcher could, for example, order a dozen primary amine crystals, a dozen hydroxyl crystals and a dozen sulfhydryl crystals. These crystals would be manufactured by the supplier according to procedures investigated and optimized expressly for use with TSM sensor crystals. Such a development would represent a significant and welcome advance to the field.

References

1. R.T. Morrison and R.N. Boyd, *Organic Chemistry, 4th Edition*; Allyn and Bacon Inc., Newton, MA, 1983; Chapter 11.
2. R.J. Fessenden and J.S. Fessenden, *Organic Chemistry, 3rd Edition*; Wadsworth, Inc., Belmont, CA, 1986; Chapter 7.
3. C.D. Bain and G.M. Whitesides, *Angew. Chem., Int. Ed. Engl.* **1989**, *28*, 506, and references therein.
4. A. Ulman, *Introduction to Ultrathin Organic Films*; Academic Press Inc., San Diego, CA, 1991; Chapter 3.
5. P.E. Laibinis, G.M. Whitesides, D.L. Allara, Y. Tao, A.N. Parikh and R.G. Nuzzo, *J. Am. Chem. Soc.* **1991**, *113(19)*, 7152-7167.
6. (a) R.B. Merrifield, *Fed. Proc.* **1962**, *21*, 412. (b) R.B. Merrifield, *J. Am. Chem. Soc.* **1963**, *85*, 2149.
7. C. Birr, *Aspects of the Merrifield Peptide Synthesis*; Springer-Verlag, Berlin, 1978.
8. M.D. Porter, T.B. Bright, D.L. Allara and C.E.D. Chidsey, *J. Am. Chem. Soc.* **1987**, *109(12)*, 3559-3568.
9. R.G. Nuzzo, L.H. Dubois and D.L. Allara, *J. Am. Chem. Soc.* **1990**, *112(2)*, 558-569.
10. H.O. Finklea and J.A. Melendez, *Spectroscopy* **1986**, *1(4)*, 47-48.
11. R.V. Duevel and R.M. Corn, *Anal. Chem.* **1992**, *64(4)*, 337-342.
12. M.J. Green, B.J. Barner and R.M. Corn, *Rev. Sci. Instrum.* **1991**, *62*, 1426-1430.
13. B.J. Barner, M.J. Green, E.I. Saez and R.M. Corn, *Anal. Chem.* **1991**, *63(1)*, 55-60.
14. L. Stolberg, J. Richer, J. Lipkowski and D.E. Irish, *J. Electroanal. Chem.* **1986**, *207*, 213-234.
15. L. Sun, B. Johnson, T. Wade and R.M. Crooks, *J. Phys. Chem.* **1990**, *94(26)*, 8869-8871.
16. J.M.S. Cabral and J.F. Kennedy, in *Protein Immobilization*; R.F. Taylor, Ed.; Marcel Dekker, Inc, New York, NY, 1991; Chapter 3.
17. A. Williams and I.T. Ibrahim, *Chem. Rev.* **1981**, *81(4)*, 589-636.
18. T. Wieland, in *Perspectives in Peptide Chemistry*; A. Eberle, R. Geiger and T. Wieland, Eds.; Karger Press, Basel, 1981; pp. 1-13.
19. D. Hudson, *J. Org. Chem.* **1988**, *53(3)*, 617-624.
20. J. Zhu, F. Xu, S.J. Schofer and C.A. Mirkin, *J. Am. Chem. Soc.* **1997**, *119(1)*, 235-236.
21. L. Sun, R.C. Thomas, R.M. Crooks and A.J. Ricco, *J. Am. Chem. Soc.* **1991**, *113(22)*, 8550-8552.
22. Y. Kajiya, T. Okamoto and H. Yoneyama, *Chem. Lett.* **1993**, 2107-2110.
23. E.Y. Katz and A.A. Solov'ev, *J. Electroanal. Chem.*, **1990**, *291*, 171-186.
24. W.B. Caldwell, K. Chen, C.A. Mirkin and S.J. Babinec, *Langmuir*, **1993**, *9(8)*, 1945-1947.
25. T. Sawaguchi, T. Matsue and I. Uchida, *Bioelectrochem. Bioenerg.* **1992**, *29*, 127-133.
26. D.D. Schlereth, E. Katz and H. Schmidt, *Electroanalysis*, **1994**, *6*, 725-734.
27. J.G. Rico, R.J. Lindmark, T.E. Rogers and P.R. Bovy, *J. Org. Chem.* **1993**, *58(27)*, 7948-7951.
28. D.G. Kurth and T. Bein, *Langmuir* **1993**, *9(11)*, 2965-2973.
29. J.K. Whitesell and H.K. Chang, *Science* **1993**, *261*, 73-76.
30. D.S. Karpovich and G.J. Blanchard, *Langmuir* **1994**, *10(9)*, 3315-3322.
31. R.L. McCarley, D.J. Dunaway and R.J. Willicut, *Langmuir* **1993**, *9*, 2775-2777.
32. E. Sabatani, J. Cohen-Boulakia, M. Bruening and I. Rubinstein, *Langmuir* **1993**, *9(11)*, 2974-2981.
33. K. Edinger, A. Gölzhäuser, K. Demota, Ch. Wöll and M. Grunze, *Langmuir* **1993**, *9(1)*, 4-8.
34. R.L. McCarley, Y. Kim and A.J. Bard, *J. Phys. Chem.* **1993**, *97(1)*, 211-215.
35. C. Barnes, C. D'Silva, J.P. Jones and T.J. Lewis, *Sensors and Actuators B* **1991**, *3*, 295-304.
36. C. Barnes, C. D'Silva, J.P. Jones and T.J. Lewis, *Sensors and Actuators B* **1992**, *7*, 347-350.
37. J.P. Jones and T.J. Lewis, *J. Chem. Soc. Faraday Trans.* **1995**, *91(18)*, 3147-3155.
38. D.G. Kurth and T. Bein, *Angew. Chem. Int. Ed. Engl.* **1992**, *31(3)*, 336-338.
39. L.V. Rajakovic, B.A. Cavik-Vlasak, V. Ghaemmaghami, K.M.R. Kallury, A. Kipling and M.

Thompson, *Anal. Chem.* **1991**, *63(6)*, 615-621.
40. M. Plomer, G.G. Guilbault and B. Hock, *Enzyme Microb. Technol.* **1992**, *14*, 230-235.
41. J.H.T. Luong, E. Prusak-Sochaczewski and G.G. Guilbault, *Ann. N.Y. Acad. Sci.* **1990**, *613*, 439-443.
42. M. Minunni, P. Skladal and M. Mascini, *Anal. Lett.* **1994**, *27(8)*, 1475-1487.
43. Z.A. Shana and F. Josse, *Anal. Chem.* **1994**, *66(13)*, 1955-1964.
44. K. Bodenhöfer, A. Hierlemann, G. Noetzel, U. Weimar and W. Göpel, *Anal. Chem.* **1996**, *68(13)*, 2210-2218.
45. L.H. Grande, C.R. Geren and D.W. Paul, *Sensors and Actuators* **1988**, *14*, 387-403.
46. R. Bahulekar, N.R. Ayyangar and S. Ponrathnam, *Enzyme Microb. Technol.* **1991**, *13(11)*, 858-868.
47. E. Prusak-Sochaczewski and J.H.T. Luong, *Anal. Lett.* **1990**, *23(2)*, 183-194.
48. E. Prusak-Sochaczewski and J.H.T. Luong, *Anal. Lett.* **1990**, *23(3)*, 401-409.
49. T.S. Koloski, C.S. Dulcey, Q.J. Haralson, and J.M. Calvert, *Langmuir* **1994**, *10(9)*, 3122.
50. Y. Ikeura, K. Kurihara and T. Kunitake, *J. Am. Chem. Soc.* **1991**, *113(19)*, 7342.
51. Y. Zhou, M.L. Bruening, D.E. Bergbreiter, R.M. Crooks and M. Wells, *J. Am. Chem. Soc.* **1996**, *118(15)*, 3773.
52. M. Wells and R.M. Crooks, *J. Am. Chem. Soc.* **1996**, *118(16)*, 3988.
53. Y. Zhou, M.L. Bruening, Y. Liu, R.M. Crooks and D.E. Bergbreiter, *Langmuir* **1996**, *12(23)*, 5519.
54. L. Sun, R.M. Crooks and A.J. Ricco, *Langmuir* **1993**, *9(7)*, 1775.
55. L.J. Kepley, R.M. Crooks and A.J. Ricco, *Anal. Chem.* **1992**, *64(24)*, 3191.
56. B.L. Frey and R.M. Corn, *Anal. Chem.* **1996**, *68(18)*, 3187.
57. C.E. Jordon, B.L. Frey, S. Kornguth and R.M. Corn, *Langmuir* **1994**, *10(10)*, 3642.
58. B. Sellergren, A. Swietlow, T. Arnebrant and K. Unger, *Anal. Chem.* **1996**, *68(2)*, 402.
59. Z.Q. Feng, S. Imabayashi, T. Kakiuchi and K. Niki, *J. Electroanal. Chem.* **1995**, *394(1-2)*, 149.
60. J.H. Reeves, S. Song and E.F. Bowden, *Anal. Chem.* **1993**, *65(6)*, 683.
61. M. Collinson, E.F. Bowden and M.J. Tarlov, *Langmuir* **1992**, *8(5)*, 1247.
62. After rinsing the PEI-coated crystal with water and DMF, the frequency became stable, and further rinsing with DMF caused negligible frequency changes (±5 Hz). The PEI film is thus stable after one DMF rinse.
63. Exposure of bare gold to succinic anhydride in DMF followed by rinsing with DMF produced negligible frequency change. This demonstrates that the much larger frequency changes resulting from immersion of PEI-coated crystals in succinic anhydride/DMF are due to irreversible attachment of mass to the polymer support.
64. The XPS data support the conclusion that under the completely anhydrous conditions employed, most of this frequency decrease is due to attachment of dopamine via amide bond formation. We note however that subsequent rinsing with water causes TSM sensor frequency increases which may be due to hydrolysis of small amounts of remaining ester-linked *O*-acylisourea intermediate and/or some removal of the polymer support.
65. The impurity peaks are identified in footnote d of Table 4.5. We note that the XPS PEI sample was not rinsed with DMF, and that the other samples are not expected to retain traces of DMF solvent under the UHV condition (< 10^{-8} torr) present in the instrument.
66. Although we might expect an increase in the peak at 285.8 eV from the methylene carbons of the attached anhydride, its decrease is likely simply a reflection of a lower absolute amount of polymer present in the PEI+SA samples vs. the PEI sample. This is consistent with the fact that the latter sample was not rinsed with DMF and therefore contains an excess of polymer which is normally removed with this rinse.
67. G. Krekel, K.J. Huettinger and W.P. Hoffman, *J. Mater. Sci.* **1994**, *29(13)*, 3461.
68. K. Waltersson, *Composites Science and Technology* **1985**, *23*, 303.
69. K. Waltersson, *Composites Science and Technology* **1985**, *22*, 223.
70. J. Janata, M. Josowicz and D.M. DeVaney, *Anal. Chem.* **1994**, *66(12)*, 207R.
71. W.P. Jencks, *Catalysis in Chemistry and Enzymology*; McGraw-Hill: New York, 1969; pp. 95-96.
72. D.A. Hutt, E. Cooper, L. Parker, G.J. Leggett and T.L. Parker, *Langmuir* **1996**, *12(22)*, 5494.

73. J. Wang, L.M. Frostman and M.D. Ward, *J. Phys. Chem.* **1992**, *96(13)*, 5224.
74. S.E. Creager and C.M. Steiger, *Langmuir* **1995**, *11(6)*, 1852.
75. D.D. Schlereth, E. Katz and H. Schmidt, *Electroanalysis* **1994**, *6(9)*, 725.
76. L.M. Frostman, M.M. Bader and M.D. Ward, *Langmuir* **1994**, *10(2)*, 576.
77. F. Malem and D. Mandler, *Anal. Chem.* **1993**, *65(1)*, 37.
78. E.L. Smith, C.A. Alves, J.W. Anderegg and M. Porter, *Langmuir* **1992**, *8(11)*, 2707.
79. S.L. Beaucage and M.L. Caruthers, *Tetrahedron Lett.* 1981, *22*, 1859.

Appendix 1

GPIB Software Routine for Data Acquisition

Where not taken manually, frequency readings were acquired automatically using the program *Asystant GPIB* (Asyst Software Technologies, Inc.). A GPIB interface card was installed in one of the expansion slots on a 486dx computer, and a 7-ft. long GPIB cable (bus) was used to connect the card to the frequency counter and hence allow the software to communicate with the frequency counter.

The software routine is stored in a separate file (filename.sav) and invoked at the time of starting *Asystant GPIB* by typing "asystant /f=filename.sav". The "GPIB" option is selected at the first screen to access the GPIB Main Menu. The GPIB Main Menu has three options: Configure Device, Program Mode and Interactive Mode. Configure Device is used mainly to specify the GPIB address of the frequency counter (address 10 was used since it was the default setting on the counter). Program Mode allows for programming of data acquisition routines. Interactive Mode allows for sending commands along the GPIB bus one at a time. The "Execute Routine" command in Interactive Mode is selected to run the data acquisition routine.

The software routine that was used consisted of a short, simple set of commands that belong to the GPIB standard set of commands. This was a distinct advantage in simplifying data acquisition programming compared with writing a program from scratch in a language such as C++. The GPIB commands used in the routine were *Talk, Initialize, Wait, Listen, Selected Dev Clr,* and *End Routine.* The routine is shown below.

```
Talk:
   Literal: *RCL 1
Initialize
Wait: Delay
Talk:
   Literal: :CALC:AVER:STAT ON;TYPE MEAN
   Literal: :CALC:DATA?
Listen:
   File: c:datafile.1
Selected Dev Clr
Initialize
End Routine
```

The "*RCL 1" argument forms a command that tells the frequency counter settings to recall a series of settings that were programmed on the front panel of the counter and saved in the counter memory. The settings instruct the counter how often to read the frequency and to perform statistical averaging of the frequency (e.g., read the frequency every 2s and compute the mean of every five readings). The CALC arguments form commands that instruct the counter to prepare a mean frequency value to be transmitted along the bus back to the computer. The software receives the number via the *Listen* command. *Selected Dev Clr* (selected device clear) and *Initialize* are simply commands sent to prepare the counter for the next time the routine is run. The number of routine iterations is specified at the time the *Execute Routine* command is invoked when in Interactive Mode. The *Wait* command hence serves as a time spacer between each time the routine is run; the duration of this time delay is specified in the "Delay" argument. All frequency readings are saved to an ASCII file "datafile.1", which can be imported into a word processor or spreadsheet at a later time.

Appendix 2

Publications, Presentations and Industry Consulting

The work described in this thesis has resulted in the following publications:

1. J.J. Chance and W.C. Purdy, "***Bile Acid Measurements Using a Cholestyramine-Coated TSM Acoustic Wave Sensor***", *Anal. Chem.* **1996**, 68(18), 3104-3111.

2. J.J. Chance and W.C. Purdy, "***Fabrication of Carboxylic Acid Terminated Thin Films Using Poly(ethyleneimine) on a Gold Surface***", *Langmuir*, in press.

3. J.J. Chance and W.C. Purdy, "Bile Salt Surfactants in Electroanalytical Chemistry", in *Organized Assemblies in Chemical Analysis: Vol. 2 - Bile Acid/Salt Surfactant Systems*; W.L. Hinze, Ed.; JAI Press, Greenwich, CT; in press.

4. J.J. Chance and W.C. Purdy, "***Evaluation of Amine-Functionalized Coatings for Liquid-Phase QCM Applications***", submitted to *Sensors and Actuators B*.

5. J.J. Chance and W.C. Purdy, "***TSM Sensor Signal Enhancement Via Viscoelastic Modulation of an Immobilized Swellable Polymer***", in preparation.

The work described in this thesis has been presented at a number of scientific conferences:

1. J.J. Chance and W.C. Purdy, "***Probing Coupling Reactions with a Piezoelectric Sensor***", 47th Pittsburgh Conference on Analytical Chemsistry and Applied Spectroscopy, March 3-8 1996, Chicago, Illinois, poster presentation.

2. J.J. Chance and W.C. Purdy, "***Full-Immersion QCM Monitoring in Non-Aqueous Solution***", 46th Pittsburgh Conference on Analytical Chemsistry and Applied Spectroscopy, March 5-10 1995, New Orleans, Louisiana, poster presentation.

3. J.J. Chance and W.C. Purdy, "***Investigation of Bile Salt Binding Using the Quartz Crystal Microbalance***", 45th Pittsburgh Conference on Analytical Chemsistry and Applied Spectroscopy, February 27 - March 4 1994, Chicago, Illinois, poster presentation.

4. J.J. Chance and W.C. Purdy, "***Applications of the Quartz Crystal Microbalance Technique to Studies of Atherosclerosis***", 76th Canadian Society for Chemistry Conference, May 30 - June 3 1993, Sherbrooke, Québec, oral presentation.

The work on bile acid measurements has also resulted in consulting work for a U.S. pharmaceutical company to assist them in assembling a TSM acoustic wave sensor system for study of novel bile acid sequestrants.

Appendix 3

Contributions to Original Knowledge

In this work the following contributions to original knowledge are claimed.

1. The use of cholestyramine resin as a coating material on a TSM acoustic wave sensor crystal serves as the basis for a novel bile acid sensor. Detection limits in water are in the range 0.2 - 9 nmol and are better than those observed in phosphate buffer. A multi-step regeneration protocol allows the coating to be reused more than 400 times over a period of several months. The TSM bile acid sensor is simple, inexpensive and easy to operate, and can likely be used to study other bile acid sequestrants.

2. At equimolar concentrations of citrate and bile salt, the trivalent citrate anion reduces the amount of bile salt binding by about 40%. This suggests that the efficiency of cholestyramine-based bile salt sequestering drugs used in the reduction of hypercholesterolemia may be improved by eliminating citric acid as an excipient and avoiding the use of fruit juices during ingestion.

3. Poly(ethyleneimine) is superior to several thiol-, silane- and pyridine-based coating materials for fabrication of primary amine-functionalized thin films which are stable and reactive in the liquid-phase.

4. Reaction of a poly(ethyleneimine) thin film with succinic anhydride in anhydrous DMF generates a thin film with terminal, reactive carboxylic acid groups. The method is quick and simple, and the films are also sufficiently robust for liquid-phase acoustic wave sensor applications.

IMAGE EVALUATION TEST TARGET (QA-3)

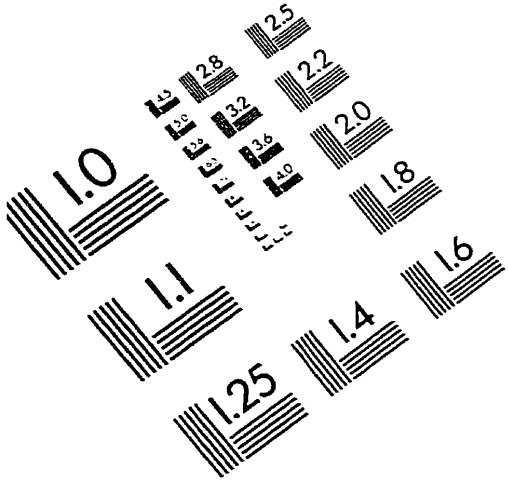

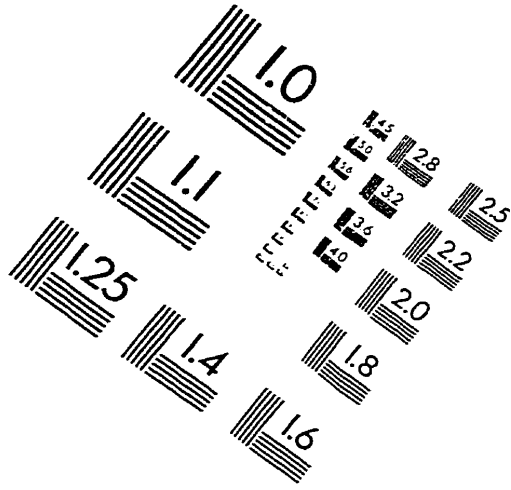

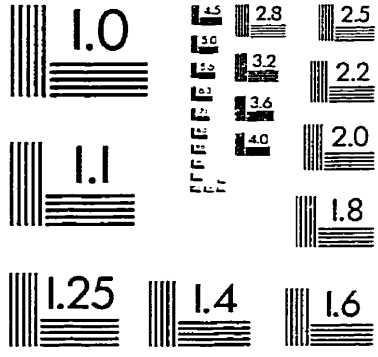

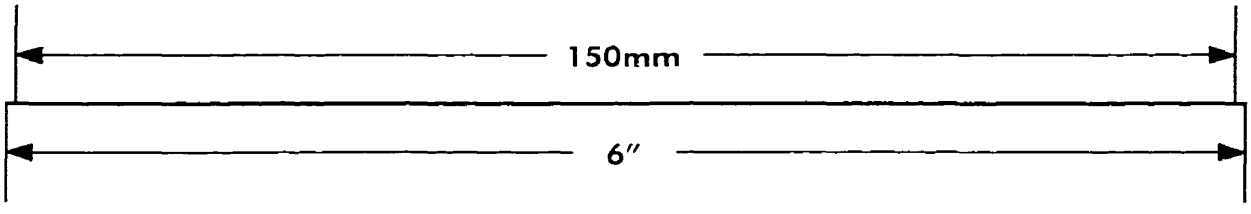

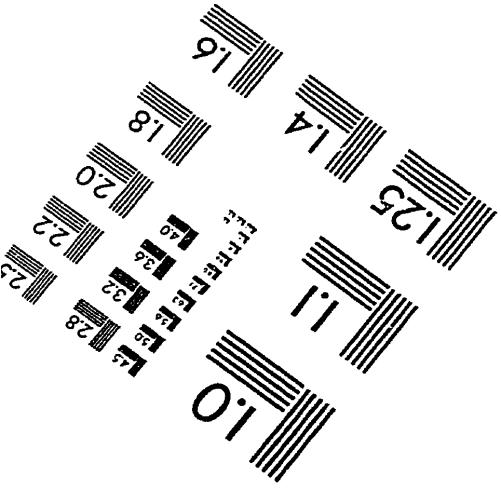

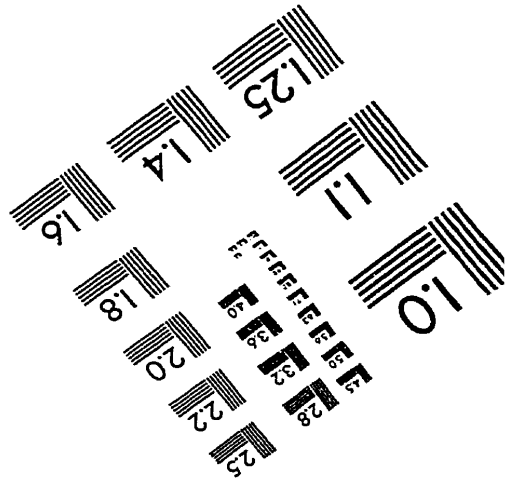

APPLIED IMAGE, Inc
1653 East Main Street
Rochester, NY 14609 USA
Phone: 716/482-0300
Fax: 716/288-5989